ABSTRACT

FERGUSON, SYLVIA, HOENIG. Interferon-λ Promotes Epithelial Defense and Barrier Function Against *Cryptosporidium parvum* Infection (Under the direction of Dr. Jody Gookin)

Cryptosporidium spp., is the second leading cause of infectious diarrheal death in children under 5 in developing countries, and a leading cause of diarrheal disease and death in the U.S. dairy industry. The intestinal epithelial cell (IEC) is the primary site of *Cryptosporidium parvum* (*C. parvum*) infection. The epithelial response is critical for orchestrating host defense against *C. parvum*, but is still mechanistically poorly understood. Accordingly, to elucidate the host strategy for defense against *C. parvum*, we examined the transcriptional response of IECs to *C. parvum* in a novel large animal model that effectively recapitulates human disease, neonatal piglets. Upregulated genes were dominated by targets of interferon (IFN) with interferon stimulated gene 15 (ISG15) being most highly induced. We next investigated the exact mediator of this IFN-response by performing qRT-PCR for Type I-III IFNs, and identified that a novel interferon, IFN-λ3, was the most upregulated in *C. parvum* infected piglet ileal mucosa. While IFN-λ has been described as a mediator of epithelial defense against viral pathogens, there is limited knowledge of any role against non-viral pathogens. We hypothesized that *C. parvum* induces an IFN-λ mediated immune response which plays a role in epithelial defense. The overall aim of the study was to determine the significance of IFN-λ to epithelial defense and barrier function during *C. parvum* infection.

The significance of *C. parvum* induced IFN-λ expression was determined using an immunoneutralization approach in neonatal C57BL/6 mice. The ability of the intestinal epithelium to upregulate IFN-λ expression in response to *C. parvum* infection and the influence of IFN-λ on epithelial defense against *C. parvum* invasion, intracellular development and loss

of barrier function was examined using polarized, non-transformed porcine intestinal epithelial cell monolayers (IPEC-J2). Specifically, changes in barrier function were quantified by measurement of TEER and transepithelial flux studies of creatinine, variably sized dextrans (4 and 70 kDa), and radiolabeled sodium ($^{22}Na^{+}$).

Immunoneutralization of IFN-λ in *C. parvum* infected neonatal mice resulted in significantly increased parasite burden, fecal shedding, and villus blunting with crypt hyperplasia during peak infection. *In vitro*, *C. parvum* was sufficient to induce autonomous IFN-λ and ISG15 expression by IECs. Priming of IEC with rHuIFN-λ promoted cellular defense against *C. parvum* infection and abrogated *C. parvum*-induced loss of barrier function by decreasing paracellular permeability to sodium. These studies are the first to identify IFN-λ as a key epithelial defense mechanism against *C. parvum* infection.

© Copyright 2018 by Sylvia Hoenig Ferguson

All Rights Reserved

Interferon-λ Promotes Intestinal Epithelial Defense and Barrier Function during *Cryptosporidium parvum* Infection.

by
Sylvia Hoenig Ferguson

A dissertation submitted to the Graduate Faculty of
North Carolina State University
in partial fulfillment of the
requirements for the degree of
Doctor of Philosophy

Comparative Biomedical Sciences

Raleigh, North Carolina

2018

APPROVED BY:

_____	_____
Jody Gookin Committee Chair	Derek Foster
_____	_____
Scott Magness	Barbara Sherry

DEDICATION

I dedicate this to my parents, who instilled in me a love of science and understanding, and to my husband Lou, and daughter, Ella.

BIOGRAPHY

Sylvia Hoenig Ferguson was born May 29th, 1985 in Ithaca, NY, and graduated from Clarke Central High School in 2003. From there, she attended the University of Georgia to study Biology. While completing her undergraduate coursework, Sylvia developed a love of infectious disease, particularly those with zoonotic and public health importance. Inspired by her parents, both of whom are veterinarians and researchers, and her desire to understand the pathogenesis of infectious diseases, Sylvia decided to attend veterinary school. In 2007, she was accepted into the University of Georgia College Of Veterinary Medicine. Through her veterinary school coursework and participation in externship opportunities at Tifton Diagnostic laboratory in Georgia and Friedrich-Loeffler institute in Germany, she developed a curiosity and love for understanding pathological mechanisms of disease.

Accordingly, following veterinary school, Sylvia completed a residency in anatomic pathology at the University of Tennessee and became board certified by the American College of Veterinary Pathologists in 2014. Then, as a result of her strong interest in zoonotic infectious disease and immunology kindled during her DVM and pathology training, and a desire to gain a better understanding of translational research and basic laboratory techniques in cellular biology, she began her study at North Carolina State University under the direction of Dr. Jody Gookin. Her dissertation project was focused on investigating the importance of the innate epithelial defense against an important zoonotic diarrheal pathogen, *Cryptosporidium*.

ACKNOWLEDGMENTS

Science and research are a team effort and accordingly, I have many people to thank. Firstly, I must thank Dr. Jody Gookin for giving me a chance by taking me on as a graduate student. I appreciate the time and effort that she put into being my mentor, always pushing me to dig deeper and think outside of the box when it comes to my research. She advised me not only about science, but also my professional development. Secondly, I would also like to thank my committee members Drs. Derek Foster, Barbara Sherry and Scott Magness. They were instrumental in keeping me focused and moving down the right path throughout my research training. I will miss the wonderful discussions that occurred during my committee meetings. Of course, I cannot forget the people that had to put up with me every day in the lab, Stephen Stauffer and Dr. Tory Watson. Stephen was instrumental in teaching me cell culture and most of the molecular techniques contained within this project. Additionally, Stephen's troubleshooting abilities were invaluable. Tory, as a fellow graduate student and anatomic pathologist, provided great friendship and guidance to me throughout my PhD. Having Tory there to share the highs and lows was immensely helpful.

On a more personal note, I must thank my husband Lou, daughter Ella, my parents, Duncan and Margarethe, and sister Julia, for providing me with unwavering support and understanding throughout this journey.

TABLE OF CONTENTS

LIST OF TABLES

CHAPTER I

CHAPTER II

LIST OF FIGURES

CHAPTER II

CHAPTER I

Intestinal epithelial responses to *Cryptosporidium* infection

Introduction

Cryptosporidium is a protozoal parasite that is responsible for an estimated 8 million cases of diarrhea in young children (<2 years of age) in developing countries every year, leading to 200,000 deaths annually (Kotloff et al., 2013; Sow et al., 2016) with more deaths in young children than malaria and HIV/AIDS combined (Kotloff et al., 2013; Liu et al., 2012; Striepen, 2013). The majority of this diarrheal disease is attributable to two species of the parasite, *Cryptosporidium hominis* (*C. hominis*) and *parvum* (*C. parvum*) (77% and 10%, respectively) (Sow et al., 2016). Cryptosporidiosis also targets the severely immunocompromised worldwide (Kotloff et al., 2013; McDonald et al., 2013); conditions leading to immunodeficiency and enhanced cryptosporidial susceptibility include congenital immunodeficiency (e.g.CD40L deficiency) (Cosyns et al., 1998), immunosuppressive drug treatment (Florescu and Sandkovsky, 2016), concurrent infections, and acquired immunodeficiency syndrome (AIDS) (O'Connor R et al., 2011).

To add to its overall impact, *C. parvum* infection occurs naturally in a wide variety of animal species, including dairy calves, neonatal pigs, goats, and sheep. Approximately 90% of U.S. dairy farms are endemically infected with *C. parvum*, which is a leading cause of dairy calf diarrhea and causes inestimable economic losses for the dairy industry (Nydam and Mohammed, 2005; Sischo et al., 2000). Additionally, *C. parvum* is the most commonly detected diarrheal pathogen in calves less than one month of age in the UK (Thomson et al., 2017). These infections in animals are equally devastating, resulting in severe diarrhea and dehydration, morbidity and mortality (Daniels et al., 2015).

Cryptosporidium is a minimally invasive, apicomplexan protozoal parasite that primarily infects small intestinal epithelial cells causing both a malabsorptive and secretory diarrhea that is self-limiting in healthy, immunocompetent individuals (Farthing, 2000), however, it leads to chronic, debilitating diarrhea, and even death in immunocompromised patients (O'Connor R et al., 2011). Accordingly, a host's immune response, particularly that orchestrated by the intestinal epithelial cells, plays a critical role in determining the susceptibility and clinical outcome of cryptosporidiosis (Bouzid et al., 2013; Gookin et al., 2002; McDonald et al., 2013). Therefore, a lot of research effort has gone towards understanding the epithelial response to *C. parvum* in hopes that it can provide insight into novel therapeutic targets capable of ameliorating disease, expediting recovery from, and even possibly preventing infection. Our current knowledge of the epithelial cells role in response to *Cryptosporidium* will be reviewed here.

Infection of enterocyte by *Cryptosporidium*

Excystation and attachment

Transmission of *C. parvum* is fecal-oral, and outbreaks are typically waterborne (Putignani and Menichella, 2010). Infection occurs following ingestion of environmentally resistant, thick-walled, sporulated oocysts. Upon ingestion, the oocysts pass into the small intestinal tract and excyst in the presence of bile acids and salts to release infective sporozoites (Putignani and Menichella, 2010; Striepen, 2013). Once in contact with the intestinal epithelial apical membrane, sporozoites express proteins on their surface as well as within an apical collection of organelles (rhoptry, micronemes, and dense granules) that directly interact with surface receptors on the intestinal epithelial surface and mediate

attachment and subsequent invasion (Blackman and Bannister, 2001; Chen et al., 2004b). Although many of these proteins are uncharacterized, we do know that *C. parvum* expresses several surface proteoglycans. Examples include circumsporozoite-like glycoprotein (CSL), C-type lectins (CpClec), and elongation factor-1α (EF-1α), which can bind lectins (CSL and CpClec) and heparin sulfate (EF-1α) expressed on the epithelial surface (Bhalchandra et al., 2013; Inomata et al., 2015; Langer and Riggs, 1999; Langer et al., 2001; Ludington and Ward, 2016; Matsubayashi et al., 2013). Interestingly, in a study performed in Chinese Hamster Ovary (CHO) cells that varied only in their expression of heparin sulfate, it was determined that efficient invasion of sporozoites requires surface expression of heparin sulfate. The authors hypothesized that differential expression of heparin sulfate and other sulfated polysaccharides in hosts and throughout the length of the intestine might explain variability in *C. parvum*'s host or tissue tropism (Inomata et al., 2015). In contrast, there was a dose-dependent inhibition of *C. parvum* invasion in the presence of heparin (Inomata et al., 2015).

Upon sporozoite attachment, the host apical membrane protrudes and envelopes the parasite; this process is necessary for the establishment of *C. parvum* infection. The steps involved in membrane protrusion involves epithelial cytoskeletal rearrangement through the recruitment of host-actin (Elliott and Clark, 2000; Elliott et al., 2001; O'Hara et al., 2008), as well as redistribution of Na^+-glucose and water transport proteins, sodium-dependent-glucose co-transporter 1 (SGLT-1) and Aquaporin 1 (AQP1), respectively (Chen et al., 2005a). Recruitment of SGLT-1 and AQP1 facilitate water influx that is required for maximal apical membrane protrusion (Chen et al., 2005a). As expected, functional inhibition of AQP1 and SGLT1 significantly reduced *C. parvum* invasion, whereas the overexpression of AQP1

promoted invasion (Chen et al., 2005a). Once internalized, *C. parvum* resides within a unique, intracellular yet extracytoplasmic compartment known as the parasitophorous vacuole (PV) which is separated from the host cytoplasm by an electron dense junctional complex predominately composed of host-actin and actin-related proteins (Chen et al., 2004a; Elliott and Clark, 2000; Elliott et al., 2001). Host actin recruitment is dependent on Cdc42 GTPase activation; this process has been shown to be necessary for parasite invasion in a biliary epithelial (H69) model of infection (Chen et al., 2004a).

Intracellular development

Cryptosporidium spp. is an obligate intracellular parasite and therefore depends on the host epithelial cell for survival. For example, once enveloped by the host cell within the PV, *C. parvum* forms a feeder organelle at the parasite-host interface. The feeder organelle is unique to apicomplexans and, as the name suggests, it is hypothesized that this organelle allows *C. parvum* to siphon off essential nutrients and energy from the host cytosol (Bouzid et al., 2013; Zhang et al., 2015). This hypothesis was substantiated by a study that demonstrated that *C. parvum* localizes important transport proteins that are structurally similar to both cystic fibrosis conductance regulator (CFTR) chloride channel and other multidrug resistance protein family of ATP-binding cassette proteins, to this organelle (Perkins et al., 1999). Additionally, the parasite is equipped with its own L-lactate dehydrogenase, which is associated with the parasitophorous vacuole that aids *C. parvum* in ATP generation through lactate fermentation (Zhang et al., 2015). Two separate researchers have demonstrated that drug inhibition or morpholino knock-down of this enzyme decreased intracellular growth and development of *C. parvum* in an HCT-8 model of infection (Witola

et al., 2017; Zhang et al., 2015). Lastly, *C. parvum* actively scavenges low-density lipoprotein (LDL) cholesterol from the host enterocyte which also is thought to support its intracellular development. (Ehrenman et al., 2013).

Once infection is established, *C. parvum* undergoes multiple rounds of asexual (merogony) and sexual (gametogony) reproduction within the same host, ultimately resulting in the production of both thin-walled and thick-walled oocysts (Gookin et al., 2002; Putignani and Menichella, 2010). Thin-walled oocysts are involved in a cycle of autoinfection of intestinal epithelial cells whereas thick-walled oocysts are environmentally resistant and shed into the environment where they can eventually infect a new host (Gookin et al., 2002).

Pathogenesis of Cryptosporidial Diarrhea

C. parvum is considered a minimally invasive parasite that primarily infects the small intestine resulting in absorptive enterocyte loss and subsequent villus blunting crypt elongation, and malabsorptive diarrhea (Argenzio et al., 1990). Villous atrophy, in addition to crypt elongation, has been described in animal models during peak infection (day 3-5) in neonatal mice and piglets (Argenzio et al., 1990; Rasmussen and Healey, 1992). However, although epithelial changes are commonly observed, in some patients, diarrhea can result without many histopathologic changes, and it is believed that *C. parvum*-induced prostaglandins may be responsible. Upon infection, the intestinal mucosa produces both prostacyclin (PGI2) and prostaglandin E2 (PGE2). In vitro, *C. parvum* stimulates prostaglandin G/H synthase 2 production, and PGE_2 synthesis by intestinal epithelial cells (Argenzio et al., 1996; Laurent et al., 1998). Then PGE_2 can bind to prostaglandin receptors

on intestinal epithelial cells, ultimately enhancing chloride secretion via stimulation of chloride channels that are enriched in the intestinal crypts (e.g., CFTR) and by concurrently inhibiting NaCl absorption by the villus enterocytes. Supporting this mechanism, in a piglet model of infection, indomethacin, a prostaglandin synthesis inhibitor, restored normal NaCl absorption despite a significant loss of villous surface area (Argenzio et al., 1993). Together, enhanced secretion and decreased absorption results in profuse, watery diarrhea (Clark, 1999).

Barrier Function Loss through Modulation of Tight Junctions

Intestinal epithelial cells (IECs) form a confluent monolayer held together by a linked network of tight junctional proteins that impart both size and charge selectivity to the intercellular junctions and space. Collectively, tight junctional proteins form an important, selectively permeable barrier that functions to absorb water and nutrients as well as to prevent the translocation of pathogens or commensal bacteria, toxins, and antigens from the intestinal lumen to the systemic circulation. Although minimally invasive, *C. parvum* does decrease intestinal barrier function; this has been seen in naturally infected humans (Dagci et al., 2002; Goodgame et al., 1995; Zhang et al., 2000), and numerous animal models (Argenzio et al., 1990; Foster et al., 2012; Gookin et al., 2004; Hunt et al., 2002; Kumar et al., 2018; Zadrozny et al., 2006), as well as *in vitro* models of infection (Adams et al., 1994; Griffiths et al., 1994; Kumar et al., 2018; Planchon et al., 1994; Roche et al., 2000). A major pathway by which intestinal epithelial barrier defects occur is through disruption of epithelial tight junctional complexes. Tight junctional proteins play an important role in maintaining electrochemical gradients necessary for transcellular ion transport (Fromter and Diamond,

1972; Tang and Goodenough, 2003), and they facilitate paracellular diffusion of sodium and water. Despite their likely importance in *C. parvum* pathophysiology**,** less than a handful of papers have investigated *C. parvum*'s influence on tight junctional protein expression or distribution (Anbazhagi et al., 2007; Bartelt et al., 2016; de Sablet et al., 2016). While there is a consensus that *C. parvum* alters tight junctional proteins, there seems to be little agreement on which proteins are affected, likely due to the wide variety of models used and the inconsistency in which tight junctional proteins are investigated. Furthermore, we still know very little about the functional consequences of *C. parvum*-induced tight junctional disturbances.

The main groups of tight junctional proteins that have been investigated during *C. parvum* are claudins, zonula occludens 1 (ZO-1), and occludin. Claudin-2 protein was shown to be upregulated in a murine model of cryptosporidiosis (Bartelt et al., 2016). This finding could have relevance to the pathophysiology and resolution of cryptosporidial diarrhea, given that claudin-2 upregulation has been demonstrated to enhance diarrhea and mediate pathogen clearance during *Citrobacter rodentium* infection (Anbazhagi et al., 2007). In a separate study, claudin-4 protein expression was decreased in the face of infection (Kumar et al., 2018); alterations in the expression of other claudin proteins have not been identified (de Sablet et al., 2016; Kumar et al., 2018). It is possible that different species of *Cryptosporidium* target unique epithelial tight junctional proteins. For example, while studies using *C. parvum* did not observe changes in zonula occludens-1 (ZO-1) expression or localization, (Bartelt et al., 2016; de Sablet et al., 2016), another study using *C. andersoni* demonstrated disruptions in ZO-1 pericellular localization with redistribution to the cytoplasm (Buret et al., 2003). Although *C. parvum*'s influence on occludin has been

investigated in three different studies, the findings were descriptive and overall contradictory, even when using similar in vitro models (Bartelt et al., 2016; de Sablet et al., 2016; Kumar et al., 2018).

Some intestinal pathogens, like *Salmonella typhimurium*, non-selectively damage tight junctions by recruiting neutrophils to the site of infection, facilitating their paracellular movement and mucosal invasion and translocation (Kohler et al., 2007). Interestingly, while *Cryptosporidium* also promotes neutrophil influx to the intestinal mucosa (Gookin et al., 2004; Zadrozny et al., 2006), this influx has been linked to an increase in barrier function without having a significant influence on epithelial parasitism or villus atrophy (Gookin et al., 2004; Zadrozny et al., 2006).

Models of Cryptosporidiosis

A wide variety of *in vivo* and *in vitro* animal models have been employed to study *Cryptosporidium.* An overview of the most commonly used cell culture and animal models of cryptosporidiosis are summarized in Tables 1 and 2**.** Although the small intestine is considered the primary site of natural *Cryptosporidium* infection in humans and most immunocompetent animal models (Farthing, 2000), extra-intestinal cryptosporidiosis has been reported in immunocompromised humans (HIV/AIDs or CD40 ligand deficiency) and mouse models, with biliary cryptosporidiosis and occasionally colonic cryptosporidiosis being the most common extra-intestinal sites (Hayward et al., 1997; Mead et al., 1991; Reijasse et al., 2001; Stephens et al., 1999; Vakil et al., 1996).

Accordingly, *in vitro* cell culture models predominately consist of primary or transformed epithelial cells lines of intestinal, colonic, or biliary origin. Historically, colonic

adenocarcinoma cell lines, particularly the HCT-8 line, are most commonly used. They are known to harbor the largest burden of infection, which can be particularly useful in studies aimed at identifying novel therapeutics by performing high-throughput screening (Manjunatha et al., 2017; Meloni and Thompson, 1996; Upton et al., 1994; Zhang and Zhu, 2015). Overall, despite their frequent use in prior studies, the utility of cancerous cell lines is limited by the fact that they are not derived from the small intestine and are transformed. This fact raises particular concern when these cell lines are used to study host-pathogen interactions, as it is likely that these cancerous epithelial cells respond differently to *C. parvum* infection. Furthermore, *Cryptosporidium* undergoes both asexual and sexual development *in vivo*; however, most cell culture models only support asexual development (Aji et al., 1991; Flanigan et al., 1991).

In an effort to use more biologically relevant models to study *C. parvum*'s host-pathogen interactions, researchers have increased use of non-transformed or primary cell lines (e.g., FHs 74 Int. and IPEC-J2) or ex-vivo techniques (enteroids) to study *Cryptosporidium-epithelium* interactions (Mirhashemi et al., 2018; Varughese et al., 2014; Zhang et al., 2016). Alternatively, some researchers have recently attempted to enhance the utility of neoplastic cell lines (HCT-8 and Caco-2) by seeding cells onto 3-dimensional (3D) scaffolds composed of silk or polysulfone hollow fibers to allow for complete asexual and sexual development of *C. parvum*. These 3D models are equipped with a constant flow of nutrients and oxygen to help mimic normal intestinal circulation. Ultimately, as evidenced by significant oocyst "shedding" into the fiber lumen, such models did achieve the goal of *in vitro* propagation of *C. parvum* (DeCicco RePass et al., 2017; Morada et al., 2016). This methodological breakthrough is exciting and incredibly useful given that, before these

studies, long-term propagation of *C. parvum* was only achieved in large animal models of infection (calves, gnotobiotic pigs).

By far the most commonly utilized models of *Cryptosporidium parvum* infection are in mice; both immunocompromised and immunocompetent strains have been used. Mice are popular models because they can be genetically or therapeutically manipulated, and a wide range of murine-specific experimental reagents are available. While they are useful for answering certain questions and for investigating key signaling pathways, it is important to remember that they are unnatural hosts, being inherently resistant to *Cryptosporidium parvum*, and completely resistant to *Cryptosporidium hominis*, the two most common strains of *Cryptosporidium* causing human disease. Additionally, mice do not become diarrheic in the face of infection, making them unsuitable models to study mechanisms of or therapy for clinical disease.

Calves and piglets are superior animal models than mice given that they are natural hosts of infection and develop clinical signs of infection. For example, piglets develop clinical disease that is very similar to humans, characterized by villous atrophy, crypt hyperplasia and impaired sodium-glucose absorption (Argenzio et al., 1990; Farthing, 2000). Despite their relevance as a model, unfortunately, the use of piglets and calves in *Cryptosporidium* research is frequently precluded by the fact that they require large animal BSL-2 facilities, are expensive, and cannot be readily genetically or therapeutically manipulated.

Even though *C. hominis* is genetically similar to *C. parvum*, natural infections are host-restricted to humans (Xu et al., 2004). Experimental *C. hominis* infections are limited to gnotobiotic pigs and human intestinal cell culture models (Lee et al., 2017; Manjunatha et al.,

2017). Accordingly, as *C. parvum* is capable of infecting most mammalian species and a wide variety of cell lines, it is used as the infectious agent in the majority of cryptosporidiosis models.

Although the majority of the studies reviewed here used mice to study the immune response to *C. parvum*, it is important to reiterate that mice do fully recapitulate the disease seen in humans, and therefore are less powerful models than calves or piglets. Adult wild-type mice are resistant to *C. parvum* infection and, therefore, either neonatal or immunocompromised mouse models must be used (e.g. severe combined immunodeficiency disease (SCID), interferon-γ, STAT1 knockouts, and protein malnourished) (Bartelt et al., 2016; Benamrouz et al., 2012; Ehigiator et al., 2007; Griffiths et al., 1998; Rasmussen and Healey, 1992).

The literature also contains studies that utilized a variety of uncommon *Cryptosporidium* model species, including rats, hamsters, guinea pigs, lambs, primates, and immunocompromised (SCID) foals (Bjorneby et al., 1991; Chrisp et al., 1990; Gibson and Wagner, 1986; Miller et al., 1990; Rehg, 1995; Rossi et al., 1990; Tzipori et al., 1982).

Host epithelial responses to *Cryptosporidium parvum* infection

Understanding how the epithelial cell responds to *C. parvum* infection is vital because they represent the primary cellular site of infection. As such, they constitute the first line of defense against infection and have the ability to produce cytokines and antimicrobial peptides that can act directly to limit infection or indirectly mobilize other immune effect cells to the infection site.

Toll-like receptors and NF-kB

Unlike the adaptive immune system, the innate immune response is not specific, nor does it have memory. The innate immune system's strength lies in its ability to recognize and respond quickly to conserved portions of pathogens (pathogen associated molecular patterns or PAMPs). Toll-like receptors (TLR) are extra- and intracellular pathogen sensors that recognize PAMPs, and, when bound, they can quickly trigger an innate immune response (Chen et al., 2005b; Costa et al., 2011; Yang et al., 2015). More specifically, upon stimulation of most TLRs, a signaling cascade occurs that stimulates the innate adaptor protein MyD88 (TLR-3 is MyD88 independent), resulting in subsequent activation of the transcription factor, NF-κB, as well as other pro-inflammatory pathways. Nuclear translocation of NF-κB promotes the transcription of pro-inflammatory cytokines (e.g.TNF-α, IL-8), enzymes (e.g. iNOS and cyclooxygenase 2), antimicrobial peptides and miRNAs by the epithelial cells that are ultimately translated and secreted (Abal-Fabeiro et al., 2014; Abreu, 2010; Eckmann et al., 1993; Gookin et al., 2006; Hu et al., 2013; McClure and Massari, 2014; Zhou et al., 2012). Some of these epithelial-derived cytokines will be discussed in greater detail in the following sections.

The exact mechanisms by which TLRs promote epithelial defense against *C. parvum* are still poorly understood. Two extracellular TLRs, TLR2 and 4, which bind lipopeptides and lipopolysaccharide (LPS), respectively (Fusunyan et al., 2001; Yamamoto and Takeda, 2010), are upregulated during *C. parvum* infection in mice (Costa et al., 2011) and thought to recognize and initiate an immune response against *C. parvum,* at least in humans (cholangiocytes), mice and calves (Chen et al., 2005b; Chen et al., 2007; Costa et al., 2011; Hu et al., 2013; O'Hara et al., 2011; Yang et al., 2015). *C. parvum*-induced TLR4 stimulation

in human enterocytes and cholangiocytes *in vitro* resulted in secretion of exosomes that contained antimicrobials (Hu et al., 2013). Mice deficient in TLR4, that were infected with *C. parvum* by direct inoculation of oocysts into the gallbladder, developed exacerbated and more persistent infections compared to wild-type controls (O'Hara et al., 2011).

Interestingly, three studies have demonstrated that intraperitoneal or oral treatment of mice with TLR 3 and 9 agonists, Poly I: C and CpG, respectively, prior to orogastric infection with *C. parvum*, resulted in significant reductions in parasite burden (80-95% in one report that used CpG) (Barrier et al., 2006; Bartelt et al., 2016; Lantier et al., 2014). The epithelial defense-promoting effects of these TLR agonists was mainly attributed to promotion of IL-12, Type I, and II IFN production. The exact origin of these cytokines was not investigated; however immune cells, not epithelial cells, are considered the primary cellular sources. The possibility that these TLR agonists also promoted the newly discovered cytokine, Type III IFN (IFN-λ) was not investigated in these studies. Stimulation of a large number of TLRs on IECs has been demonstrated to promote Type III IFN production (Odendall et al., 2017). Accordingly, it is likely that IFN- λ played a role in these studies and impacted their results.

Finally, while most studies have demonstrated that TLR/NF-κB activation promotes epithelial clearance of *C. parvum*, NF-κB activation can also have the exact opposite effect. As a result of *C. parvum* infection, there is initial, severe loss of infected enterocytes via apoptosis (mediated by executioner caspase 3 activation) which ultimately results in villous atrophy. One study identified that following this initial loss of enterocytes, activated NF-κB promotes the production of the X-linked inhibitor of apoptosis (XIAP). As the name suggests, XIAP is then able to suppress further the loss of apoptotic cells by binding to and

promoting the degradation of activated/cleaved caspase-3 (Foster et al., 2012). This study identified a unique mechanism by which *C. parvum* can resist its own clearance.

iNOS, nitric oxide and the nitric oxide derivative, peroxynitrite

Inducible nitric oxide synthase (iNOS) is required for the formation of nitric oxide (NO) and promoted by NF-κB activation (Gookin et al., 2006). Intestinal epithelial cells are the primary producers of iNOS during *C. parvum* infection (Gookin et al., 2004; Leitch and He, 1999). Subsequent increased production of NO by the intestinal mucosa during *C. parvum* infection results in anti-microbial/anti-parasitic effects (Gookin et al., 2005; Leitch and He, 1999). Two research groups have investigated the *in vivo* significance of iNOS/NO expression during *C. parvum* infection (Gookin et al., 2005; Gookin et al., 2006; Gookin et al., 2004; Leitch and He, 1994, 1999). In one study, iNOS was systemically inhibited in *C. parvum*-infected neonatal BALB/c mice, blocking downstream NO production resulting in exacerbation *of C. parvum* infection (Leitch and He, 1999). In another study, iNOS was inhibited in neonatal pigs, resulting in enhanced epithelial parasitism and fecal oocyst shedding. These authors demonstrated that iNOS/NO's anti-*C. parvum* effects were in part due to localized production of peroxynitrite, a potent oxidant that forms when NO interacts with superoxide (Gookin et al., 2005).

Tumor Necrosis Factor-α (TNF-α)

Tumor necrosis factor-α (TNF-α) is an important pro-inflammatory cytokine mediator that has been shown to be vital for defense against intracellular infections, and has been shown to be increased during *C. parvum* infection in humans as well as in a variety of *in*

vitro, *ex vivo* and *in vivo* models (Kirkpatrick et al., 2006; Lacroix et al., 2001; Lean et al., 2006; Robinson et al., 2001; Seydel et al., 1998).However, there is also a study in humans that demonstrated that TNF-α induction may not always be a consistent feature of infection (Alcantara et al., 2003). In an *ex vivo* study, TNF-α production significantly increased in both human intestinal xenografts in SCID mice and wild-type infected mice during *C. parvum* infection (Seydel et al., 1998). The *in vivo* significance of TNF-α has been demonstrated in two separate studies; SCID mice treated with TNF-α neutralizing antibodies and TNF-α knockout mice were utilized. Both researchers found that depletion of TNF-α did not affect *C. parvum* susceptibility or disease outcome (Chen et al., 1993; Lean et al., 2006). This is in contrast to another study where IFN-ɣ knockout mice were treated with exogenous TNF-α, and they found that infection severity was ameliorated (Lacroix et al., 2001). While those findings were somewhat conflicting, some *in vitro* studies have had more consistent findings. For example, one study determined that pretreatment with exogenous TNF-α on HT-29 cell line inhibited *C. parvum* infection (Pollok et al., 2001). Another study of the human enterocyte line CMT-93, pre-treated with TNF-α, found that *C. parvum* invasion was inhibited in a dose-dependent manner (Lean et al., 2006). In summary, conflicting reports exist about the role of TNF-α on *C. parvum* infection; however, the variation in infection model may explain the disparate conclusions.

Antimicrobial peptides (AMPs)

Epithelial cells produce antimicrobial peptides (AMP), often packaged within exosomes or granules (e.g., specialized epithelial cells, paneth cells), as the first line of defense against a wide variety of pathogens, including *C. parvum* (Cobo and Chadee, 2013;

Hu et al., 2013). Stimulation of TLRs and other PRRs is thought to be the primary mechanism by which epithelial secretion of AMPs is enhanced (Hu et al., 2013). Of the many different AMPs that exist, β-defensin's role in epithelial defense against *C. parvum* is best characterized. Several studies have touched on the significance of β-defensins during *C. parvum* infection in humans, mice as well as in calves (Carryn et al., 2012; Chen et al., 2005b; Tarver et al., 1998; Zaalouk et al., 2004). One study quantified the expression of 3 different human β-defensins (hBD1-3) in a human colonic cell line (HT-29 cell line) and found that *C. parvum* induced differential expression of each defensin, specifically a partial reduction in hBD-1, an induction of hBD-2, and no effect on hBD-3 gene expression (Zaalouk et al., 2004). Exposure of *C. parvum* sporozoites to exogenous hBD-1 and hBD-2 prior to infection limited their ability to infect murine colonic cells (CMT-93) in *vitro* (Zaalouk et al., 2004). In a separate study, this direct antimicrobial effect of β-defensin 1 and 2 was enhanced when combined with a monoclonal antibody (Mab 3E2) that targets *C. parvum*'s apical complex and surface glycoprotein ligand CSL (Riggs et al., 1997).

Differential expression of β-defensins has also been described *in vivo*. *C. parvum* significantly downregulated constitutive expression of β-defensins in wild-type neonatal mice. Interestingly, this downregulation was partially rescued in IFN-γ KO mice, even thought they had higher burdens of infection, indicating that IFN-γ may be partially responsible for *C. parvum*'s ability to downregulate host defensin expression. Downregulation of AMPs may represent a conserved mechanism of host evasion for apicomplexans. For example, intestinal infection of mice with *Toxoplasma gondii* led to a dramatic decrease in lysozyme, defensin, and RegIII-γ production which was linked to an

IFN-γ dependent decrease in the number of paneth cells in the small intestine (Raetz et al., 2013).

Interleukin-8 (IL-8) and neutrophils

Interleukin-8 is a potent epithelium-derived neutrophil chemotactic agent shown to be significantly up-regulated in humans *in vivo* in *Cryptosporidium*-infected children, *ex vivo* in human intestinal xenograft models in SCID mice, and in vitro in human Caco-2 intestinal epithelial cells (Alcantara et al., 2003; Maillot et al., 2000; Seydel et al., 1998). Corresponding to this increase in IL-8, neutrophils have been shown to be increased in the intestinal mucosa of infected humans, as well neonatal piglets (Gookin et al., 2005; Seydel et al., 1998).

Furthermore, a study using a well-established neonatal piglet model of *C. parvum* quantified an increased influx of neutrophils into the small intestinal lamina propria during infection, as well as increased myeloperoxidase production (an indicator of neutrophil activation/degranulation) (Gookin et al., 2005). Inhibition of neutrophils influx (β-2 integrin, CD18 neutralizing antibodies) into the intestine did not alter *C. parvum* infection outcomes, ultimately indicating that neutrophil influx had no demonstrable impact on the severity of epithelial infection, villus atrophy or diarrhea. Nonetheless, inhibition of neutrophil influx did partially ameliorate the loss in barrier function that is typical of *C. parvum* infection (Gookin et al., 2005).

Host-derived MicroRNAs/ Parasite derived non-coding RNAs

Epithelial cells produce miRNAs in response to a wide-variety of pathogens, including *C. parvum* (Gong et al., 2011; Hu et al., 2013; Hu et al., 2010; Maudet et al., 2014; Piedade and Azevedo-Pereira, 2016). One study identified that a panel of miRNAs (mir-125b-1, mir-21, mir-30b, and mir-23b-27b-24-1) were up-regulated in infected human cholangiocytes (H69). Functional inhibition of some of these miRNAs resulted in an increased *C. parvum* burden (Zhou et al., 2009). To date, the predominant mechanisms by which miRNAs influence epithelial defense against *C. parvum* is by regulating secretion of antimicrobial products or by facilitating leukocyte adhesion and transmigration. For example, miR-27b stabilizes iNOS mRNA, ultimately facilitating NO production. However, in a separate study, downregulation of let-7 miRNAs promoted luminal exosome release from IECs; these exosomes contained antimicrobial peptides, beta-defensin 2, and LL-37 (Abal-Fabeiro et al., 2014). Infected intestinal epithelial cells also down-regulate miRNA-221, resulting in up-regulation of intercellular adhesion molecule 1(ICAM-1) and facilitation of T-lymphocyte adhesion (specifically Jurkat cell line) to infected epithelial cells (Gong et al., 2011). The majority of the work examining the significance of miRNAs during *C. parvum* infection has been conducted using a cholangiocyte model of infection. Given that intestinal epithelial cells are the most common site of infection, the influence of IEC miRNAs on *C. parvum* infection deserves to be explored.

Interestingly, although *C. parvum* does not possess the machinery to make miRNAs (Abrahamsen et al., 2004; Ming et al., 2017), it was recently discovered that during infection, *C. parvum* injects non-protein coding RNA's (ncRNAs) into epithelial cells which translocate to the host nucleus and influence epithelial gene expression. Specifically, these *C.*

parvum-derived RNAs have demonstrated ability to suppress the expression of host cadherin 3 (CDH3), also known as P-cadherin, lysyl-oxidase like 4 (LOXL4), β-defensin-1 (DEFB1), and DAZ-interacting zinc finger protein (DZ1P1). The transcriptional suppression of β-defensin-1 by *C. parvum* is particularly intriguing, given that, as mentioned earlier, β-defensins are thought to have anti-*C. parvum* potential (Zaalouk et al., 2004).

Interferons

Interferons (IFN) are secreted cytokines that are categorized into Types I-III. They are produced mainly in response to intracellular pathogens and are most well known for their ability to "interfere" with virus infection and replication, playing a critical role in anti-viral defense (Barakat et al., 2009b; Chen et al., 1993; Hayward et al., 2000; Pollok et al., 2001). Each type of IFN mediates their anti-pathogen effects by binding to and stimulating distinct heterodimeric receptors that ultimately lead to activation of the JAK/STAT pathway and upregulate the transcription of interferon-stimulated genes (ISGs) (Platanias, 2005).

Many intracellular pathogens can induce an IFN response in the intestine, including *C. parvum.* Specifically, Type I (IFN α/β) and Type II (IFN-γ) have been shown to play an important role during *C. parvum* infection (Barakat et al., 2009b; Chen et al., 1993; Hayward et al., 2000; Leav et al., 2005; Pollok et al., 2001), while role of the more recently described Type III IFN during *C. parvum* infection has not been described in the literature.

Type I interferon (Interferon-α/β)

To date, only one study has been published examining the role of IFN α/β during the *C. parvum* infection. This study examined IFN α/β significance both *in vitro* using murine rectal polypoid carcinoma cells (CMT-93) and human colonic adenocarcinoma cells (Caco-2) and *in vivo* in SCID mice treated with or without IFN α/β neutralizing antibodies. In both models, IFN-α/β mRNA was significantly up-regulated within 24 hours of C. parvum infection. When Caco-2 cells were primed with various isotypes of IFN-α and IFN-β before infection, there was significant inhibition of *C. parvum* parasite burden. *In vivo*, SCID mice were treated with IFN-α/β neutralizing antibodies before infection and the parasite burden increased drastically. This study was the first to identity an innate host response capable of defending IECs against *C. parvum* involving IFN-α/β (Barakat et al., 2009b).

Type II interferon (Interferon-γ)

Interferon-γ's role in *C. parvum* defense is perhaps the best studied among the different types of IFN. As for IFN α/β, it has been shown that IFN-γ mRNA is increased during *C. parvum* infection within the first 24 hours of infection (Leav et al., 2005). Many studies have identified that the presence or absence of IFN-γ is a key determinant of susceptibility and clinical outcome to cryptosporidiosis (Hayward et al., 2000). The line between innate and adaptive immune responses becomes slightly blurred when it comes to IFN-ɣ production during *C. parvum* infection because this cytokine plays an important role in both. Both, dendritic cells and CD8+ intraepithelial T lymphocytes, have been shown to be important sources of IFN-γ; however, the intestinal epithelium is also capable of producing and responding to IFN-γ in response to *C. parvum* (Leav et al., 2005; Pollok et al., 2001). In

one study, researchers infected IFN-γ-KO mice and found that mice either died or developed chronic *C. parvum* infections. They then went on to compare the cytokine response in both groups and found that wild-type neonatal mice up-regulated IFN-γ, IL-1, and TNF-α. However, in KO mice, TNF-α was not up-regulated. This outcome indicated that TNF-α production seems to be IFN-ɣ-dependent and that a loss in TNF-α production may be linked to increased susceptibility to infection (Lacroix et al., 2001). As discussed previously, studies have ascribed variable importance to TNF-α in *C. parvum* pathogenesis.

The importance of IFN-γ is further evidenced by the fact that SCID and IFN-γ knockout mice when treated with IFN-γ neutralizing antibodies, became increasingly susceptible to *C. parvum* infection (Chen et al., 1993; Leav et al., 2005). In another study, pre-treatment with IFN-γ of three different human enterocyte cell lines, each with varied expression of the IFN-γ receptor, induced resistance to *C. parvum* in a seemingly receptor-dependent fashion. This result indicates that IFN-γ, directly via its receptor, mediates the anti-*C. parvum* response, rather than having a direct anti-parasitic effect (Pollok et al., 2001). Overall, there seems to be a consensus that IFN- γ is vital for host resistance against and clearance of *C. parvum* infection.

Type III Interferon (Interferon-λ)

Type III IFN, also known as IFN-λ, is the most recently discovered group of IFNs. There are four main subtypes (λ 1-4). IFN-λ 1-3 genes were first described in 2003 (Kotenko et al., 2003a; Sheppard et al., 2003), and IFN-λ4 was first described in 2013 (Prokunina-Olsson et al., 2013). Across species, there is great variability in the presence or expression of certain IFN-λ genes. For example, IFN-λ1 is a pseudogene in mice, pigs do not have a gene

for IFN λ2, and mice lack an IFN-λ 4 gene (Coordinators, 2018). For humans, IFN-λ4 is unique in that it can be either a gene or pseudogene, depending on the absence or presence of a frameshift mutation capable of preventing the expression/secretion of IFN-λ4, respectively. The prevalence of this mutation in the human population is high, particularly in Asian (93%), African (63%) and European (23%) populations, indicating that it has likely undergone positive selection (Prokunina-Olsson et al., 2013). One explanation for this positive selection is that a failure to secrete IFN-λ4 has been linked to improved clearance of Hepatitis C virus (HCV). This seems somewhat counter-intuitive given that IFN-λ4 can stimulate weak anti-viral responses; however, these responses are ineffective at clearing HCV, and additionally, they decrease the responsiveness of cells to other more powerful Type I and Type III IFNs that are actually capable of clearing HCV (Hong et al., 2016; Prokunina-Olsson et al., 2013).

In the intestine, IFN-λ is primarily produced by IECs (Hernandez et al., 2015; Mahlakoiv et al., 2015; Pott et al., 2011), however dendritic cells, eosinophils and mast cells are also reported sources (Chen et al.; Chiriac et al., 2017; He et al., 2012; Raki et al., 2013). The production of IFN-λ can be induced in response to mucosal injury (Chiriac et al., 2017), as well as in response to viral and bacterial pathogens, typically through stimulation of PRRs (e.g., TLRs and RIG-I) (Odendall et al., 2014; Odendall et al., 2017). All TLRs have been shown to induce IFN-λ gene transcription in intestinal cells. However, stimulation of some TLRs (e.g., TLR 2 and 5) have been shown to induce it more strongly than others (Odendall et al., 2017). Pathogen stimulation of intracellular RIG-I receptors are also linked to Type III IFN expression; RIG-I activates mitochondrial antiviral signaling protein (MAVS) which is associated with either mitochondria or peroxisomes, resulting in stimulation of transcription factors linked to IFN production(Odendall et al., 2014; Seth et al., 2005). Interestingly,

MAVS associated with peroxisomes preferentially induces transcription factors that promote IFN-λ gene transcription, and peroxisome content in cells increases with differentiation and is linked to a cell's propensity to respond with a Type III response (Odendall et al., 2014). Transcription factors primarily responsible for Type III IFN gene transcription are NF-kB, and interferon regulator factors 1, 3, and 7 (IRF1,3,7) (Syedbasha and Egli, 2017); IRF1, in particular, has been shown to selectively induce Type III IFN over Type I IFN (Odendall et al., 2014; Siegel et al., 2011; Ueki et al., 2013).

After transcription, translation, and secretion, all subtypes of IFN-λ signal through the transmembranous, heterodimeric receptor composed of IFNλR1 and IL-10R2 chains and stimulate the JAK/STAT pathway. The IFNλR1 chain is specific to IFN- λ, whereas IL10R2 is shared with IL-10 (Kotenko et al., 2003a). Interferon-λ binds first to the IFNλR1 chain leading to recruitment of IL10R2 to the complex. Both receptor chains are directly associated with Janus tyrosine kinases, specifically Jak1 and Tyk2, which mediate phosphorylation of the intracellular domain of IFNλR1, allowing for docking and phosphorylation of Signal Transducer and Activator of Transcription 1 and 2 (STAT1/2) proteins. Subsequently, in the cytoplasm, STAT1 and 2 binds to IRF 9 to form the IFN-stimulated gene factor 3 (ISGF3) complex. This complex translocates to the nucleus and binds to specific nucleotide sequences called interferon-stimulated response elements (ISREs) present in the promoter region of interferon-stimulated genes (ISGs), ultimately leading to ISG transcription (Kotenko et al., 2003b; Sheppard et al., 2003; Syedbasha and Egli, 2017).

The intracellular signaling cascade for IFN-λ is identical to that of Type I IFN, and, as such, both cytokines induce largely overlapping ISG signatures (Witte et al., 2010; Zhou et al., 2007). Not surprisingly, researchers originally thought that IFN-λ's biological

functions were largely redundant to Type I IFN. However, we now know that type III responses predominately occur at mucosal/barrier sites like the respiratory, gastrointestinal and urogenital tracts, and the liver. This is primarily due to receptor distribution; the Type I IFN receptor (IFNAR) is expressed on most nucleated cell types whereas IFNλR is primarily expressed on epithelial cells at barrier/mucosal sites. Some myeloid cells also express IFNλR but still seem to have impaired responses to Type III IFN (Witte et al., 2009). Additionally, in one study, primary intestinal epithelial cells (enteroid culture) infected with an epitheliotropic virus, upregulated both Type I and Type III IFNs, but preferentially secreted IFN-λ. This finding provides further evidence that that Type III IFN response is likely the preferred response of epithelial cells (Pervolaraki et al., 2017).

The importance of IFN-λ for IEC anti-viral defense is now well-recognized and it's *in vivo* significance has been specifically demonstrated in the intestine in response to epitheliotropic viruses (e.g. norovirus, rotavirus, and reovirus) (Baldridge et al., 2017; Hernandez et al., 2015; Mahlakoiv et al., 2015; Pott et al., 2011). Murine norovirus induces IFN-λ expression by IECs and IFNλR signaling on epithelial cells is vital for clearing persistent infections (Baldridge et al., 2017). Rotavirus infection induces IFN-λ expression by IECs in both mice and in human enteroids (Hernandez et al., 2015; Pott et al., 2011; Saxena et al., 2017). Additionally, in mice, intact IFNλR and not Type I signaling, was able to promote clearance of rotavirus infection *in vivo* (Pott et al., 2011). However this IFNλR dependent control of rotavirus in vivo cannot be entirely attributed to IFN-λ, the innate lymphoid cell derived cytokine IL-22 was also found to also signal through IFNλR and act synergistically with IFN-λ to upregulated ISGs (Hernandez et al., 2015).

To conduct these studies, the majority of researchers have utilized a mouse model first created in 2008 that are genetically modified to lack the IFNλR1 chain (IFNλR1-/) (Ank et al., 2008). One study even specifically depleted IECs of IFNλR1 (Baldridge et al., 2017). As with any immunodeficient mouse model, one of the biggest challenges researchers face when using IFNλR1-/- mice is that they are inherently more susceptible to viral co-infections. One common co-infection that immunodeficient mice often face is the gastrointestinal virus, norovirus (Doom et al., 2009; Henderson, 2008); as such, researchers have to be extremely diligent when screening and housing IFNλR1-/- mice.

While IFN-λ, like other interferons types, are most well-known for their role in anti-viral defense, we are now learning that IFN-λ has a broader role for non-viral pathogen defense, barrier defense in the brain and the intestine, and intestinal mucosal healing. Only a handful of papers have investigated IFN-λ's role for non-viral pathogens. For example, *Mycobacterium tuberculosis*, *Listeria monocytogenes*, and *Salmonella typhimurium* have all been shown to induce IFN-λ (Bierne et al., 2012; Cohen and Prince, 2013; Lebreton et al., 2011; Travar et al., 2014). Additionally, IFN-λ signaling has demonstrated importance in defending against respiratory fungal infection, specifically *Aspergillus fumigatus* (Espinosa et al., 2017). To date, there are no published reports of IFN-λ expression or signaling importance in parasitic infection.

Like other IFN types, the expression of ISGs is thought to be the primary mechanism by which IFN-λ mediates pathogen defense (Hernandez et al., 2015; Schoggins, 2014; Zhou et al., 2007). However, only a few ISGs have a demonstrated role in non-viral pathogen defense: these include interferon-stimulated gene 15 (ISG15), guanylate binding protein 1 and 2 (GBP1 and 2), ubiquitin (UBD) and the Tripartite motif family 21 (TRIM21). One

study identified that *Listeria monocytogenes* infection induces ISG15 expression and has the capability of limiting infection burden both *in vitro* and *in vivo* (Radoshevich et al., 2015). ISG15 proteins are ubiquitin-like and can covalently bind to a wide variety of proteins and influence their expression or cellular distribution through a process called ISGylation (Zhang and Zhang, 2011). Accordingly, to identify the mechanism by which ISG15 limits *Listeria* infection, these researchers explored ISGylation targets using a proteomics approach. They found that ISG15 targeted endoplasmic reticulum (ER) and Golgi proteins which increased the pro-inflammatory cytokines that are known to counteract *Listeria* infection, IL-8, and IL-6 (Radoshevich et al., 2015). The other ISGs mentioned, UBD, GBP1, 2, and TRIM21, all work together to defend against intracellular pathogens that form parasitophorous vacuoles (PV). This mechanism has been best described in the context of the protozoal infection, *Toxoplasma gondii* (*T. gondii*). In response to intracellular *T. gondii* infection, TRIM21, an E3 ubiquitin ligase, is up-regulated, facilitating the ubiquitination of the PV membrane. The presence of ubiquitin then allows the GTPases GBP1 and 2 to bind. This combined process promotes the disruption of the PV, enhancing the exposure of the parasite to the immune mediators within the cytoplasm (Foltz et al., 2017; Haldar et al., 2015).

In addition to promoting pathogen clearance, IFN-λ can promote barrier integrity by tightening paracellular junctions. This barrier-promoting effect was demonstrated both in the presence and absence of infection in two separate studies, one at the level of the blood-brain barrier and the other in the intestine (Lazear et al., 2015; Odendall et al., 2017). In brain microvascular endothelial cells (BMECs), IFN-λ specifically promoted the relocalization of the tight junctional protein claudin-5 to the junctional complex. IFN-λ's influence on other tight junctions has not been investigated (Lazear et al., 2015). Furthermore, the exact

downstream mediators responsible for IFN-λ's barrier-promoting effect have not been investigated. The only ISG that has a known barrier promoting effect in the intestine is GBP1 (Schnoor et al., 2009). Upregulation of GBP1 was shown to localize specifically to the IEC tight junctional protein coxsackie-adenovirus receptor (CAR). Knockdown of GBP1 in IECs with small interfering RNA (siRNA) specifically decreased transepithelial electrical resistance (TEER) and enhanced fluorescein isothiocyanate (FITC)-labeled 4 kDa dextran permeability (Schnoor et al., 2009).

Lastly, IFN-λ upregulation also promotes mucosal defense in response to non-infectious intestinal diseases, like inflammatory bowel disease (IBD). Expression of IFN-λ subtypes is up-regulated in IBD patients. Additionally, mice with intact IFN-λ signaling experience less mucosal damage and colitis when exposed to chemical colitis inducers, dextran sulfate sodium (DSS) or oxazolone, when compared to IFNλR-/- mice. Additionally, *ex-vivo* treatment of murine enteroids with exogenous IFN-λ not only led to increased epithelial proliferation but also up-regulated several genes known to promote epithelial defense and wound healing (e.g. USP18, IRF7, APOLP, CXCL10). Overall, these findings indicate that IFN-λ signaling promotes mucosal healing in the face of non-infectious colitis (Chiriac et al., 2017).

Conclusions and Future Directions

In conclusion, the epithelial cell is critical for instigating and orchestrating an innate immune response to *Cryptosporidium parvum*. That being said, our current understanding of the epithelial cell's role in host defense during *Cryptosporidium* infection is predominately derived from studies that have taken a candidate gene/protein approach to identifying

epithelial-derived immune mediators. Additionally, these studies have utilized animal or cell culture models that do not fully recapitulate human disease (e.g. mice and neoplastic colonic epithelium, respectively). To date, only two studies, both published by the same research group, have taken a more global (transcriptomic) approach to investigating IEC responses to *Cryptosporidium*, both utilizing in vitro models of *C. parvum* infection (Mirhashemi et al., 2018; Yang et al., 2010). Their first study utilized microarray analysis of *C. parvum* infected HCT-8 cells and identified through gene ontology (GO) analysis that glycoprotein genes were among the most significantly upregulated; they then confirmed glycoproteins were increased and expressed on the surface of HCT-8s with immunofluorescence, however did not investigate the biological significance of glycoprotein upregulation for infected IECs (Yang et al., 2010). This research group's second study, performed 8 years later, took an almost identical approach however they utilized RNA-sequencing in IPEC-J2 cells. They found that 813 genes were differentially expressed during infection and identified through GO analysis that genes related to the spliceosome and cell cycle were among the most significantly enriched. Unfortunately, while taking a global approach is apt to identifying novel mechanisms of epithelial defense, these studies failed to perform more mechanistic experiments that provide more valuable feedback regarding the biological significance of the identified transcriptomic changes. Accordingly, there is a need for more mechanistic studies that take an unbiased, global approach to identifying important IEC mechanisms of defense. Additionally, there is a need for studies to take a global approach utilizing natural models of infection that effectively recapitulate human disease, for example, calves or piglets. The added benefit to using these animal models is that IECs would be influenced by signals coming from the underlying lamina propria, which are lacking in *in vitro* models.

Table 1. Summary of *in vitro/ex vivo Cryptosporidium* models

IN VITRO MODELS OF CRYPTOSPORIDIOSIS		
Transformed/neoplastic		
Cell-line	**Origin**	**Select reference(s)**
HCT-8	**Human adenocarcinoma**	**(Alcantara Warren et al., 2008; Manjunatha et al., 2017)**
Caco-2	**Human adenocarcinoma**	**(Griffiths et al., 1994)**
IEC (4.1 or 6)	**Rat small intestine**	**(Langer et al., 2001)**
CMT-93	**Mouse rectal polypoid carcinoma**	**(Barakat et al., 2009a)**
HT-29	**Human colorectal adenocarcinoma**	**(Meloni and Thompson, 1996)**
Non-transformed		
FHs 74 Int.	**Human small intestine**	**(Varughese et al., 2014)**
IPEC-J2	**Porcine jejunum**	**(Mirhashemi et al., 2018)**
Extra intestinal cell lines		
MDBK-II	**Bovine kidney**	**(Hamer et al., 1994)**
HepG2	**Human hepatocyte**	**(Cosyns et al., 1998)**
H69	**Human cholangiocyte**	**(Chen et al., 2005a; Chen et al., 2005b; Chen et al., 2007)**
***Ex vivo* models**		
Murine (SCID mouse) colonic explants on transwell inserts		**(Baydoun et al., 2017)**
Murine enteroids		**(Zhang et al., 2016)**
Human intestinal xenotransplants		**(Seydel et al., 1998)**

Table 2. Summary of *in vivo Cryptosporidium* models

LARGE ANIMAL MODELS	
Model	**Select reference (s)**
Calves	**(Manjunatha et al., 2017; Naciri et al., 1993)**
Piglets	**(Argenzio et al., 1990; Foster et al., 2011; Gookin et al., 2004)**
Gnotobiotic piglets	**(Lee et al., 2017; Pereira et al., 2002)**
SMALL ANIMAL MODELS	
Immunocompetent mice	
Adult mice	**(Garza et al., 2008)**
Neonatal mice	**(Hou et al., 2004; Lantier et al., 2014; Leitch and He, 1999)**
Immunocompromised mice	
SCID	**(Barakat et al., 2009b; Benamrouz et al., 2012; Perryman et al., 1993)**
T cell receptor deficient	**(Waters and Harp, 1996)**
B-cell deficient	**(Chen et al., 2003)**
RAG -/-	**(Lukin et al., 2000)**
IFN-γ -/-	**(Griffiths et al., 1998)**
TLR4 -/-	**(O'Hara et al., 2011)**
MyD88 -/-	**(Rogers et al., 2006)**
CD40-CD40L	**(Cosyns et al., 1998)**
Athymic nude	**(Heine et al., 1984)**
Germ-free/antibiotic treated	**(Harp et al., 1988)**
Dexamethasone treated	**(Rasmussen and Healey, 1992)**
Protein deficient	**(Bartelt et al., 2016) (Bartelt et al., 2016)**
Uncommon Animal Models	
Lamb	**(Anderson, 1982; Giles et al., 2001)**
Gnotobiotic lamb	**(Snodgrass et al., 1984)**
SCID Foal	**(Bjorneby et al., 1991)**
Neonatal rhesus macaques	**(Miller et al., 1990)**
Rabbit (adult/neonatal)	**(Mosier et al., 1997)**
Guinea pig	**(Chrisp et al., 1990)**

Table 2. Summary of *in vivo Cryptosporidium* models (continued)

Neonatal Rat	**(Capet et al., 1999; Khaldi et al., 2009; Topouchian et al., 2001)**
Immunocompromised Rat:	
Cyclophosphamide treated	**(Rehg et al., 1987)**
Steroid treated	**(Brasseur et al., 1994; Rehg, 1995)**
Hamster	**(Rossi et al., 1990)**

CHAPTER II

Interferon-λ promotes epithelial defense and barrier function against *Cryptosporidium parvum* infection

Sylvia H. Ferguson[1,4], Derek Foster[2,4], Barbara Sherry[3,4], Scott Magness[4,7,8], Dahlia M. Nielsen[5,6], Jody L. Gookin[1,2,4]

[1]Department of Clinical Sciences, College of Veterinary Medicine, North Carolina State University, Raleigh, North Carolina, USA

[2]Department of Population Health and Pathobiology, College of Veterinary Medicine, North Carolina State University, Raleigh, North Carolina, USA

[3]Department of Molecular Biomedical Sciences, College of Veterinary Medicine, North Carolina State University, Raleigh, North Carolina, USA

[4]Comparative Medicine Institute, College of Veterinary Medicine, North Carolina State University, Raleigh, North Carolina, USA

[5]Department of Biological Sciences, North Carolina State University, Raleigh, NC, USA

[6]Bioinformatics Research Center, North Carolina State University, Raleigh, NC, USA

[7]Department of Medicine, Division of Gastroenterology and Hepatology, University of North Carolina, Chapel Hill, NC, USA

[8]Joint Department of Biomedical Engineering, University of North Carolina, Chapel Hill, and North Carolina State University, Raleigh, North Carolina, USA.

Abstract

Background and Aims:

The epithelial response is critical for epithelial defense against *Cryptosporidium* but is poorly understood. To uncover the host strategy for defense against *Cryptosporidium*, we examined the transcriptional response of intestinal epithelial cells (IECs) to *C. parvum* in experimentally infected piglets by microarray. Upregulated genes were dominated by targets of interferon (IFN) and IFN-λ was significantly upregulated in infected piglet mucosa. While IFN-λ has been described as a mediator of epithelial defense against viral pathogens, there is limited knowledge of any role against non-viral pathogens. Accordingly, the aim of the study was to determine the significance of IFN-λ to epithelial defense and barrier function during *C. parvum* infection.

Methods:

The significance of *C. parvum* induced IFN-λ expression was determined using an immunoneutralization approach in neonatal C57BL/6 mice. Ability of the intestinal epithelium to upregulate IFN-λ expression in response to *C. parvum* infection and the influence of IFN-λ on epithelial defense against *C. parvum* invasion, intracellular development and loss of barrier function was examined using polarized, non-transformed porcine intestinal epithelial cell monolayers (IPEC-J2). Specifically, changes in barrier function were quantified by measurement of TEER and transepithelial flux studies.

Results:

Immunoneutralization of IFN-λ in *C. parvum* infected neonatal mice resulted in significantly increased parasite burden, fecal shedding, and villus blunting with crypt hyperplasia during peak infection. *In vitro*, *C. parvum* was sufficient to induce autonomous

IFN-λ and ISG15 expression by IECs. Priming of IEC with rHuIFN-λ promoted cellular defense against *C. parvum* infection and abrogated *C. parvum*-induced loss of barrier function by decreasing paracellular permeability to sodium.

Conclusions:

These studies identify IFN-λ as a key epithelial defense mechanism against *C. parvum* infection.

Introduction

Cryptosporidiosis causes unrelenting diarrhea in immunocompromised individuals worldwide and is the most common cause of infectious water and foodborne diarrheal outbreaks in the United States, resulting in an estimated 750,000 cases each year (Scallan et al., 2011). In developing countries, *Cryptosporidium* spp. is the second leading cause of infectious diarrheal death in children under the age of 5 years and results in approximately 200,000 deaths annually (Kotloff et al., 2013; Sow et al., 2016).

Cryptosporidium infection occurs by fecal-oral transmission of environmentally-resistant oocysts. After ingestion, oocysts release infective sporozoites that attach and become enveloped in the apical membrane of small intestinal villous intestinal epithelial cells (IEC) where they complete a complex and recurring life cycle. When *Cryptosporidium* infects the villus epithelial cells, they are rapidly shed resulting in profound villus blunting. In this condition, nutrient malabsorption, intestinal secretion, and failure of barrier function result in severe diarrhea, dehydration, starvation, and frequently death. Despite decades of research, there are currently no consistently effective treatments for cryptosporidiosis. Clearance of the pathogen and recovery from infection are reliant on a competent host response and access to supportive care. Use of more insightful therapies to promote recovery of individuals with cryptosporidiosis is hindered by a lack of understanding of how the intestinal epithelium favorably combats the infection.

To address this gap in understanding, we began our study by investigating the transcriptional response of *C. parvum* infected IECs in a robust model of cryptosporidiosis, the neonatal pig. We hypothesized that the IEC transcriptional signature would provide clues that would aid in identifying novel epithelial-derived mechanisms of innate immune

activation and host defense against *C. parvum* infection. Accordingly, we detected that IECs upregulate numerous interferon-stimulated genes during peak *Cryptosporidium* infection. By investigating the specific stimulus for this interferon response, we identified that *C. parvum* infection induces robust mucosal expression of a recently discovered Type III interferon, IFN-λ (Kotenko et al., 2003a; Sheppard et al., 2003).

There is mounting evidence that IFN-λ is a critical mediator for the innate protection of epithelia against viral infection (Nice et al., 2015; Pott et al., 2011). Additionally, IFN-λ has demonstrated extra-intestinal epithelial barrier protective effects in the face of viral infection (Lazear et al., 2015). However, to date, the role of IFN-λ in defense against non-viral enteric diarrheal pathogens or in promotion of intestinal epithelial barrier function has been limited to a single study (Odendall et al., 2017). Accordingly, the aim of this study was to determine the significance of IFN-λ expression to epithelial defense and barrier function during *C. parvum* infection.

Materials and Methods

Piglet Model of Cryptosporidiosis

One-day-old piglets were infected by orogastric gavage with 10^8 C. parvum oocysts (Bunchgrass Farms, Deary ID) on day 3 of life and samples were collected at peak infection 3–5 days later. Sections of ileum mucosa were collected for epithelial exfoliation (microarray), fixation in 10% neutral buffered formalin (histology), or embedded in optimal cutting temperature media and frozen in liquid nitrogen (*in situ* hybridization). All studies were approved by the Institutional Animal Care and Use Committee of North Carolina State University.

RNA Microarray

The intestinal epithelium was exfoliated from freshly obtained sections of uninfected control (n=4) and *C. parvum* infected (n=8) porcine ileum mucosa in an oxygenated chelation buffer containing 2.5 mM glucose and 10 mM EDTA as previously described (Gookin et al., 2006) and frozen at -80°C. Total RNA was isolated and treated with DNase (RNeasy Mini Kit; Qiagen, Germantown, MD) according to manufacturer instructions. RNA quantity and quality were determined by capillary electrophoresis (Agilent 2100 Bioanalyzer; Agilent Technologies, Santa Clara, CA). Fluorescently-labeled cDNA was prepared and hybridized to Affymetrix Porcine GeneChip microarrays by a commercial laboratory (Expression Analysis, Durham, NC). All GeneChips were scaled to a median intensity setting of 500. The arrays were first normalized with a Loess normalization technique using JMP Genomics (SAS), and analysis of gene expression changes was performed via analysis of variance. False discovery rates were calculated according to the methods of Storey (Storey, 2002) and a false discovery threshold of 0.05 was adopted in order to identify differentially

expressed genes. A two-fold change in gene expression from the control cells was the minimum change to be considered for further analysis. Lists of differentially expressed genes were further analyzed using Ingenuity Pathway Analysis (Ingenuity Systems, Redwood City, CA). Determination of enriched biological processes was determined by entering upregulated genes into the PANTHER database. Total RNA (2 μg) was converted into cDNA using Reverse Transcriptase (Enzo Biosciences, Farmingdale, NY) and a modified oligo(dT)24 primer that contains T7 promoter sequences (GenSet). After first strand synthesis, residual RNA was degraded by the addition of RNaseH and a double stranded cDNA molecule was generated using DNA Polymerase I and DNA Ligase. The cDNA was then purified and concentrated using a phenol: chloroform extraction followed by ethanol precipitation. The cDNA products were incubated with T7 RNA Polymerase and biotinylated ribonucleotides using an *In Vitro* Transcription kit (Affymetrix). The resultant cRNA product was purified using an RNeasy column (Qiagen) and quantified with a spectrophotometer. The cRNA target (20μg) was incubated at 94ºC for 35 minutes in fragmentation buffer (Tris, MgOAc, KOAc). The fragmented cRNA was diluted in hybridization buffer (MES, NaCl, EDTA, Tween 20, Herring Sperm DNA, Acetylated BSA) containing biotin-labeled OligoB2 and Eukaryotic Hybridization Controls (Affymetrix, Santa Clara, CA). The hybridization cocktail was denatured at 99°C for 5 minutes, incubated at 45°C for 5 minutes and then injected into an Affymetrix Porcine GeneChip cartridge. The GeneChip array was incubated at 42°C for at least 16 hours in a rotating oven at 60 rpm. GeneChips were washed 91 with a series of nonstringent (25°C) and stringent (50°C) solutions containing variable amounts of MES, Tween20 and SSPE. The microarrays were then stained with Streptavidin Phycoerythrin and the fluorescent signal was amplified using a biotinylated antibody solution. Fluorescent

images were detected in a GeneChip® Scanner 3000 and expression data was extracted using the GeneChip Command Console Software (AGCC) v 2.0 or later (Affymetrix, Santa Clara, CA).

Quantitative Histopathology

Formalin fixed sections of ileum mucosa were paraffin-embedded, sectioned at a thickness of 5-µm, and stained with hematoxylin and eosin. For each piglet, the average crypt depth and villus height was calculated from measurements of 5 well-oriented villus-crypt units using a brightfield microscope and ocular micrometer. The % infection was determined by dividing the number of infected villus enterocytes by the total number of villus enterocytes.

Fluorescence *In Situ* Hybridization

Custom probes designed for hybridization with porcine interferon stimulated gene 15 (ISG15) were purchased (Affymetrix, Santa Clara, CA). Probes were hybridized to formalin-fixed and paraffin embedded (FFPE) 5-µm sections of porcine ileum mucosa (ViewRNA in situ hybridization kit; Affymetrix, Santa Clara, CA) using the manufacturer protocol for 1-plex hybridization. Slides were deparaffinized using xylene (30 minutes) and heat and protease K pre-treated (10 and 30 minutes, respectively). Following initial hybridization, signal amplification was performed using pre-amplifier and amplifier probes using a slide hybridization and denaturation system (ThermoBrite;Leica Microsystem, Wetzlar, Germany). To detect the ISG15 target, slides were incubated with fast-red chromagen (1:30 dilution for 45 minutes), washed and coverslipped using mounting media containing DAPI (VECTASHIED antifade mounting medium with DAPI; Vector Labs, Burlingame, CA). Slides were imaged using a fluorescence microscope (Leica DB 5000B with LASX software;

Leica microsystems, Wetzlar, Germany). Rat ubiquitin (UBC) probes were hybridized to FFPE rat kidney slides as a hybridization control.

Immunoneutralization of IFN-λ2/3 in Neonatal Mouse Pups with Cryptosporidiosis

Conventional (specific pathogen-free which includes common gastrointestinal pathogens like norovirus, reovirus, rotavirus, *Citrobacter rodentium*, *Salmonella*, *Helicobacter*, and *Giardia*) C57BL/6 pregnant dams (embryonic day 13-15) were purchased (Charles River Laboratories, Durham, NC) and housed in accordance to Biosafety Level 2 guidelines. Litters were assigned to 1 of 4 treatment groups: 1) uninfected control mice treated with isotype (rat IgG) antibody, 2) uninfected control mice treated with rat anti-mouse IFN-λ2/3 immunoneutralizing antibody, 3) *C. parvum* infected mice treated with isotype (rat IgG) antibody, 4) *C. parvum* infected mice treated with rat anti-mouse IFN-λ2/3 immunoneutralizing antibody. Each mouse pup was administered either 15 μg of IFNλ2/3 neutralizing antibody (Monoclonal Rat IgG_{2B} Clone #244716) or 15 μg of rat IgG isotype control antibody (Monoclonal Rat IgG_{2B} Clone #141945, R and D Systems, Minneapolis, MN) by intraperitoneal injection on days -1, 0, and 3 of infection. The dose was calculated based on the quantity required to achieve 100% immunoneutralization of IFN-λ2/3 *in vitro* (ED100) and estimated blood volume of pups on day 10 of infection (day 14 of life). Pups were infected orogastrically with 2×10^5 oocysts of *C. parvum* in 10 μL of phosphate-buffered saline (PBS) using a 25 mm, plastic gavage needle (PETSURGICAL, Westlake Village, CA). During the 10-day course of infection, pups were weighed daily. Pups were euthanized using isofluorane anesthesia followed by decapitation. Immediately following euthanasia the gastrointestinal tract was removed from the abdominal cavity. A section of the small intestine extending from the distal jejunum to the proximal ileum was snap-frozen for

RNA extraction. The ileo-ceco-colic region of the intestine was formalin fixed and paraffin embedded, sectioned at a thickness of 5-µm, and stained with hematoxylin and eosin prior to quantifying the burden of epithelial infection and histomorphometry using light microscopy (Olympus Accu-scope 3025, Corporation, Tokyo, Japan). Digital images of well-oriented individual villus-crypt units were captured (Olympus cellSens software) at a magnification of 400×. The total number of epithelial cell-associated *Cryptosporidium* parasites were counted for each of 10 well-oriented villus-crypt units. Villus height and crypt depth measurements were obtained from each villus-crypt unit using Image J software.

RNA Extraction and Real-Time PCR Analysis

For RNA extraction from tissue, snap frozen samples of ileum mucosa (piglets) or total distal jejunum/proximal ileum (mice) were placed in ice cold lysis buffer, homogenized, and sonicated to disrupt the tissue. For RNA extraction from cell culture monolayers, media was removed and monolayers were washed 3 times with PBS, lysis buffer was applied directly to monolayers, and cells were scraped off inserts with a sterile cell lifter. Total RNA was extracted using a commercial kit (Ambion PureLink Mini kit; Thermo Fisher Scientific, Raleigh, NC) including DNAse treatment (Turbo DNA free kit, Thermo Fischer Scientific). RNA concentration and purity were quantified by spectrophotometry (Nanodrop ND-1000; Thermo Fisher Scientific). One µg of total RNA was converted to single-stranded cDNA by reverse transcription (high-capacity cDNA reverse transcription kit, ThermoFisher Scientific, *Waltham,* MA). Following reverse transcription, quantitative PCR was performed in a 15 µL reaction volume with 50 nM of each primer, 60 ng cDNA, and 2 × SYBR green Mastermix (Roche Diagnostics, Basel, Switzerland) using a Roche Lightcycler 480 for 50 cycles at 95°C for 15 s and 60°C for 1 min after an initial incubation for 10 min at 95°C. PCR products were

additionally examined following electrophoresis in 1.5% agarose gels stained with GelRed DNA stain (Biotium, Freemont, CA). The identity of amplicons was confirmed by expected size, melting temperature, and commercial sequencing (GeneWiz,South Plainfied, NJ). Comparative threshold cycle analysis was used as described in the LightCycler 480 user manual to calculate relative degree of changes. Expression of the following genes were targeted: *C. parvum* glycoprotein 40/15 (*Cp* gp40/15) porcine interferon-alpha (all isoforms, poIFN-α-all), porcine interferon-alpha isoforms 7/11 (poIFN-α-7/11), porcine interferon alpha isoform 9 (poIFN-α9), porcine IFN-beta (poIFN-β), porcine interferon-gamma (poIFN-γ), porcine interferon-lambda 1 (poIFN-λ1), porcine interferon-lambda 3 (poIFN-λ3,) porcine interferon-lambda 4 (poIFN-λ4), porcine interferon-lambda-receptor 1 (poIFN-λR1) porcine interferon stimulated gene 15 (poISG15), murine interferon-lambda2/3 (muIFN-λ2/3), murine interferon-beta (muIFN-β), and murine interferon stimulated gene 15 (muISG15). All primers were purchased from Integrated DNA technologies, Skokie, Illinois. Abundance of specific mRNA transcripts ($2^{-\Delta\Delta Ct}$) were calculated by normalization against expression of a housekeeping gene (porcine: cyclophilin, murine: GAPDH). Primer sequence data and references of origin are shown in Supplementary Table 1). Primers were designed either by the authors or as previously described.

Polarized Intestinal Epithelial Cell Culture Response to Cryptosporidiosis

Non-transformed porcine jejunal epithelial cells (IPEC-J2) were grown in co-culture media which included Dulbecco's minimal essential medium: Nutrient Mixture F-12 (DMEM/F12) supplemented with 5 µg/ml each of insulin, transferrin, and selenium, EGF (5 ng/ml), penicillin (50,000 IU/ml), streptomycin (50,000 mg/ml) and 5% porcine serum, and incubated at 37°C in 5% CO_2. Cells were seeded onto permeable polycarbonate filters (0.4

μm pore size, either 0.6 cm^2 or 4.67cm^2; Millipore, Burlington, MA) and cultured until confluent (Transepithelial Electrical Resistance (TEER) ≥ 2,000 Ω × 0.6 cm^2 or ≥ 1,300 Ω × 4.67 cm^2). TEER was measured using an EVOM2 epithelial voltohmmeter with chopstick electrodes (World Precision Instruments, Sarasota, FL). For immunofluorescence assessment of *C. parvum* burden, IPEC-J2 cells were seeded onto 8-well chamber slides (Nunc Lab-Tek II; Thermo Fisher, Raleigh, NC) and grown to confluence over a period of 3-4 days prior to use. IPEC-J2 cells were used at passage numbers 38-50. Media was changed every 3-4 days.

Infection of IPEC-J2 cells with *C. parvum*

Cryptosporidium parvum oocysts (Bunchgrass Farms, Deary, ID) were pelleted by centrifugation (13,000 x g for 3 minutes) and treated with 10 mM HCl (Millipore Sigma, St. Louis, MO) in PBS for 60 minutes in a 37° C water bath The oocysts were then pelleted by centrifugation to remove the HCl, reconstituted with 0.2 mM taurodeoxycholate and 22 mM NaHCO3 (Millipore Sigma, Millipore Sigma, St. Louis, MO) in PBS, and incubated for 30 minutes in a 37° C water bath to excyst infective sporozoites. The excysted oocysts were centrifuged and reconstituted in IPEC-J2 culture media. The number of excysted oocysts was counted using a hemacytometer to establish a final concentration of excysted oocysts. A multiplicity of infection of 2:1 of excysted oocysts to IPEC-J2 cells was used to inoculate monolayers. Based on established counts of approximately 5 x 10^5 IPEC-J2 cells per 30 mm (4.2 cm^2) insert at confluence, each monolayer was infected with 1 x 10^6 excysted oocysts.

Stimulation of IPEC-J2 cells with IFN-λ3

Monolayers of IPEC-J2 cells were treated at the time of confluence with 100-2500 U/mL of recombinant human interferon λ3 (rHuIFN-λ3) in PBS (PBL Assay Science, Piscataway, NJ). For determination of effects on *C. parvum* infection, cells were pretreated

with rHuIFN-λ3 beginning 12 hours prior to infection of the monolayer and sustained within the culture medium throughout the course of infection.

Crystal Violet Cytotoxicity Assay

Uninfected control and *C. parvum* infected IPEC-J2 cells were grown to confluence on 24-well polystyrene plates. At designated post-infection time intervals, epithelial monolayers were gently washed with PBS to remove detached epithelial cells, fixed with 2% paraformaldehyde in PBS for 15 min at RT, washed with HBSS, and stained with 100 µL of 0.13% crystal violet solution dissolved in a 5:2 (vol/vol) ethanol-paraformaldehyde solution. Monolayers were washed twice with dH_20 and allowed to air dry. Stained cells were solubilized in 100 µL 1% SDS in 50% ethanol and transferred to 96-well plates. The intensity of staining was quantified using a spectrophotometer at a wavelength of 570 nM with a reference wavelength of 650 nM to account for optical interference.

Epithelial Permeability Assays

IPEC-J2 monolayers were grown to confluence on 12-mm-diameter, 0.4 µm pore size polycarbonate filters. A subset of monolayers were infected with *C. parvum*, and the permeability of uninfected control and *C. parvum*-infected monolayers was measured at 24 and 48 hours post-infection by concurrent transepithelial passage of three permeability probes: creatinine, fluorescein isothiocyanoate-4 kDa dextran, and rhodamine-70 kDa dextran (R and D systems, Minneapolis, MN). Probes were prepared in cell culture media at a final concentration of 11 mg/mL. At the beginning of each flux period, 100 µL of the flux solution was added to the apical side of each insert to give a final volume and concentration of 500 µL and 2.2 mg/mL respectively. After 2 hours of incubation, basolateral recovery of each probe was measured in a plate reader (Synergy HT; BioTek, Winooski, VT) using

freshly prepared standards. Fluorescence of fluorescein and Rhodamine B were measured at 490 and 555 nm using emission wavelengths of 520 and 585 nm, respectively. Creatinine was measured separately using a colorimetric assay (Sigma Aldrich, Raleigh, NC).

Epithelial permeability to $^{22}Na^{+}$

Basolateral to apical isotopic flux studies of $^{22}Na^{+}$ (1 μCi/mL, Perkin Elmer, Waltham MA) was performed in uninfected control and *C. parvum* infected IPEC-J2 monolayers with or without pre-treatment with 1000 U/mL of rHuIFN-λ3 12 hours prior to infection. Barrier function (TEER) was measured at time points 6, 12, 24, 36, 48 hours over the course of infection. At 24 hours post-infection, a 50 μL aliquot of $^{22}Na+$ working stock was added to a 450 μL existing volume of basolateral media. Following a flux period of 2 hours, paired 200 μL samples were obtained from both the apical and basolateral compartments. Sample emissions were counted using a gamma counter (Perkin Elmer Wallac Wizard 1470-020, Waltham, Massachusetts) and basolateral to apical flux of Na^{+} was calculated using standard equations.

Determination of IFN-λ Effects on *C. parvum* Burden and Intracellular Development in Epithelial Monolayers

IPEC-J2 cells were cultured to confluency (3-4 days) in 8 well chamber slides and treated or not with 1000 U/mL of rHuIFN-λ3 for 12 hours prior to infection with *C. parvum* or vehicle (0.1% BSA in PBS). At 4, 6, 12, 24, and 48 hours post-infection, slides were washed 3 times with PBS and fixed with 4% paraformaldehyde for 10 minutes at RT. Following fixation, cells were washed 3 times with PBS, incubated in a blocking solution of 1% BSA in PBS for 30 minutes, and permeabilized for 5 minutes with 0.5% Triton X-100 in PBS at room temperature and then washed once with PBS for 30 seconds. To visualize epithelial invasion sites of *C. parvum* organisms, slides were incubated with a red fluorescent

phalloidin conjugate (Acti-stain 555 phalloidin; Cytoskeleton, Inc., Denver, CO) at a concentration of 100 nM at RT for 30 minutes. The monolayers were then washed 3 times with PBS. For simultaneous visualization of *C. parvum* organisms, monolayers were subsequently incubated at RT for 45 minutes with a FITC-labeled rat anti-*Cryptosporidium* parvum polyclonal antibody (1X Sporo-Glo;Waterborne, Inc., New Orleans, LA). Finally, monolayers were washed 3 times with PBS, partially air-dried and then cover slipped with mounting media containing DAPI (VECTASHIELD antifade mounting medium with DAPI; Vector Labs, Burlingame, CA). Monolayers were imaged using a fluorescence microscope (Leica DMB5000B with LASX software; Leica microsystems, Wetzlar, Germany). Quantification of *C. parvum* burden was determined by counting the total number of FITC-labeled parasites that were also associated with characteristic F-actin invasion sites within 10, 400× fields per infected well. For characterization of life stages present, attached parasites were measured using LASX software (Leica microsystems, Wetzlar, Germany) in 5 individual 1000× fields per well and categorized as either sporozoite (~4 × 1 µm, elongate, eccentric F-actin invasion site), early trophozoite (≤1 × 1 to 2 × 2 µm, round, centralized F-actin invasion site), trophozoite (2 ×2 to 3 × 3 µm, round, centralized F-actin invasion site), or meront (<3 × 3 cm, round, often with multiple nuclei visible).

Data Analysis

Data were tested for normal distribution and variance and analyzed using parametric or nonparametric statistics as appropriate (SigmaStat; Jandel Scientific, San Rafael, CA). Parametric data were analyzed using Student's *t* tests. Nonparametric data were analyzed using Mann–Whitney or Kruskal-Wallis rank sumand Wilcoxon signed rank tests. Differences in proportion of observations between groups was analyzed using Chi-square

tests. Data represent means ± SEM. For all analyses, $P \leq 0.05$ was considered significant. All authors had access to the study data and reviewed and approved the final manuscript.

Results

The intestinal epithelial transcriptional response to *C. parvum* infection *in vivo* is dominated by targets of interferon signaling.

Our understanding of host strategy for epithelial defense against infection by *C. parvum* remains poorly understood. In an effort to distinctively characterize the innate response of the intestinal epithelium to *C. parvum* infection we utilized a host species that fully reproduces the diarrheal disease as observed in children with cryptosporidiosis (Argenzio et al., 1990). Accordingly, we infected neonatal piglets with *C. parvum* and harvested the ileal epithelium at peak infection (days 3-5) for microarray analysis of the IEC transcriptional response. Piglets that were selected had a heavy burden of infection (57 ± 8.0% of villus enterocytes harbored *C. parvum*) and demonstrated marked villus blunting when compared to control piglets (P=0.004)(Figure 1A,B). Based on the microarray analysis, 61 genes were significantly upregulated and 21 genes significantly downregulated in IEC from *C. parvum* infected compared to control piglets (Table 1). Gene ontology analysis identified Type I interferon signaling (~25 fold, P<0.001) as the most enriched biological process in IEC from infected piglets. Twelve (20%) of the 61 significantly upregulated genes were identified as targets of interferon signaling including interferon stimulated gene 15 (ISG15), guanylate binding protein 1 and 2 (GBP1 and GBP2), proteasome subunit-β type 8 (PSMB8), interferon-α inducible protein 27 (IF127), interferon stimulated gene 20 (ISG20), calcium-binding and coiled-coil domain-2 (CALCOCO2), CXC motif chemokine ligand 16 (CXCL16), tripartite motif containing 34 (TRIM34), ubiquitin D (UBD), placenta specific gene 8 (PLAC8), and ribonuclease 4 (RNASE4). The gene identified as most highly expressed in response to *C. parvum* infection was ISG15 (21-fold). Significantly increased mucosal expression of ISG15 mRNA *in vivo* was additionally confirmed by targeted qPCR.

To further localize cellular ISG15 expression in context of the entire ileum mucosa, fluorescence in situ hybridization was performed on uninfected control and *C. parvum* infected piglet ileum using custom-designed anti-porcine ISG15 oligonucleotide probes. Interferon stimulated gene 15 mRNA was expressed predominately in the villous intestinal epithelial cells in infected piglets (Figure 1C).

Cryptosporidium parvum infection significantly increases _in vivo_ expression of the Type III interferon, IFN-λ3.

Having identified that targets of interferon signaling constitute a major transcriptional response of the intestinal epithelium to *C. parvum* infection, we sought to determine what type(s) of interferon were likely stimulating this response *in vivo*. Accordingly, we used our own and published primers to quantify, by means of qRT-PCR, specific members of all three classes of interferon (Type I-III) using RNA extracted from the ileum mucosa. There was no difference in expression of Type I interferon (i.e. IFN-α and IFN-β) observed between ileum mucosa of uninfected control and *C. parvum* infected piglets. Type II interferon (IFN-γ) expression was upregulated approximately 20-fold. However, Type III interferon, specifically IFN-λ3, was increased over 200-fold in the ileum mucosa of infected piglets (Figure 2).

A Type III interferon response is conserved in suckling mice infected with _C. parvum_.

To further investigate the mechanistic relationship between *C. parvum* infection, transcription of IFN-λ3, and increased expression of interferon-stimulated genes by the intestinal epithelium *in vivo*, we first sought to establish whether these observations were conserved in a mouse model. For these studies we used wild-type neonatal suckling mice due

to their innate susceptibility to infection and its associated intestinal pathology. Over a 10 day time-course of infection, wild-type pups exhibited peaks in colonic content of *C. parvum* mRNA, ileum IEC-associated *C. parvum* organisms, and histological indices of intestinal injury (villus blunting and crypt elongation) between 4-6 days post-infection, with clearance typically occurring by day 10 (Figure 3A-D). At peak infection, expression of IFN-λ2/3 and ISG15 mRNA was significantly increased in total distal jejunum/proximal ileum samples from *C. parvum* infected compared to uninfected mouse pups (Figure 3E).

Immunoneutralization of IFN-λ2/3 increases severity of epithelial infection and mucosal injury in suckling mice infected with *C. parvum*.

To determine the impact of IFN-λ on host defense against *C. parvum* infection, neonatal mouse pups were treated parenterally with human anti-mouse IFN-λ2/3 immunoneutralizing versus isotype control antibodies on days –1, 0, and 3 of *C. parvum* infection. As assessed at the time of peak infection (days 4-6), pups treated with anti-IFN-λ 2/3 antibodies had a significantly greater number of organisms infecting the villous IEC (Figure 4A) and were more likely to shed *C. parvum* in feces (19/20; 95%) compared to pups treated with isotype control antibodies (13/19; 68%), although the quantity of *C. parvum* shed in the feces was similar between the treatment groups (Figure 4B). When examined during the recovery stage of infection (day 10), pups treated with anti-IFN-λ2/3 antibodies had retained greater numbers of organisms infecting the villous epithelium (Figure 4C) and continued to shed *C. parvum* in feces and in significantly greater quantities compared to mice treated with isotype control antibodies (Figure 4D). In addition to a more severe epithelial burden and prolonged fecal shedding of *C. parvum*, pups treated with anti-IFN-λ2/3

antibodies had quantitatively greater villus blunting and crypt elongation compared to infected pups treated only with the isotype control antibody (Figure 4E-G).

Intestinal epithelial cells are sufficient to serve as a source of IFN-λ and -β and autonomously mediate an interferon response to *C. parvum* infection

Having demonstrated a significant and specific influence of IFN-λ in promoting intestinal defense against *C. parvum* in immunoneutralized mouse pups, we sought to next determine the direct involvement of the intestinal epithelium in mediating the interferon response to infection. These studies were performed using a non-transformed porcine-derived small intestinal epithelial cell line (IPEC-J2) as a reductionist model for comparative studies to the neonatal piglets. We first confirmed that IPEC-J2 cells constitutively express IFN-λR1 mRNA by means of RT-PCR (Figure 5A). We subsequently examined functionality of the receptor to stimulation using recombinant human IFN-λ3 (rHuIFN-λ3). Treatment of polarized IPEC-J2 cell monolayers with rHuIFN-λ3 resulted in a dose and time-dependent induction of ISG15 mRNA expression that peaked at a concentration of 1000 U/mL at 24 hours post-stimulation (Figure 5B). Other studies have demonstrated that epithelial cells express IFN-λ in response to viral infection (Nice et al., 2015; Pott et al., 2011), however few studies have examined whether or not this response occurs with non-viral pathogens (Bierne et al., 2012; Lebreton et al., 2011; Travar et al., 2014). To determine if *C. parvum* infection is sufficient to induce a Type III interferon response by the intestinal epithelium, we infected polarized monolayers of IPEC-J2 cells with *C. parvum* and quantified expression of IFN-λ3 and ISG15 mRNA over a 48 hour time course using qRT-PCR (Figure 6). The burden of *C. parvum* infection oscillated over time within the monolayers, as reflective of the phasic nature of the life cycle (Bouzid et al., 2013) and was accompanied by a significant decrease

in transepithelial electrical resistance (TEER) beginning at 24 hours after infection (Figure 6A-B). The epithelial infection was associated with a significant increase in expression of IFN-λ3 mRNA beginning at 24 hours followed by a significant increase in expression of ISG15 mRNA beginning at 36 hours post infection (Figure 6C-D). To determine if *C. parvum* stimulated the expression of other types of interferon that could also contribute to the observed ISG15 response, qRT-PCR was used to also quantify Type I and II interferon (supplementary Figure 1). Apart from IFN- λ, significant increases in expression was also observed for IFN-β beginning 24 hours after infection. Significant increases in expression of IFN-α were not observed at any time point post-infection, despite the use of published primer pairs designed to amplify all of the known isoforms of porcine IFN-α (Sang et al., 2010b). Amplification of IFN-γ was not observed in either control or *C. parvum* infected IPEC-J2 cells at any time point.

Intestinal epithelial cells primed with IFN-λ have enhanced resistance to *C. parvum* infection and improved barrier function

To determine if the intestinal epithelium is sufficient to mediate the anti-cryptosporidial and mucosal protective effects of IFN-λ, as observed to be impaired in immunoneutralized mice, we primed intestinal epithelial monolayers with rHuIFN-λ3 for 12 hours prior to introduction of *C. parvum*, thereby enabling the peak interferon response (e.g. ISG15 upregulation) to coincide with establishment of cellular *C. parvum* infection (12-24 hours post-infection). A dose-response increase in ISG15 mRNA expression was observed in *C. parvum* infected intestinal epithelial monolayers that were primed with exogenous rHuIFN-λ3 (range, 100 to 2500 U/ml) (Figure 7A). Priming of monolayers with rHuIFN-λ3 was accompanied by correspondingly significant inhibitory effects on *C. parvum* infection

burden (Figure 7B). Percent inhibition of *C. parvum* burden was positively correlated to upregulation of ISG15 expression (Pearson's correlation coefficient R=0.574, P=0.0082). In addition to promoting epithelial defense against infection, rHuIFN-λ3 priming significantly abrogated *C. parvum*-associated loss of TEER at concentrations ranging from 500 to 1000 U/ml. This barrier protective effect waned in cells treated with a higher dose of rHuIFN-λ3 (i.e. 2500 U/mL) (Figure 7C) and was not observed in monolayers not infected with *C. parvum* (Figure 7D). Importantly, neither *C. parvum* nor rHuIFN-λ3 alone, or in combination, resulted in loss of epithelial cells from treated monolayers (supplementary Figure 2), suggesting that IFN-λ enhanced defense against *C. parvum* using effector mechanisms contained within the intact monolayer.

Interferon-λ decreases *C. parvum* invasion of IEC and disrupts early intracellular development

To gain additional insight into the cell-based mechanism(s) by which IFN-λ promotes epithelial defense against *C. parvum* infection, we quantified the influence of rHuIFN-λ3 priming (1000 U/ml) on subsequent parasite invasion and cell-associated development. For these studies, infected epithelial monolayers were treated with a FITC-labeled anti-*Cryptosporidium* spp. antibody and counterstained with DAPI. Recruitment of host-F-actin to cell-associated *Cryptosporidium* spp. (Elliott and Clark, 2000; Elliott et al., 2001) organisms was used to identify host-parasite invasion sites and the associated intracellular life stages were identified on the basis of organism size and number of nuclei. Significant inhibitory effects of rHuIFN-λ3 on visualized *C. parvum* invasion occurred within 12 hours of infection (Figure 8A). The magnitude of inhibition of *C. parvum* invasion was similar to earlier indirect measurements of infection burden based on qRT-PCR for *C. parvum* gp40/15 after

priming of IPEC-J2 cells with rHuIFN-λ3 (Figure 7). In unprimed cells, *C. parvum* was observed to develop through an orderly progression of intracellular life stages over 48 hours. However, in rHuIFN-λ3-primed cells, a delay in maturation of *C. parvum* was observed as early as 6 hours post-infection with persistence of sporozoites and early trophozoites within the monolayers (Figure 9B-C). By 12 hours post-infection, rHuIFN-λ3-primed monolayers resumed a distribution of life stages similar to unprimed cells but with 30% less parasites suggesting loss of developmentally delayed sporozoites and early trophozoites from rHuIFN-λ3-treated monolayers.

Interferon-λ mitigates loss of barrier function by decreasing paracellular sodium conductance of *C. parvum* infected epithelium

To further characterize the mechanism by which priming of epithelial monolayers with rHuIFN-λ ameliorates subsequent loss of TEER associated with *C. parvum* infection, we conducted studies to define the nature of the barrier function defect. Having established, by means of crystal violet retention, that decreases in TEER were not associated with loss of cells from the monolayer, we focused on examination of the leak, pore, and ion/charge selective pathways which are governed by the modification of tight junctional proteins (Colegio et al., 2002; Shen et al., 2011; Tsai et al., 2017; Turner, 2009). Accordingly, we probed the pathway by which *C. parvum* and IFN-λ influence barrier function by measuring the transepithelial flux of 70-kDa dextran, 4-kDa dextran, creatinine, and $^{22}Na^{+}$. At the time of peak *C. parvum*-induced decreases in TEER, there was no significant difference in the transepithelial flux of 70-kDa dextran, 4-kDa dextran, or creatinine across *C. parvum* infected compared to uninfected monolayers. The only probe identified as corresponding to changes in TEER was a significant increase in the flux of $^{22}Na^{+}$ (Figure 9A-B). Moreover, in

C. parvum infected monolayers, the mitigating effect of rHuIFN-λ3 on loss of TEER was similarly associated with a significant decrease in the transepithelial flux of $^{22}Na^{+}$ (Figure 9C-D). A univariate non-linear regression using the least squares method was used to determine the relationship between TEER and $^{22}Na^{+}$ conductance across all treatment groups (uninfected versus infected) and conditions (rHuIFN-λ versus vehicle) identified a statistically significant, inverse relationship (correlation matrix of -0.83, $P<0.0001$) (Figure 9E).

Discussion

By interrogating intestinal epithelial cell (IEC) defense strategies against C. parvum, these studies have identified that Type III interferon, IFN-λ, is a conserved innate mediator of epithelial defense against this significant protozoal pathogen. We examined the significance of IFN-λ and specific mechanisms by which IFN-λ influences epithelial defense against *C. parvum* using three different models of infection, the neonatal piglet, suckling mouse, and non-transformed porcine intestinal epithelial cell monolayers (IPEC-J2). Results of these studies demonstrate that IFN-λ directly promotes epithelial resistance to parasite invasion and abrogates the loss of barrier function caused by *C. parvum* infection. While there is a wealth of literature supporting the role of IFN-λ in defending mucosal sites against viral pathogens (Mahlakoiv et al., 2015; Nice et al., 2015; Pott et al., 2011), few studies have suggested a broader role for IFN-λ in mucosal defense against non-viral pathogens (Bierne et al., 2012; Cohen and Prince, 2013; Odendall et al., 2017). To our knowledge, this is the first report demonstrating the importance of IFN-λ in epithelial defense against a protozoal infection.

Cryptosporidium spp. is a minimally invasive epithelial pathogen that can be cleared in an immunocompetent host through an immune response largely instigated by the IECs (O'Hara et al., 2011). Accordingly, we hypothesized that the transcriptional responses of IEC to *C. parvum in vivo* would provide key insights into how a competent host effectively resolves infection. Using a piglet model that uniquely recapitulates childhood cryptosporidiosis (Argenzio et al., 1990) and microarray analysis to quantify gene expression by IECs obtained from the ileum of control and infected animals, we identified that the prevailing transcriptional response of IECs to C. parvum is to upregulate gene targets of

interferon signaling. In situ localization of ISG15 mRNA to the villous IECs of *C. parvum* infected piglets supported that the IFN-response was enriched within the epithelium. Among the significantly upregulated interferon-stimulated genes, ISG15, is most well-known for its ability to promote anti-viral defense by directly disrupting viral replication, budding, and release (Kuang et al., 2011; Malakhova and Zhang, 2008; Okumura et al., 2006; Okumura et al., 2008; Pincetic et al., 2010). While we know that ISG15 is upregulated during *Leishmania brazilensis* and *Theileria annulata* infections, we still have limited knowledge of its function in anti-parasitic defense (Oura et al., 2006; Vargas-Inchaustegui et al., 2008). Guanylate binding protein 1 (GBP1), GBP2, and TRIM34 were also significantly upregulated during *C. parvum* infection; these genes have known functions in promoting host defense against non-viral pathogens, including protozoa. For example, in response to *Toxoplasma*, *Salmonella typhimurium*, and *Legionella* infection of IECs, GBP1 and 2, and TRIM family proteins, are recruited to the pathogen-host interface, specifically the parasitophorous vacuole (PV) (Feeley et al., 2017; Foltz et al., 2017; Meunier et al., 2014). Their recruitment ultimately promotes PV disruption, enhances exposure to host-immune responses, and facilitates pathogen clearance (Meunier et al., 2014). As PV formation is a hallmark feature of *C. parvum* interface with host IEC (Huang et al., 2004; Zhang et al., 2015), it is probable that upregulation of these particular genes represents a conserved mechanism of epithelial defense that may be similarly effective against *C. parvum*.

Upon investigating *C. parvum* infected piglet ileum mucosa for the source of an epithelial-targeted interferon response, we determined that Type I interferons (IFN-α and IFN-β) were not upregulated during peak infection. However, there was significantly-induced expression of a novel Type III interferon, IFN-λ3 (200-fold). Mucosal expression of Type II

interferon (IFN-γ), long recognized as an indispensable immune cell-derived cytokine associated with *C. parvum* infection, was also upregulated although to a log-fold lesser degree than IFN-λ. Expression of IFN-λ3 in response to *C. parvum* infection has not been previously described, nor has IFN-λ been demonstrated to influence the *in vivo* pathogenesis of a non-viral infection. Accordingly, identification of IFN-λ3 expression in cryptosporidiosis is a remarkable finding. Until recently, IFN-λ was considered to be largely redundant to the cellular effects of Type I interferon. However, it is now recognized that IFN-λ receptors are selectively expressed by IEC resulting in an epithelial-targeted mucosal immune response that plays a decisive role in the clearance of epitheliotropic viruses such as rotavirus, norovirus, and reovirus (Baldridge et al., 2017; Hernandez et al., 2015; Mahlakoiv et al., 2015; Mordstein et al., 2010a; Mordstein et al., 2010b; Nice et al., 2015; Pott et al., 2011). In light of this knowledge, our findings suggest that *C. parvum* likewise stimulates an epithelial targeted interferon response that is mediated, at least in part, by IFN-λ.

To test a hypothesis that IFN-λ contributes specifically to epithelial defense against *C. parvum* infection, we utilized a neonatal mouse model of the infection which enabled immunological manipulation of IFN-λ signaling. The use of IFN-λR1 knock-out mice was considered a superior approach for these studies, however their use was repeatedly precluded by pre-screening diagnosis of norovirus infection (Doom et al., 2009). In mice, norovirus stimulates a Type III interferon response that is critical for mediating viral clearance (Nice et al., 2015) and we expected this would confound interpretation of this study. Consequently, we obtained pregnant C57BL/6 wild-type mice that were established to be specific pathogen free from murine norovirus as well as other common, and potentially confounding, gastrointestinal co-infections. We subsequently infected the neonatal mouse pups with *C.*

parvum and confirmed conserved upregulation of IFN-λ during peak-infection. We then infected pups with or without pre-infection systemic immunoneutralization of IFN-λ2/3. Compared to mice treated with an isotype control antibody, mice receiving anti-mouse IFN-λ2/3 immunoneutralizing antibody harbored a significantly larger number of epithelial parasites, developed more severe villous blunting and crypt hyperplasia, and were more likely to shed *C. parvum* and for a longer period of time. These findings strongly support a significant and specific influence of IFN-λ in promoting epithelial defense against *C. parvum* infection.

In response to viral pathogens, IECs are not only a target of IFN-λ, but also serve as a significant source of the cytokine (Hernandez et al., 2015; Mahlakoiv et al., 2015). Using porcine IEC monolayers as a reductionist model of the intestinal epithelium, we identified that *C. parvum* infection alone is sufficient to induce endogenous IFN-λ expression and induction of ISG15 by IEC. Paracrine stimulation of ISG15 gene expression by IFN-λ was supported by the ability of exogenous HuIFN-λ to similarly stimulate an IEC ISG15 response in the absence of *C. parvum*. Infected IECs did not upregulate IFN-γ, most likely because immune cells and not IECs are considered the predominant sources of IFN-γ *in vivo* (Leav et al., 2005). The only other interferon induced by *C. parvum* infected IEC in the time frame of these studies was the Type I interferon, IFN-β. Others have similarly demonstrated expression of Type I interferon (IFN-α or IFN-β) by *C. parvum* infected IEC, but did not examine expression of IFN-λ (Barakat et al., 2009b). Although Type I interferon and IFN-λ have distinct receptor types, both stimulate the same intracellular signaling pathway (STAT1/STAT2) which results in indistinguishable overlap in target gene expression. Accordingly, we did not examine the responsiveness of our IEC monolayers to treatment

with exogenous Type I interferon and it is likely that endogenously-produced IFN-β also contributed to the ISG15 response observed in our *C. parvum* infected IEC. Importantly, many studies provide additional context for understanding the differential influence of Type I and Type III interferon, at least as it pertains to viral infection. For example, restriction of the IFN-λ receptor to IEC *in vivo* targets the effect of IFN-λ to the epithelium, while Type I interferon has a ubiquitous receptor expression. Recent studies using enteroid cultures suggest that epithelial cells may upregulate both Type I and Type III interferons in response to viral infection, but only translate and secrete Type III interferon (Pervolaraki et al., 2017). Therefore, recognition that *C. parvum* induces IFN-λ gene expression and that epithelial defense mechanisms are dependent on IFN-λ has important implications for further development of targeted therapies for the infection.

In the present study, IECs primed with IFN-λ were more resistant to infection by *C. parvum.* The principle mechanism of IFN-λ action was to impair parasite invasion of enterocytes. This finding substantiates our observation of increased burden of epithelial parasitism in mouse pups treated with IFN-λ immunoneutralizing antibodies. Once *C. parvum* invaded the IEC cells however, there were no appreciable changes in ability of the parasites to develop intracellularly. Enterocyte resistance to *C. parvum* has also been described in monolayers pretreated with Type I and II interferon [19], however given preferential targeting of intestinal epithelial cells by IFN-λ *in vivo*, our results likely have more biological relevance. In addition to enhanced resistance to infection by *C. parvum*, IEC primed with IFN-λ were protected from decreases in barrier function resulting from the infection. Barrier protective effects of IFN-λ at the level of the blood-brain barrier, as well as in polarized T84 cells (colonic adenocarcinoma), have been observed in the presence and

absence of viral or bacterial injury. [4, 22]. In contrast, we observed IFN-λ's barrier mitigating effect only in the face of *C. parvum* infection. The reason for this observational difference is unknown. Regardless of IFN-λ's role in influencing IEC barrier function at homeostasis, our findings now provide further proof that IFN-λ's defends IECs against pathogen-induced barrier disruption. We probed the paracellular pathway by which *C. parvum* and IFN-λ influenced the TEER of IEC monolayers and isolated the barrier defect to a corresponding change in flux of $^{22}Na^{+}$, indicating the characteristics of an ion/charge selective pathway. Interestingly, IFN-λ has been demonstrated to promote barrier function in the blood brain barrier by enhancing junctional localization of the tight junctional protein, claudin-5 (Lazear et al., 2015). Furthermore, overexpression of claudin-5 in MDBK epithelial cells led to an increase in TEER and selectively decreased the relative permeability of Na^{+} ions (Wen et al., 2004). In light of these findings, the influence of IFN-λ on expression and localization of claudin-5 during *C. parvum* infection is worth investigating.

In closing, these studies have identified a novel mechanism for intestinal epithelial defense against *C. parvum* involving IFN-λ. In our studies, IFN-λ promoted epithelial defense by not only limiting parasite invasion but also promoting intestinal epithelial barrier function. These findings broaden the scope and depth of our current understanding of IFN-λ's significance for epithelial defense and provide a mechanistic focus for development of targeted therapies for *Cryptosporidium* spp. infection.

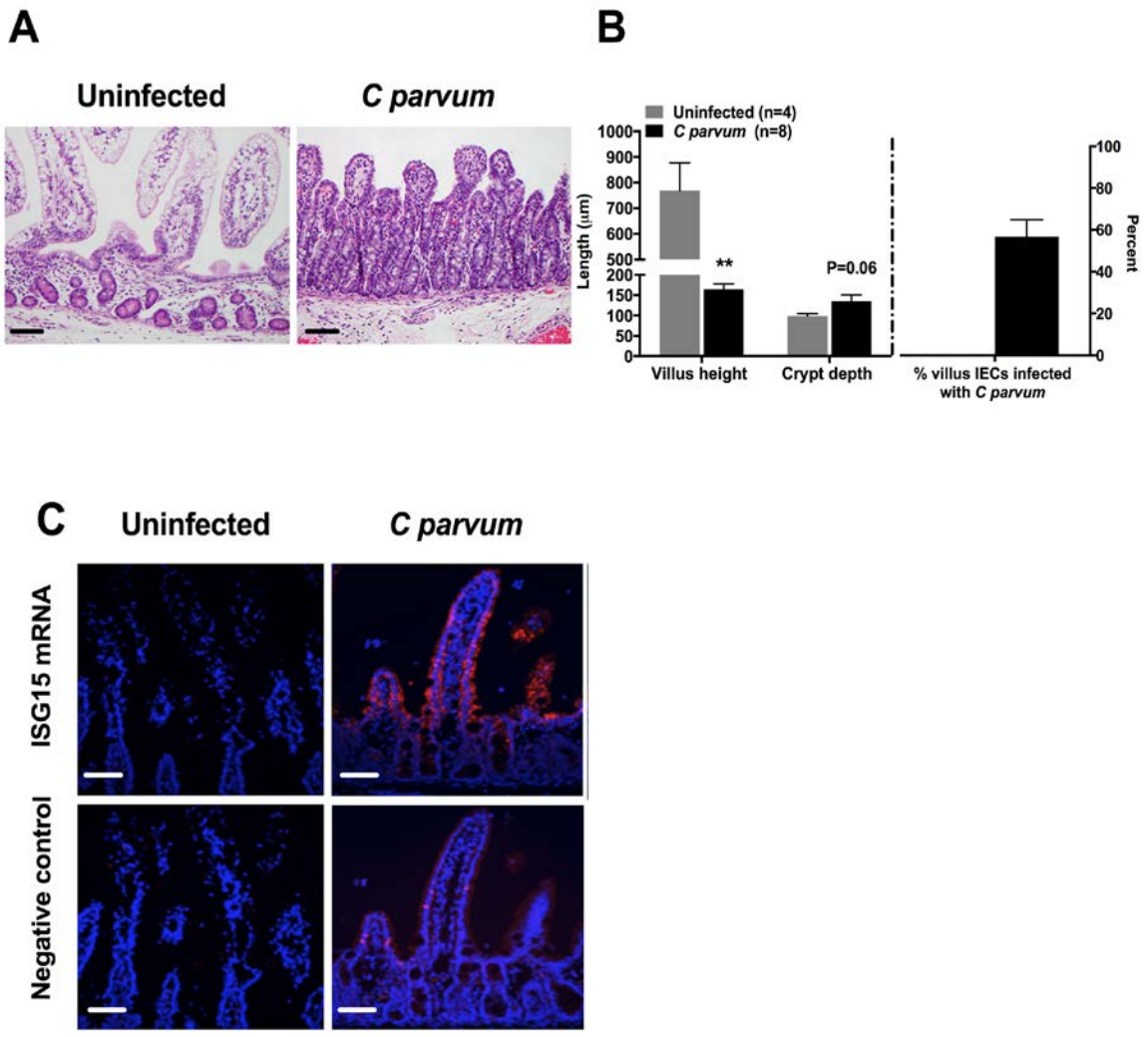

Figure 1. Intestinal epithelial cells upregulate numerous interferon stimulated genes in response to *C. parvum* infection. Intestinal epithelium was harvested from ileum mucosa of neonatal piglets at the time of peak infection (day 3-5 post-infection) (n=8) and from age-matched uninfected controls (n=4) for performance of gene analysis using microarrays. **(A)** Representative photomicrograph of ileum mucosa from an uninfected control and *C. parvum* infected piglet used for microarray analysis. Hematoxylin and Eosin stain. Bar=20 μm. **(B)** Quantitative morphometry of the mean ±SEM villus height and crypt depth (μm) and percent of total villous intestinal epithelial cells (IEC) infected with *C. parvum* in piglets utilized for microarray analysis. **(C)** Fluorescence *in situ* hybridization demonstrating ISG15 mRNA (red fluorescence) in villous epithelial cells of ileum mucosa from piglets at peak *C. parvum* infection and absent in villous epithelium of control piglets. Bar = 50 μm. **P<0.01, Student's t-test.

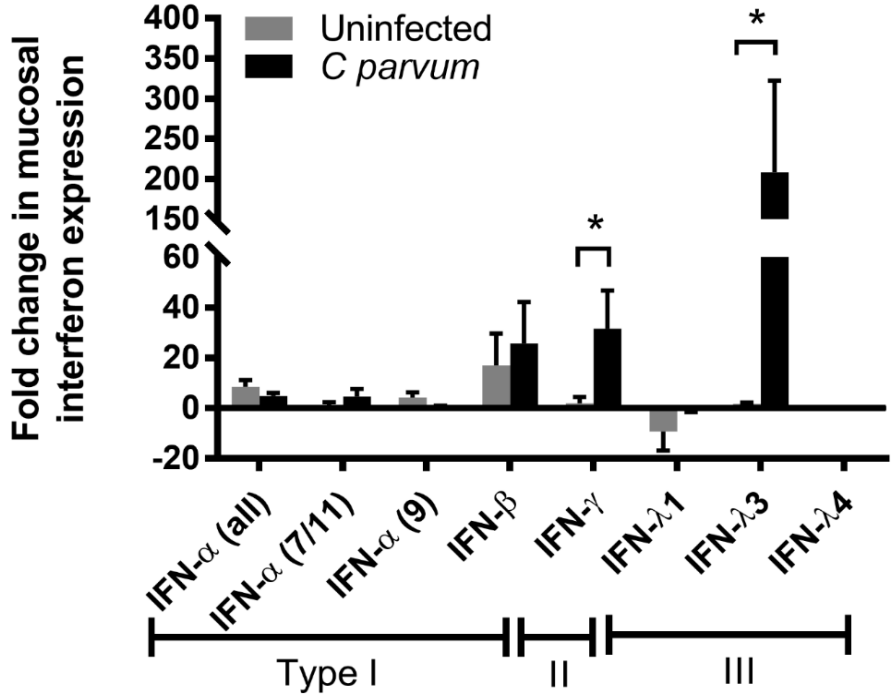

Figure 2. *C. parvum* stimulates ileum mucosal expression of IFN-λ3 and IFN-ɣ mRNA. (A) Quantitative RT-PCR analysis of porcine ileum mucosal total cellular mRNA for the presence of IFN-α (isoforms all, 7/11, and 9), IFN-β, IFN-γ, and IFN-λ 1, 3, and 4. Samples were obtained from piglets at peak *C. parvum* infection (days 3-5) and age-matched controls. Infected piglets demonstrated significantly increased expression of both IFN-λ3 (~200 fold) and IFN-γ mRNA (~20 fold) * $p<0.05$, Kruskal-Wallis ANOVA. n=3-11 piglets per group.

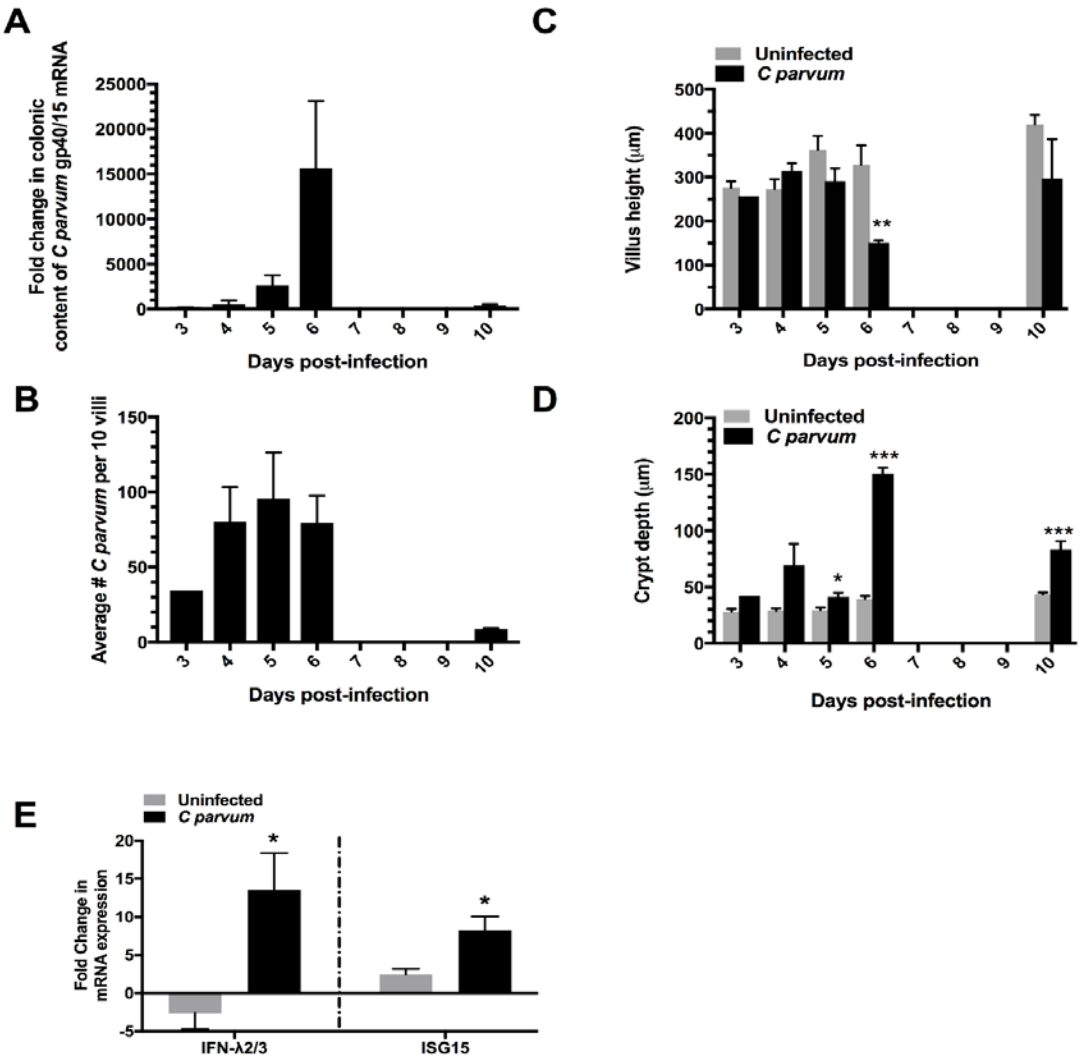

Figure 3. A Type III interferon response is conserved in neonatal mice infected with *C. parvum*. Characterization of a 10-day time course of *C. parvum* infection in suckling C57BL/6 pups following orogastric gavage of 2×10^5 *C. parvum* oocysts or mock-infection with PBS. Sampling took place on days 3-6, and day 10 post-infection. **(A)** Quantitative RT-PCR analysis of *Cryptosporidium* glycoprotein 40/15 mRNA in total distal colon for quantification of fecal shedding of *C. parvum*. Day 3 infected pup used for fold change comparison. **(B)** Quantification of the average number of epithelium-associated *C. parvum* per 10 villi per pup by light microscopy. **(C-D)** Quantitative morphometry of villus height and crypt depth as averaged for 10 villus crypt units per pup. **(E)** Quantitative RT-PCR analysis of IFN-λ2/3 and ISG15 mRNA in samples of total ileum from control and infected pups at peak infection (days 4-6). Bars represent mean ±SEM. n=3-7 pups per group per time point. *P<0.05, **P<0.01, ***P<0.001 compared to uninfected pups at same time point, Student's t-test.

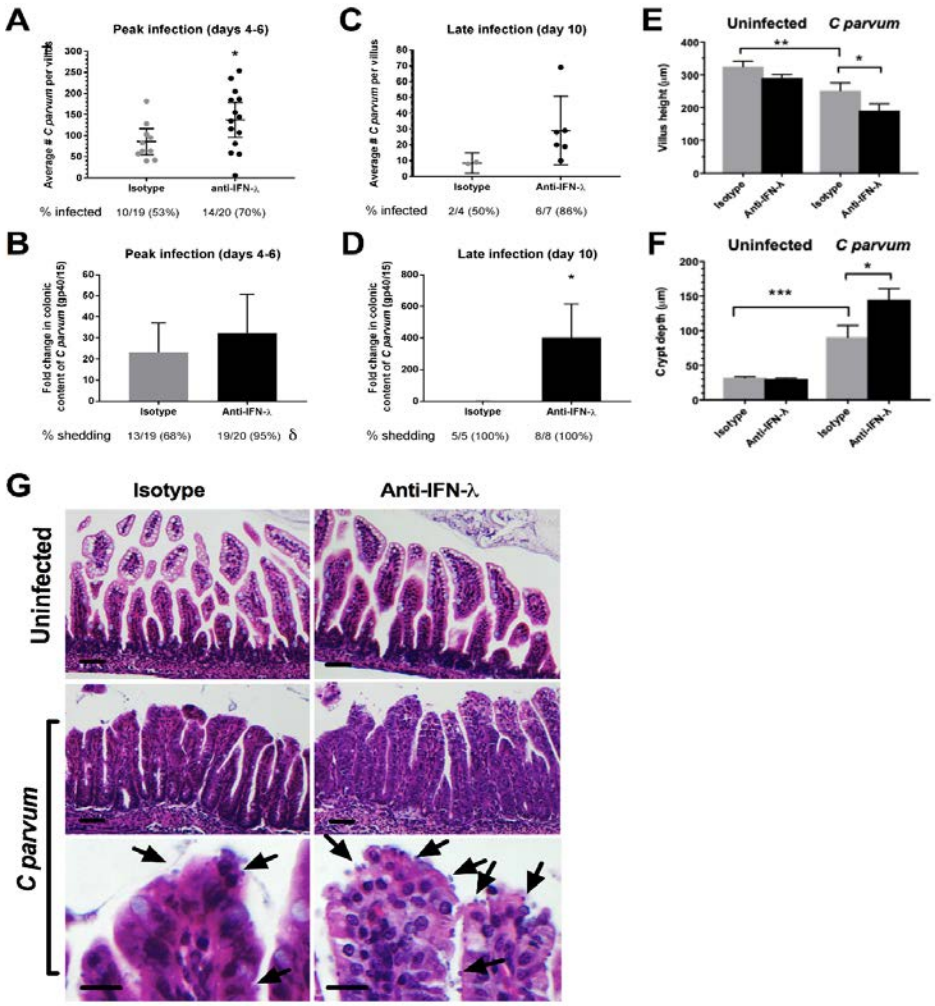

Figure 4. Immunoneutralization of IFN-λ exacerbates *C. parvum* infection. Mice were treated with either 15 μg of rat isotype or rat-anti-mouse IFN-λ2/3 neutralizing antibodies on days -1, 0, and 3 following orogastric gavage of *C. parvum* or mock-infection with PBS. Quantitative assessment of *C. parvum* epithelial burden **(A;** *P<0.05, Student's t-test**)** and colonic content of *C. parvum* as determined by quantitative RT-PCR analysis of *Cryptosporidium* gp40/15 mRNA **(B)** at peak (days 4-6 post-infection), or late stage (day 10) of infection **(C and D;** *P<0.05, Student's t-test**)**. Quantitative morphometry of average villus height **(E)** and crypt depth **(F)** for 10 villus crypt units per pup at peak infection (*P<0.05, **P<0.01; ***P<0.001, Student's t-test). Data represent mean ± SEM. n=19 to 20 pups per treatment at peak infection and n=4 to 8 pups at late infection time point. δ P<0.05 χ^2. **(G)** Representative photomicrographs of uninfected control and *C. parvum* infected ileum mucosa obtained on day 6 post-infection from mouse pups treated with rat isotype or rat-anti-IFN-λ2/3 neutralizing antibodies. Arrows highlight *C. parvum* infecting IECs. Bar = 20 μm for top four panels and 10 μm for bottom two panels.

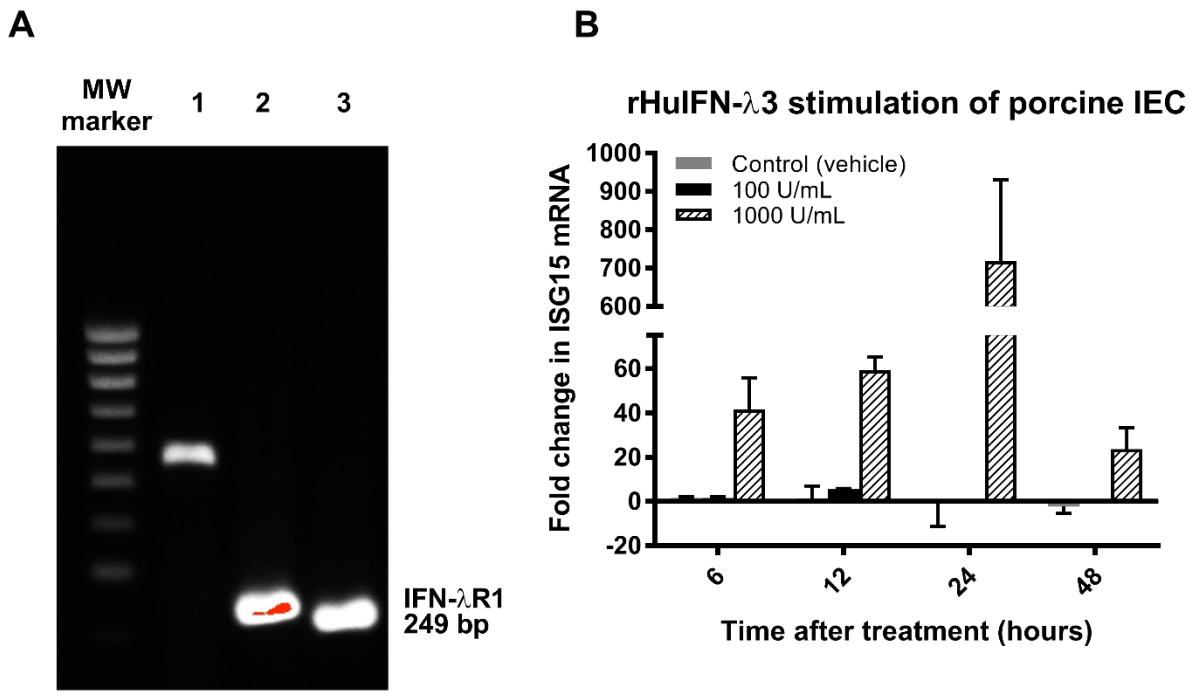

Figure 5. Non-transformed porcine intestinal epithelial (IPEC-J2) cells express IFNλR1 and respond to exogenous rHuIFN-λ3 to upregulate ISG15 mRNA expression in a dose and time-dependent manner. **(A)** Amplicons generated following PCR amplification of IFNλR1 (249 bp) using porcine genomic DNA (lane 1), cDNA prepared from IPEC-J2 cell mRNA (lane 2), and cDNA prepared from porcine ileum mucosa mRNA (lane 3) as template. **(B)** Quantitative RT-PCR analysis of ISG15 mRNA expression in IPEC-J2 cell monolayers at time points of 6, 12, 24, or 48 hours following stimulation with rHuIFNλ3 (100 or 1000 U/mL) or vehicle (0.1% BSA in PBS) . Data represent mean ± SEM. n=2-4 monolayers per time point.

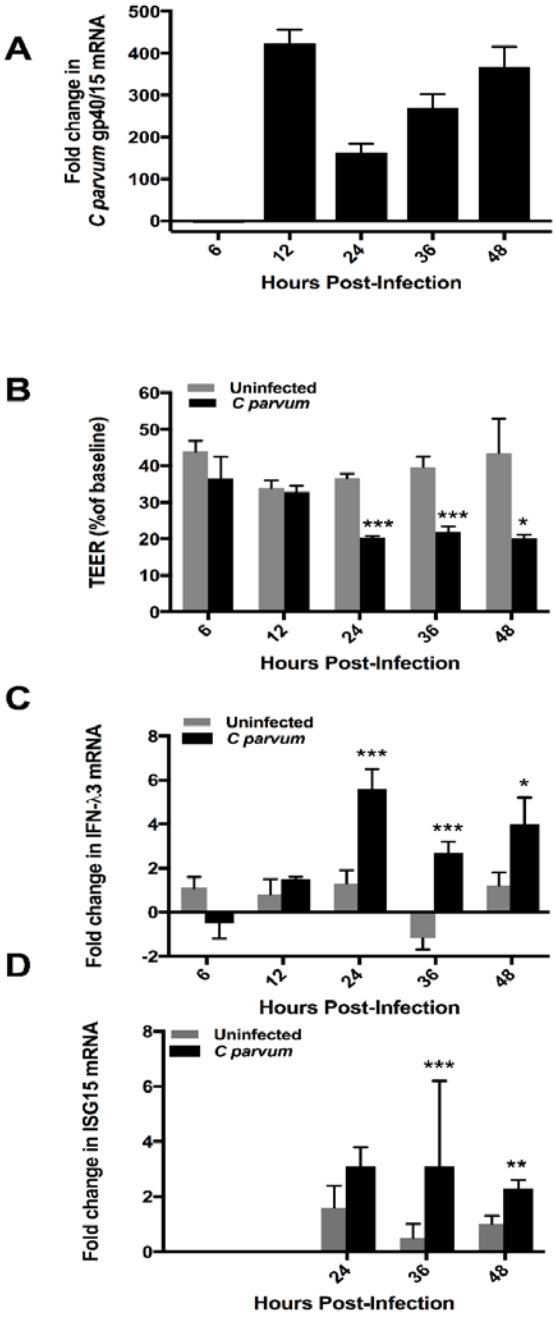

Figure 6. *C. parvum* is sufficient to stimulate IEC expression of IFN-λ3 and ISG15 mRNA. (A) Measurement of infection burden on the basis of quantitative RT-PCR analysis of *Cryptosporidium* glycoprotein 40/15 mRNA from control and infected IPEC-J2 monolayers, n=4 monolayers per group. **(B)** Transepithelial electrical resistance (TEER) of control and infected IPEC-J2 monolayers expressed as % of each individual monolayer's TEER at T=0. **(C-D)** Quantitative RT-PCR analysis of IFN-λ3, and ISG15 mRNA from control and infected IPEC-J2 monolayers. n=8 monolayers per group. Data represent mean±SEM. *P<0.05, **P<0.01, ***P<0.001 compared to uninfected monolayers at same time point; Student's t-test.

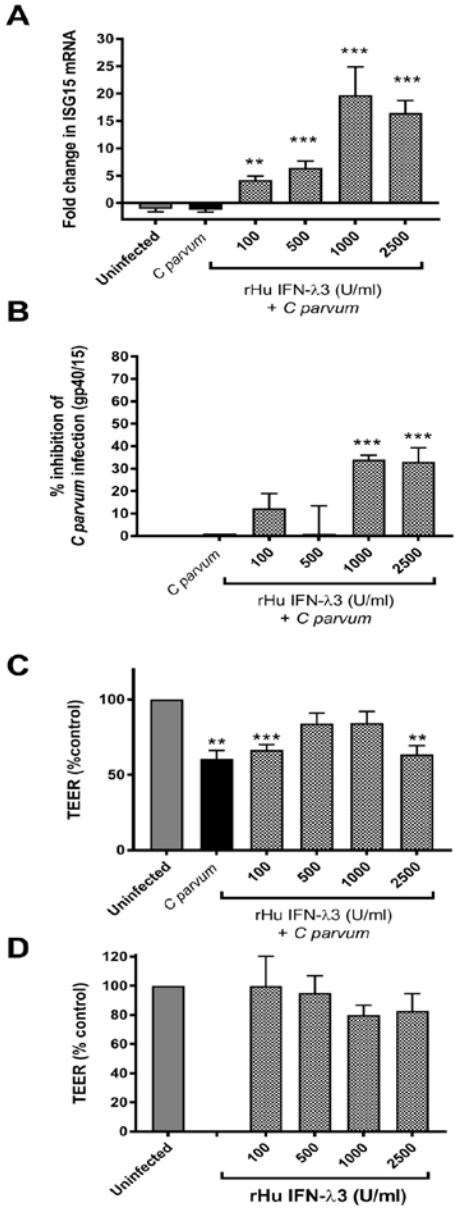

Figure 7. Priming of IEC with exogenous IFN-λ decreases the burden of *C. parvum* infection and abrogates loss of transepithelial electrical resistance. Polarized monolayers of IPEC-J2 cells were pre-treated with either vehicle, 100, 500, 1000, or 2500 U/mL of rHuIFN-λ3 for 12 hours prior to *C. parvum* infection. At the time of peak *C. parvum* infection (12-24 hours post-infection) the effect of rHuIFN-λ3 was assessed by quantitative RT-PCR analysis of ISG15 mRNA **(A)** and *Cryptosporidium* gp40/15 mRNA expression **(B)**, as well as by measurement of TEER. **(C)**. Priming of uninfected IEC with rHuIFN-λ3 had no significant effect on TEER of the monolayers **(D)**. Data for C and D expressed as % of 12-24 hour uninfected monolayers. n=3-6 monolayers per group. *P<0.05, **P<0.01, ***P<0.001, Student's t-test.

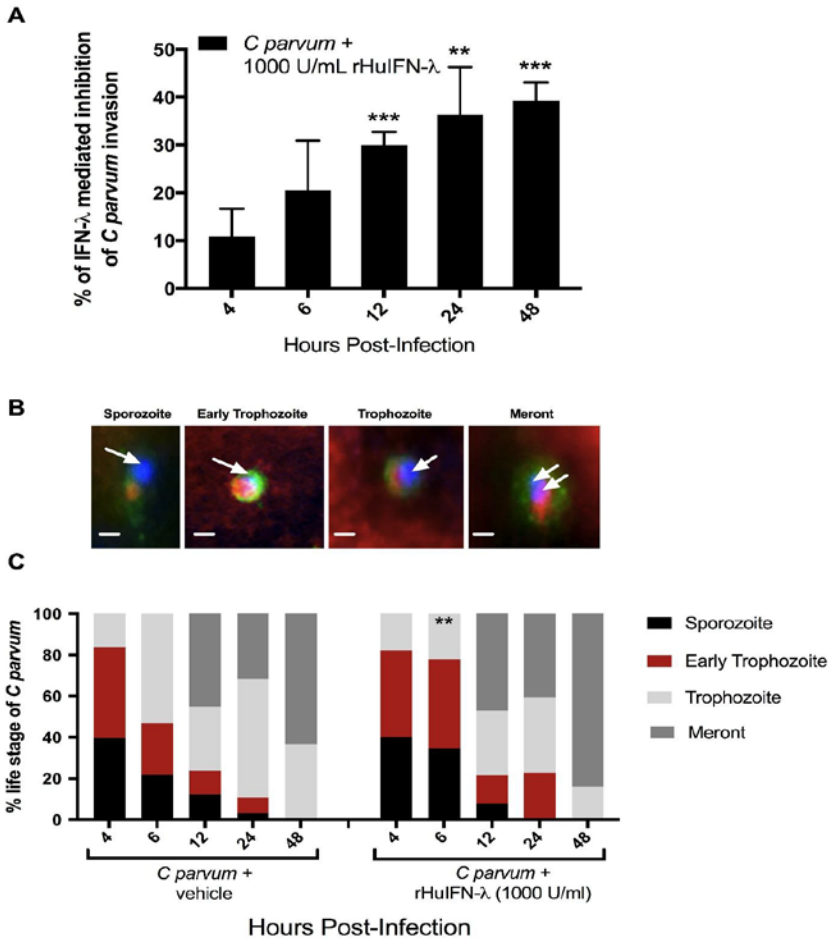

Figure 8. Priming IEC with IFN-λ enhances resistance to *C. parvum* invasion. Intestinal epithelial (IPEC-J2) monolayers were grown on chamber slides and pre-treated with either vehicle or 1000 U/mL of rHuIFN-λ3 for 12 hours prior to a 48-hour time course of *C. parvum* infection. Monolayers were examined using fluorescence microscopy at 4, 6, 12, 12, 24, 48 hours post-infection. **(A)** Quantification of invading *C. parvum* parasites was determined by counting the total number of FITC-*C. parvum* and Alexa-555 phalloidin co-labeled parasites within 10, 400× fields for each chamber well. n=3 monolayers per time and treatment group **P<0.01 and ***P<0.001 compared to vehicle treated, *C. parvum* infected controls. Student's t-test. Data represent mean ±SEM. **(B)** Representative fluorescence microscopy images of *C. parvum* asexual intracellular life stages. Parasites shown reflect positive labeling with FITC-*C. parvum* (green), DAPI positive *C. parvum* nuclei (blue and indicated by arrows), and Alexa-555-phalloidin cellular invasion sites (red). Bar = 1 µm. **(C)** The relative percentage of *C. parvum* asexual life stages at each time-point in vehicle treated (left) and rHuIFN-λ3 pre-treated infected monolayers. Parasite life stages were counted and classified within 5, 1000× fields for each chamber well. n=3 monolayers per time and treatment group *P<0.01 compared to trophozoite % of vehicle treated monolayers at same time point, χ^2.

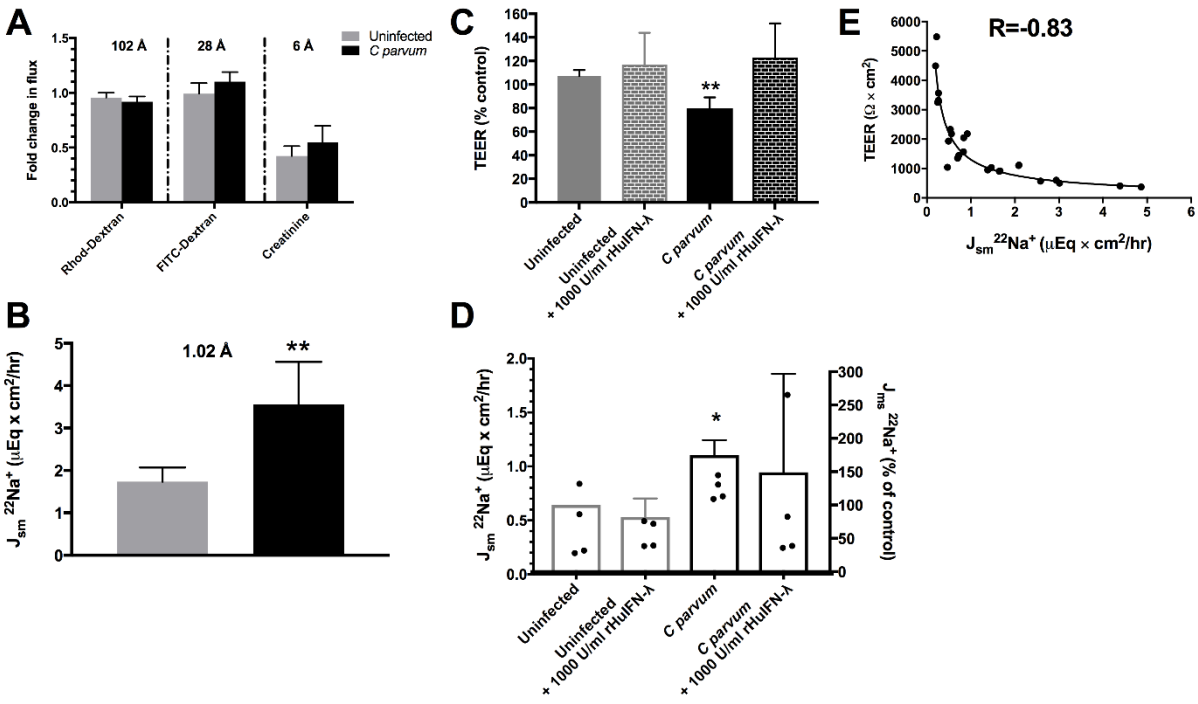

Figure 9. Interferon-λ mitigates *C. parvum*-induced loss of TEER by decreasing sodium permeability. (A) Mucosal to serosal flux of rhodamine-dextran, FITC-dextran, and creatinine and **(B)** serosal to mucosal flux of $^{22}Na^{+}$ across uninfected control and *C. parvum* infected IPEC-J2 monolayers at time of peak loss of TEER (24-48 hours post-infection), n=4-6 each, **P<0.01, Student's t-test. Transepithelial electrical resistance at 24 hours post-infection (expressed as % of the mean of 24-hour uninfected controls) **(C)** and serosal to mucosal flux of $^{22}Na^{+}$ **(D)** across uninfected control and *C. parvum* infected IPEC-J2 monolayers pre-treated with vehicle or 1000 U/mL of rHuIFN-λ3 for 12 hours prior to infection. For **(D)**, left axis shows individual data points for each flux measurement while right axis shows mean ± SEM of flux as a % of uninfected control. n=4 each, *P<0.05, compared to vehicle-treated controls; Student's test. **(E)** Correlation between TEER (Ω × cm^2) and flux of $^{22}Na^{+}$. n=26, includes uninfected and *C. parvum* infected monolayers both with and without rIFN-λ3 pre-treatment. Correlation coefficient of -0.83, P<0.0001.

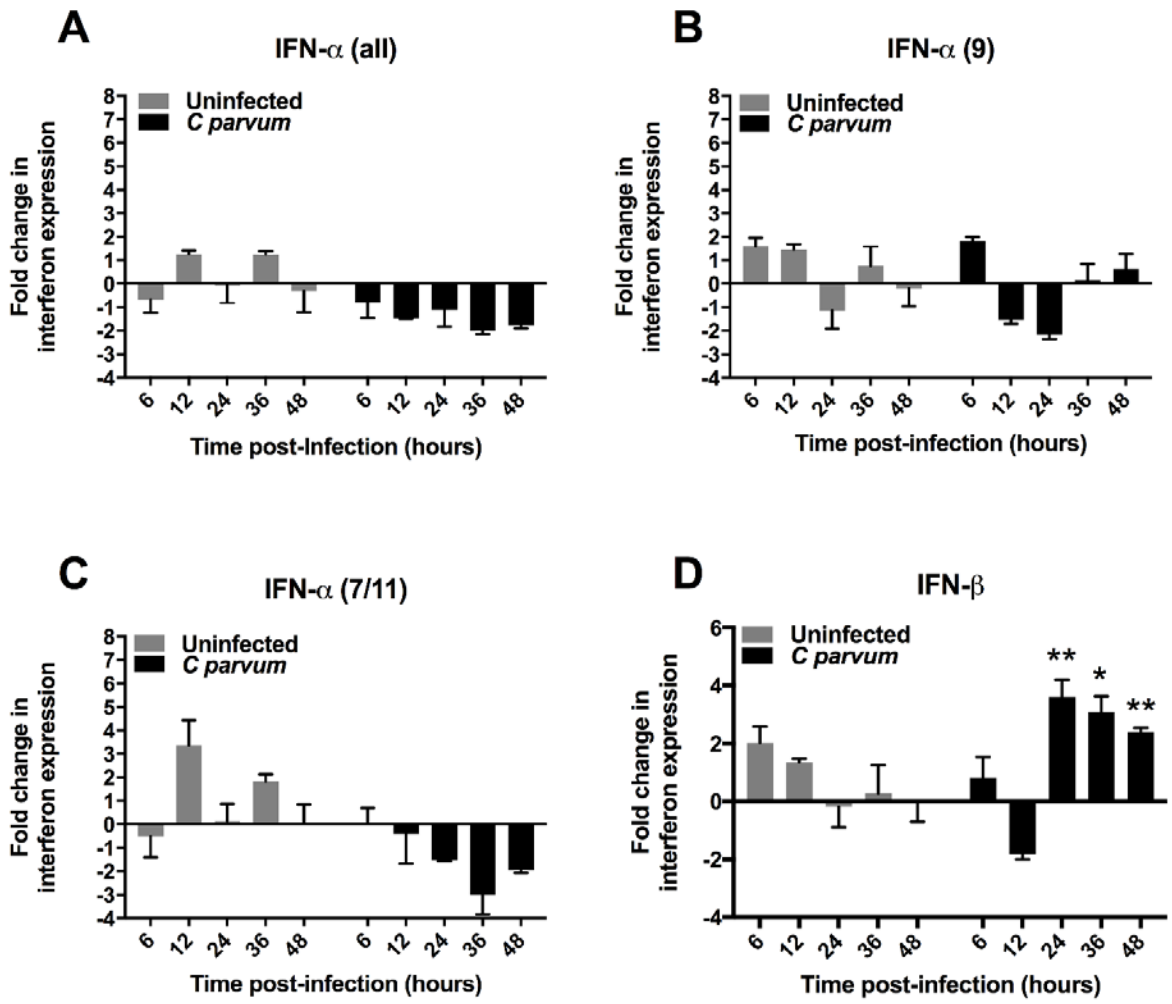

Supplementary Figure 1. Intestinal epithelial (IPEC-J2) cell monolayers express IFN-β but not IFN-α mRNA in response to *C. parvum* infection. Quantitative PCR analysis of IFN-α (all) isotypes **(A)**, IFN-α7/11 isotypes **(B)**, IFN-α9 **(C)**, and IFN-β **(D)** during a 48-hour time course of *C. parvum* infection in IPEC-J2 cells. n=4 monolayers per group and time point. Data represent mean ± SEM. *P<0.05, **P<0.01, ***P<0.001, Student's t-test compared to uninfected monolayers at same time point.

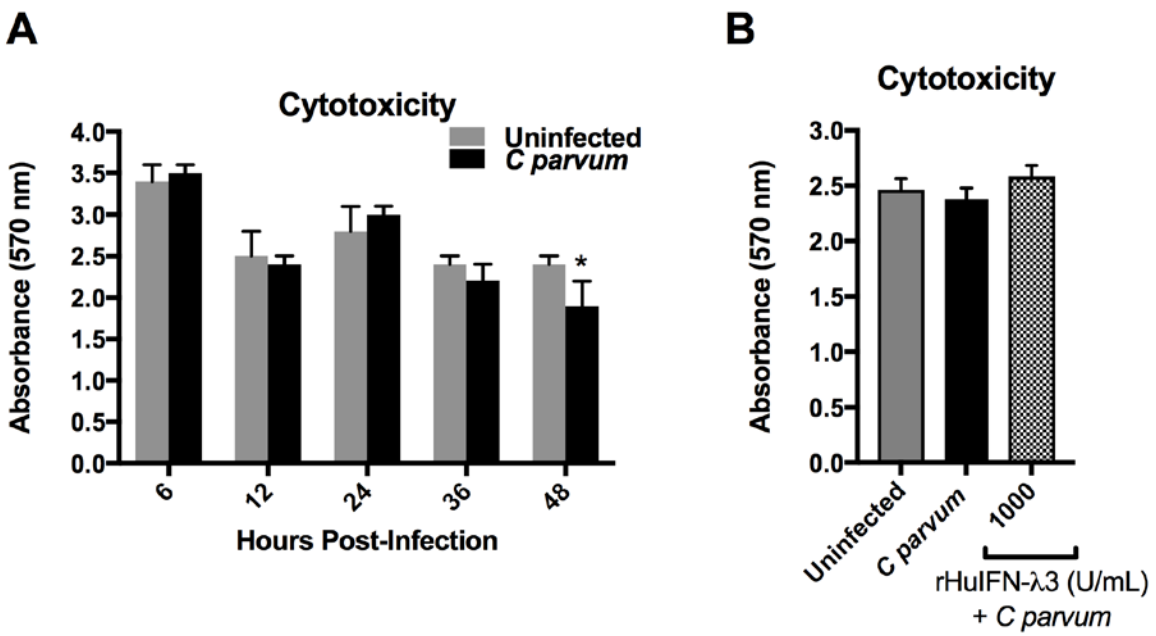

Supplementary Figure 2. Neither *C. parvum* infection or priming with exogenous IFN-λ3 alone or in combination cause significant cell loss from IPEC-J2 monolayers. Spectrophotometric assay of crystal violet absorbance (570 nm) by IPEC-J2 monolayers following a 48-hour time-course of *C. parvum* infection **(A)**. Spectrophotometric assay of crystal violet absorbance in uninfected control and *C. parvum* infected monolayers 24 hours after infection and in monolayers primed with 1000 U/mL of rHuIFN-λ3 12 hours prior to the infection **(B).** n=6 monolayers per treatment and time group. Data represent mean ± SEM. *P<0.05 compared to uninfected monolayers at same time point; Student's t-test.

Table 1: Differentially expressed genes in *C. parvum* infected intestinal epithelial cells.

	Gene Name	Fold Change
UPREGULATED		
ISG15 Ubiquitin-like modifier	ISG15	21.34
Regenerating islet-derived 3 alpha	REG3A	17.17
Guanylate binding protein 2	GBP2	11.95
Ubiquitin D	UBD	11.70
Placenta-Specific 8	PLAC8	11.33
Matrix Gla protein	MGP	9.78
Chromosome 10 open reading frame 116	C10orf116	8.27
Interferon alpha-inducible protein 27	IF127	8.06
Guanylate binding protein 1	GBP1	7.81
Complement component 1, s subcomponent	C1S	7.18
Ribonuclease, RNase A family, 4	RNASE4	5.43
Glucosaminyl (N-acetyl) transferase 3, mucin type	GCNT3	5.22
Annexin 2	ANXA2	5.16
Glutathione S-transferase omega 1	GSTO1	4.98
S100 Calcium binding protein A6	S100A6	4.92
Pyrophosphatase 1	PPA1	4.84
Proline rich 13	PRR13	4.83
Chemokine (C-X-C motif) ligand 16	CXCL16	4.74
Membrane-spanning 4-domains, subfamily A, member 12	MS4A12	4.70
Sterol-C4-methyl oxidase-like	SC4MOL	4.37
Tropomyosin 4	TPM4	4.08
Tripartite motif-containing 34	TRIM34	3.97

Table 1: Differentially expressed genes in *C. parvum* infected intestinal epithelial cells (continued).

Interferon-induced protein 44 –like	IFI44L	3.69
Farnesyl diphosphate synthase	FDPS	3.67
Isopentenyl-diphosphate delta isomerase 1	IDI1	3.59
HIG1 hypoxia inducible domain family, member 1A	HIGD1A	3.50
Chloride intracellular channel 1	CLIC1	3.49
Tropomyosin 3	TPM3	3.46
Creatinine kinase, mitochondrial 1B	CKMT1B	3.45
Interferon stimulated exonuclease gene 20 kDa	ISG20	3.42
Hematological and neurological expressed 1	HN1	3.34
Cysteine-rich protein 1 (intestinal)	CRIP1	3.31
Calpain 1, large subunit	CAPN1	3.30
Proteasome subunit, beta type, 8	PSMB8	2.92
OUT domain, ubiquitin aldehyde binding 1	OTUB1	2.77
Calmodulin 3	CALM3	2.76
Stearoyl-CoA desaturase 5	SCD5	2.72
Phosphatidylinositol transfer protein, cytoplasmic 1	PITPNC1	2.72
Actin related protein 2/3 complex, subunit 1A, 41 kDa	ARPC1A	2.65
PERP, TP53 apoptosis effector	PERP	2.60
Thioredoxin	TXN	2.51
Optineurin	OPTN	2.492
Poly (ADP-ribose) polymerase family, member 3	PARP3	2.47
Calcium binding and coiled-coil domain 2	CALCOCO2	2.45
Heat shock 70 kDa protein 4	HSPA4	2.40
DAZ associated protein 2	DAZAP2	2.32

Table 1: Differentially expressed genes in *C. parvum* infected intestinal epithelial cells (continued).

UDP-N-acetylglucosamine pyrophosphorylase 1	UAP1	2.27
DnaJ (Hsp40) homolog, subfamily B, member 11	DNAJB11	2.27
Calcium binding protein 39	CAB39	2.27
Cytochrome C oxidase subunit VIIA	COX8A	2.25
Isocitrate dehydrogenase 2	IDH2	2.24
Chromosome 15 open reading frame 63	C15ORF6	2.23
Tyrosine 3-monoxygenase/tryptophan 5-monooxygenase activation protein, zeta polypeptide	YWHAZ	2.20
Ubiquitin A-52 residue ribosomal protein fusion product 1	UBA52	2.19
Serine/threonine kinase 24	STK24	2.17
Acyl-CoA thioesterase 7	ACOT7	2.16
Archain 1	ARCN1	2.12
Casein kinase 2, beta polypeptide	CSNK2B	2.09
Coatomer protein complex, subunit epsilon	COPE	2.06
Eukaryotic translation initiation factor 6	EIF6	2.03
ADP-ribosylation factor 6	ARF6	2.02
DOWNREGULATED		
Apolipoprotein C-II	APOC2	28.48
Brain expressed, X-linked 4	BEX4	12.34
Alpha-N-acetylgalactosaminidase-like	NAGA	6.09
Nuclear pore complex protein Nup50-like	NUP50	3.89
Regulator of G-protein signaling 3	RGS3	3.37
Adenine nucleotide translocase 1-like, transcript variant 2 (ANT1)	ANT1	3.05
Oxytocin receptor	OXTR	2.72
Transcription elongation regulator 1	TCERG1	2.51
Neuroligin 1 precursor	NLGN1	2.32

Table 1: Differentially expressed genes in *C. parvum* infected intestinal epithelial cells (continued).

Tryptophan 5-hydroxylase 2	TPH2	2.26
Ethanolamine kinase-like protein	EKI2	2.18
Chymotrypsinogen 2-like	CTRB2	2.16
Conserved oligomeric Golgi complex subunit 5	COG5	2.13
Actin alpha 2	ACTA2	2.12
Solute carrier family 13 (sodium-dependent citrate transporter), member 5	SLC13A5	2.09
Uroplakin 3A, transcript variant 1	UPK3A	2.07
Sister chromatid cohesion protein PDS5 homolog B-like	PDS5B	2.07
Myosin If	MYO1F	2.06
Filamin A interacting protein 1	FILIP1	2.06
Activin A receptor, type IIB	ACVR2B	2.01

Supplementary table 1. Specific primer sequences and sources used in real-time RT-PCR and their resulting amplification product sizes and melting temperatures.

mRNA	Forward (5' to 3')	Reverse (5'to 3')	Product size	Tm (C°)	Reference (if applicable)
Cp gp40/15	TCATTTGTAATGTGGTTCGGAGAA	AGGGTAAAGGCAAACAAATCG	326	82.5-83.0	(Godiwala et al., 2
Po-IFNα (all)	GGCTCTGGTGCATGAGATGC	CAGCCAGGATGGAGTCCTCC	197	88.45-88.80	(Sang et al., 2010b)
Po-IFNα 7/11	GGGACTTTGGATCCCCTCAT	GTGGAGGAAGAGAAGGATG	369	89.0-89.5	(Sang et al., 2010a)
Po-IFNα9	GTGCTGCTCAGCTGCAAG	AGTCCTCCTCCAGCAGGGGC	384	87.5-88.5	(Sang et al., 2010a)
Po-IFNβ	ATGTCAGAAGCTCCTGGGACAGTT	AGGTCATCCATCTGCCCATCAAGT	246	82.20-82.70	(Sang et al., 2010b)
Po-IFNγ	GTTTTTCTGGCTCTTACTGC	CTTCCGCTTTCTTAGGTTAG	410	86.3-87.0	(Dijkmans et al., 1990)
Po-IFNλ1	ACATCCACGTCGAACTTCAGGCTT	TCAGATGTGCAAGTCTCCACTGGT	209	87.5-88.0	(Sang et al., 2010a)
Po-IFNλ3	AAGAGGGCCAAGGATGCCTTTGAA	AGGCGGAAGAGGTTGAACATGACA	374	92.9-93.3	(Sang et al., 2010a)
Po-IFNλ4	GTCACAGAGCTGACTCGCCT	TCACAGACAAGGCCCCGAAT	110	89.2-89.5	Authors
Po-ISG15	GATGCTGGGAGGCAAGGA	CAGGATGCTCAGTGGGTCTCT	229	90.0-90.3	Authors
Po-IFNλR1	CGGTGGCAAAGAGTGAAAAT	GATCTCCTCTGTCCGGGTGA	249	86.7-86.8	Authors
Po-cyclophilin	CCGTCGATGGCGAGCCC	CCCGTATGCTTCAGGATAAAA	250	82.5-84.5	(Gookin et al., 2004)
Mu-IFNλ2/3	AGCTGCAGGCCTTCAAAAAG	TGGGAGTGAATGTGGCTCAG	244	88.5-89.1	(Pott et al., 2011)
Mu-ISG15	GAGCTAGAGCCTGCAGCAAT	TTCTGGGCAATCTGCTTCTT	122	84.3-84.5	(Pott et al., 2011)
Mu-IFNβ	GGAGATGACGGAGAAGATGC	CCCAGTGCTGGAGAAATTGT	103	79.9-80.6	(Stewart et al., 2005)
Mu-GAPDH	TGCACCACCAACTGCTTAGC	GGCATGGACTGTGGTCATGAG	87	84.2-84.4	(Pott et al., 2011)

References

Abal-Fabeiro, J.L., Maside, X., Llovo, J., Bello, X., Torres, M., Trevino, M., Moldes, L., Munoz, A., Carracedo, A., Bartolome, C., 2014. High-throughput genotyping assay for the large-scale genetic characterization of Cryptosporidium parasites from human and bovine samples. Parasitology 141, 491-500.

Abrahamsen, M.S., Templeton, T.J., Enomoto, S., Abrahante, J.E., Zhu, G., Lancto, C.A., Deng, M., Liu, C., Widmer, G., Tzipori, S., Buck, G.A., Xu, P., Bankier, A.T., Dear, P.H., Konfortov, B.A., Spriggs, H.F., Iyer, L., Anantharaman, V., Aravind, L., Kapur, V., 2004. Complete genome sequence of the apicomplexan, Cryptosporidium parvum. Science 304, 441-445.

Abreu, M.T., 2010. Toll-like receptor signalling in the intestinal epithelium: how bacterial recognition shapes intestinal function. Nat Rev Immunol 10, 131-144.

Adams, R.B., Guerrant, R.L., Zu, S.X., Fang, G.D., Roche, J.K., 1994. Cryptosporidium-Parvum Infection of Intestinal Epithelium - Morphologic and Functional-Studies in an in-Vitro Model. J Infect Dis 169, 170-177.

Aji, T., Flanigan, T., Marshall, R., Kaetzel, C., Aikawa, M., 1991. Ultrastructural study of asexual development of Cryptosporidium parvum in a human intestinal cell line. The Journal of protozoology 38, 82S-84S.

Alcantara, C.S., Yang, C.H., Steiner, T.S., Barrett, L.J., Lima, A.A., Chappell, C.L., Okhuysen, P.C., White, A.C., Jr., Guerrant, R.L., 2003. Interleukin-8, tumor necrosis factor-alpha, and lactoferrin in immunocompetent hosts with experimental and Brazilian children with acquired cryptosporidiosis. Am J Trop Med Hyg 68, 325-328.

Alcantara Warren, C., Destura, R.V., Sevilleja, J.E., Barroso, L.F., Carvalho, H., Barrett, L.J., O'Brien, A.D., Guerrant, R.L., 2008. Detection of epithelial-cell injury, and quantification of infection, in the HCT-8 organoid model of cryptosporidiosis. J Infect Dis 198, 143-149.

Anbazhagi, M., Loganathan, D., Tamilselvan, S., Jayabalou, R., Kamatchiammal, S., Kumar, R., 2007. Cryptosporidium oocysts in drinking water supply of Chennai City, Southern India. Clean-Soil Air Water 35, 167-171.

Anderson, B.C., 1982. Cryptosporidiosis in Idaho lambs: natural and experimental infections. Journal of the American Veterinary Medical Association 181, 151-153.

Ank, N., Iversen, M.B., Bartholdy, C., Staeheli, P., Hartmann, R., Jensen, U.B., Dagnaes-Hansen, F., Thomsen, A.R., Chen, Z., Haugen, H., Klucher, K., Paludan, S.R., 2008. An important role for type III interferon (IFN-lambda/IL-28) in TLR-induced antiviral activity. J Immunol 180, 2474-2485.

Argenzio, R.A., Armstrong, M., Rhoads, J.M., 1996. Role of the enteric nervous system in piglet cryptosporidiosis. The Journal of pharmacology and experimental therapeutics 279, 1109-1115.

Argenzio, R.A., Lecce, J., Powell, D.W., 1993. Prostanoids inhibit intestinal NaCl absorption in experimental porcine cryptosporidiosis. Gastroenterology 104, 440-447.

Argenzio, R.A., Liacos, J.A., Levy, M.L., Meuten, D.J., Lecce, J.G., Powell, D.W., 1990. Villous atrophy, crypt hyperplasia, cellular infiltration, and impaired glucose-Na absorption in enteric cryptosporidiosis of pigs. Gastroenterology 98, 1129-1140.

Baldridge, M.T., Lee, S., Brown, J.J., McAllister, N., Urbanek, K., Dermody, T.S., Nice, T.J., Virgin, H.W., 2017. Expression of Ifnlr1 on Intestinal Epithelial Cells Is Critical to the Antiviral Effects of Interferon Lambda against Norovirus and Reovirus. J Virol 91.

Barakat, F.M., McDonald, V., Foster, G.R., Tovey, M.G., Korbel, D.S., 2009b. Cryptosporidium parvum Infection Rapidly Induces a Protective Innate Immune Response Involving Type I Interferon. J Infect Dis 200, 1548-1555.

Barrier, M., Lacroix-Lamande, S., Mancassola, R., Auray, G., Bernardet, N., Chausse, A.M., Uematsu, S., Akira, S., Laurent, F., 2006. Oral and intraperitoneal administration of phosphorothioate oligodeoxynucleotides leads to control of Cryptosporidium parvum infection in neonatal mice. J Infect Dis 193, 1400-1407.

Bartelt, L.A., Bolick, D.T., Kolling, G.L., Roche, J.K., Zaenker, E.I., Lara, A.M., Noronha, F.J., Cowardin, C.A., Moore, J.H., Turner, J.R., Warren, C.A., Buck, G.A., Guerrant, R.L., 2016. Cryptosporidium Priming Is More Effective than Vaccine for Protection against Cryptosporidiosis in a Murine Protein Malnutrition Model. Plos Neglect Trop D 10.

Baydoun, M., Vanneste, S.B., Creusy, C., Guyot, K., Gantois, N., Chabe, M., Delaire, B., Mouray, A., Baydoun, A., Forzy, G., Chieux, V., Gosset, P., Senez, V., Viscogliosi, E., Follet, J., Certad, G., 2017. Three-dimensional (3D) culture of adult murine colon as an in vitro model of cryptosporidiosis: Proof of concept. Sci Rep 7, 17288.

Benamrouz, S., Guyot, K., Gazzola, S., Mouray, A., Chassat, T., Delaire, B., Chabe, M., Gosset, P., Viscogliosi, E., Dei-Cas, E., Creusy, C., Conseil, V., Certad, G., 2012. Cryptosporidium parvum Infection in SCID Mice Infected with Only One Oocyst: qPCR Assessment of Parasite Replication in Tissues and Development of Digestive Cancer. Plos One 7.

Bhalchandra, S., Ludington, J., Coppens, I., Ward, H.D., 2013. Identification and Characterization of Cryptosporidium parvum Clec, a Novel C-Type Lectin Domain-Containing Mucin-Like Glycoprotein. Infect Immun 81, 3356-3365.

Bierne, H., Travier, L., Mahlakoiv, T., Tailleux, L., Subtil, A., Lebreton, A., Paliwal, A., Gicquel, B., Staeheli, P., Lecuit, M., Cossart, P., 2012. Activation of type III interferon genes by pathogenic bacteria in infected epithelial cells and mouse placenta. Plos One 7, e39080.

Bjorneby, J.M., Leach, D.R., Perryman, L.E., 1991. Persistent cryptosporidiosis in horses with severe combined immunodeficiency. Infect Immun 59, 3823-3826.

Blackman, M.J., Bannister, L.H., 2001. Apical organelles of Apicomplexa: biology and isolation by subcellular fractionation. Mol Biochem Parasitol 117, 11-25.

Bouzid, M., Hunter, P.R., Chalmers, R.M., Tyler, K.M., 2013. Cryptosporidium Pathogenicity and Virulence. Clin Microbiol Rev 26, 115-134.

Brasseur, P., Favennec, L., Lemeteil, D., Roussel, F., Ballet, J.J., 1994. An immunosuppressed rat model for evaluation of anti-Cryptosporidium activity of sinefungin. Folia Parasitol (Praha) 41, 13-16.

Buret, A.G., Chin, A.C., Scott, K.G., 2003. Infection of human and bovine epithelial cells with Cryptosporidium andersoni induces apoptosis and disrupts tight junctional ZO-1: effects of epidermal growth factor. Int J Parasitol 33, 1363-1371.

Capet, C., Kapel, N., Huneau, J.F., Magne, D., Laikuen, R., Tricottet, V., Benhamou, Y., Tome, D., Gobert, J.G., 1999. Cryptosporidium parvum infection in suckling rats: impairment of mucosal permeability and Na(+)-glucose cotransport. Exp Parasitol 91, 119-125.

Carryn, S., Schaefer, D.A., Imboden, M., Homan, E.J., Bremel, R.D., Riggs, M.W., 2012. Phospholipases and Cationic Peptides Inhibit Cryptosporidium Parvum Sporozoite Infectivity by Parasiticidal and Non-Parasiticidal Mechanisms. J Parasitol 98, 199-204.

Chen, W., Harp, J.A., Harmsen, A.G., 2003. Cryptosporidium parvum infection in gene-targeted B cell-deficient mice. J Parasitol 89, 391-393.

Chen, W., Harp, J.A., Harmsen, A.G., Havell, E.A., 1993. Gamma interferon functions in resistance to Cryptosporidium parvum infection in severe combined immunodeficient mice. Infect Immun 61, 3548-3551.

Chen, X., He, S.-H., Feng, B.-S., Yang, P.-C., 364 Role of Mast Cell-Derived Interferon Lambda in Intestinal Inflammation Induced By Microbial Antigens. Gastroenterology 136, A-59.

Chen, X.M., Huang, B.Q., Splinter, P.L., Orth, J.D., Billadeau, D.D., McNiven, M.A., LaRusso, N.F., 2004a. Cdc42 and the actin-related protein/neural Wiskott-Aldrich syndrome protein network mediate cellular invasion by Cryptosporidium parvum. Infect Immun 72, 3011-3021.

Chen, X.M., O'Hara, S.P., Huang, B.Q., Nelson, J.B., Lin, J.J., Zhu, G., Ward, H.D., LaRusso, N.F., 2004b. Apical organelle discharge by Cryptosporidium parvum is temperature, cytoskeleton, and intracellular calcium dependent and required for host cell invasion. Infect Immun 72, 6806-6816.

Chen, X.M., O'Hara, S.P., Huang, B.Q., Splinter, P.L., Nelson, J.B., LaRusso, N.F., 2005a. Localized glucose and water influx facilitates Cryptosporidium parvum cellular invasion by means of modulation of host-cell membrane protrusion. Proc Natl Acad Sci USA 102, 6338-6343.

Chen, X.M., O'Hara, S.P., Nelson, J.B., Splinter, P.L., Small, A.J., Tietz, P.S., Limper, A.H., LaRusso, N.F., 2005b. Multiple TLRs are expressed in human cholangiocytes and mediate host epithelial defense responses to Cryptosporidium parvum via activation of NF-kappaB. J Immunol 175, 7447-7456.

Chen, X.M., Splinter, P.L., O'Hara, S.P., LaRusso, N.F., 2007. A cellular Micro-RNA, let-7i, regulates toll-like receptor 4 expression and contributes to cholangiocyte immune responses against Cryptosporidium parvum infection. J Biol Chem 282, 28929-28938.

Chiriac, M.T., Buchen, B., Wandersee, A., Hundorfean, G., Gunther, C., Bourjau, Y., Doyle, S.E., Frey, B., Ekici, A.B., Buttner, C., Weigmann, B., Atreya, R., Wirtz, S., Becker, C., Siebler, J., Neurath, M.F., 2017. Activation of Epithelial Signal Transducer and Activator of Transcription 1 by Interleukin 28 Controls Mucosal Healing in Mice With Colitis and Is Increased in Mucosa of Patients With Inflammatory Bowel Disease. Gastroenterology 153, 123-138 e128.

Chrisp, C.E., Reid, W.C., Rush, H.G., Suckow, M.A., Bush, A., Thomann, M.J., 1990. Cryptosporidiosis in guinea pigs: an animal model. Infect Immun 58, 674-679.

Clark, D.P., 1999. New insights into human cryptosporidiosis. Clin Microbiol Rev 12, 554.

Cobo, E.R., Chadee, K., 2013. Antimicrobial Human beta-Defensins in the Colon and Their Role in Infectious and Non-Infectious Diseases. Pathogens 2, 177-192.

Cohen, T.S., Prince, A.S., 2013. Bacterial Pathogens Activate a Common Inflammatory Pathway through IFN lambda Regulation of PDCD4. Plos Pathog 9.

Colegio, O.R., Van Itallie, C.M., McCrea, H.J., Rahner, C., Anderson, J.M., 2002. Claudins create charge-selective channels in the paracellular pathway between epithelial cells. American journal of physiology. Cell physiology 283, C142-147.

Coordinators, N.R., 2018. Database resources of the National Center for Biotechnology Information. Nucleic Acids Res 46, D8-D13.

Costa, L.B., JohnBull, E.A., Reeves, J.T., Sevilleja, J.E., Freire, R.S., Hoffman, P.S., Lima, A.A., Oria, R.B., Roche, J.K., Guerrant, R.L., Warren, C.A., 2011. Cryptosporidium-malnutrition interactions: mucosal disruption, cytokines, and TLR signaling in a weaned murine model. J Parasitol 97, 1113-1120.

Cosyns, M., Tsirkin, S., Jones, M., Flavell, R., Kikutani, H., Hayward, A.R., 1998. Requirement of CD40-CD40 ligand interaction for elimination of Cryptosporidium parvum from mice. Infect Immun 66, 603-607.

Dagci, H., Ustun, S., Taner, M.S., Ersoz, G., Karacasu, F., Budak, S., 2002. Protozoon infections and intestinal permeability. Acta Trop 81, 1-5.

Daniels, M.E., Shrivastava, A., Smith, W.A., Sahu, P., Odagiri, M., Misra, P.R., Panigrahi, P., Suar, M., Clasen, T., Jenkins, M.W., 2015. Cryptosporidium and Giardia in Humans, Domestic Animals, and Village Water Sources in Rural India. Am J Trop Med Hyg 93, 596-600.

de Sablet, T., Potiron, L., Marquis, M., Bussiere, F.I., Lacroix-Lamande, S., Laurent, F., 2016. Cryptosporidium parvum increases intestinal permeability through interaction with epithelial cells and IL-1 and TNF released by inflammatory monocytes. Cell Microbiol 18, 1871-1880.

DeCicco RePass, M.A., Chen, Y., Lin, Y., Zhou, W., Kaplan, D.L., Ward, H.D., 2017. Novel Bioengineered Three-Dimensional Human Intestinal Model for Long-Term Infection of Cryptosporidium parvum. Infect Immun 85.

Dijkmans, R., Vandenbroeck, K., Beuken, E., Billiau, A., 1990. Sequence of the porcine interferon-gamma (IFN-gamma) gene. Nucleic Acids Res 18, 4259.

Doom, C.M., Turula, H.M., Hill, A.B., 2009. Investigation of the impact of the common animal facility contaminant murine norovirus on experimental murine cytomegalovirus infection. Virology 392, 153-161.

Eckmann, L., Kagnoff, M.F., Fierer, J., 1993. Epithelial cells secrete the chemokine interleukin-8 in response to bacterial entry. Infect Immun 61, 4569-4574.

Ehigiator, H.N., McNair, N., Mead, J.R., 2007. Cryptosporidium parvum: the contribution of Th1-inducing pathways to the resolution of infection in mice. Exp Parasitol 115, 107-113.

Ehrenman, K., Wanyiri, J.W., Bhat, N., Ward, H.D., Coppens, I., 2013. Cryptosporidium parvum scavenges LDL-derived cholesterol and micellar cholesterol internalized into enterocytes. Cell Microbiol 15, 1182-1197.

Elliott, D.A., Clark, D.P., 2000. Cryptosporidium parvum induces host cell actin accumulation at the host-parasite interface. Infect Immun 68, 2315-2322.

Elliott, D.A., Coleman, D.J., Lane, M.A., May, R.C., Machesky, L.M., Clark, D.P., 2001. Cryptosporidium parvum infection requires host cell actin polymerization. Infect Immun 69, 5940-5942.

Espinosa, V., Dutta, O., McElrath, C., Du, P., Chang, Y.J., Cicciarelli, B., Pitler, A., Whitehead, I., Obar, J.J., Durbin, J.E., Kotenko, S.V., Rivera, A., 2017. Type III interferon is a critical regulator of innate antifungal immunity. Science immunology 2.

Farthing, M.J., 2000. Clinical aspects of human cryptosporidiosis. Contributions to microbiology 6, 50-74.

Feeley, E.M., Pilla-Moffett, D.M., Zwack, E.E., Piro, A.S., Finethy, R., Kolb, J.P., Martinez, J., Brodsky, I.E., Coers, J., 2017. Galectin-3 directs antimicrobial guanylate binding proteins to vacuoles furnished with bacterial secretion systems. Proc Natl Acad Sci U S A 114, E1698-E1706.

Flanigan, T.P., Aji, T., Marshall, R., Soave, R., Aikawa, M., Kaetzel, C., 1991. Asexual development of Cryptosporidium parvum within a differentiated human enterocyte cell line. Infect Immun 59, 234-239.

Florescu, D.F., Sandkovsky, U., 2016. Cryptosporidium infection in solid organ transplantation. World journal of transplantation 6, 460-471.

Foltz, C., Napolitano, A., Khan, R., Clough, B., Hirst, E.M., Frickel, E.M., 2017. TRIM21 is critical for survival of Toxoplasma gondii infection and localises to GBP-positive parasite vacuoles. Sci Rep 7, 5209.

Foster, D.M., Stauffer, S.H., Stone, M.R., Gookin, J.L., 2012. Proteasome Inhibition of Pathologic Shedding of Enterocytes to Defend Barrier Function Requires X-Linked Inhibitor of Apoptosis Protein and Nuclear Factor kappa B. Gastroenterology 143, 133-U695.

Fromter, E., Diamond, J., 1972. Route of passive ion permeation in epithelia. Nature: New biology 235, 9-13.

Fusunyan, R.D., Nanthakumar, N.N., Baldeon, M.E., Walker, W.A., 2001. Evidence for an innate immune response in the immature human intestine: toll-like receptors on fetal enterocytes. Pediatr Res 49, 589-593.

Garza, A., Castellanos-Gonzalez, A., Griffiths, J., Robinson, P., 2008. Infection of immunocompetent mice with acid-water-pretreated Cryptosporidium parvum results in weight loss, and intestinal (structural and physiological) alterations. Parasitol Res 102, 457-463.

Gibson, S.V., Wagner, J.E., 1986. Cryptosporidiosis in guinea pigs: a retrospective study. Journal of the American Veterinary Medical Association 189, 1033-1034.

Giles, M., Webster, K.A., Marshall, J.A., Catchpole, J., Goddard, T.M., 2001. Experimental infection of a lamb with Cryptosporidium parvum genotype 1. Vet Rec 149, 523-525.

Godiwala, N.T., Vandewalle, A., Ward, H.D., Leav, B.A., 2006. Quantification of in vitro and in vivo Cryptosporidium parvum infection by using real-time PCR. Appl Environ Microb 72, 4484-4488.

Gong, A.Y., Hu, G.K., Zhou, R., Liu, J., Feng, Y.Y., Soukup, G.A., Chen, X.M., 2011. MicroRNA-221 controls expression of intercellular adhesion molecule-1 in epithelial cells in response to Cryptosporidium parvum infection. Int J Parasitol 41, 397-403.

Goodgame, R.W., Kimball, K., Ou, C.N., White, A.C., Genta, R.M., Lifschitz, C.H., Chappell, C.L., 1995. Intestinal Function and Injury in Acquired-Immunodeficiency-Syndrome - Related Cryptosporidiosis. Gastroenterology 108, 1075-1082.

Gookin, J.L., Allen, J., Chiang, S., Duckett, L., Armstrong, M.U., 2005. Local peroxynitrite formation contributes to early control of Cryptosporidium parvum infection. Infect Immun 73, 3929-3936.

Gookin, J.L., Chiang, S., Allen, J., Armstrong, M.U., Stauffer, S.H., Finnegan, C., Murtaugh, M.P., 2006. NF-kappa B-mediated expression of iNOS promotes epithelial defense against infection by Cryptosporidium parvum in neonatal piglets. Am J Physiol-Gastr L 290, G164-G174.

Gookin, J.L., Duckett, L.L., Armstrong, M.U., Stauffer, S.H., Finnegan, C.P., Murtaugh, M.P., Argenzio, R.A., 2004. Nitric oxide synthase stimulates prostaglandin synthesis and barrier function in C. parvum-infected porcine ileum. American journal of physiology. Gastrointestinal and liver physiology 287, G571-581.

Gookin, J.L., Nordone, S.K., Argenzio, R.A., 2002. Host responses to Cryptosporidium infection. J Vet Intern Med 16, 12-21.

Griffiths, J.K., Moore, R., Dooley, S., Keusch, G.T., Tzipori, S., 1994. Cryptosporidium parvum infection of Caco-2 cell monolayers induces an apical monolayer defect, selectively increases transmonolayer permeability, and causes epithelial cell death. Infect Immun 62, 4506-4514.

Griffiths, J.K., Theodos, C., Paris, M., Tzipori, S., 1998. The gamma interferon gene knockout mouse: a highly sensitive model for evaluation of therapeutic agents against Cryptosporidium parvum. J Clin Microbiol 36, 2503-2508.

Haldar, A.K., Foltz, C., Finethy, R., Piro, A.S., Feeley, E.M., Pilla-Moffett, D.M., Komatsu, M., Frickel, E.M., Coers, J., 2015. Ubiquitin systems mark pathogen-containing vacuoles as targets for host defense by guanylate binding proteins. Proc Natl Acad Sci U S A 112, E5628-5637.

Hamer, D.H., Ward, H., Tzipori, S., Pereira, M.E., Alroy, J.P., Keusch, G.T., 1994. Attachment of Cryptosporidium parvum sporozoites to MDCK cells in vitro. Infect Immun 62, 2208-2213.

Harp, J.A., Wannemuehler, M.W., Woodmansee, D.B., Moon, H.W., 1988. Susceptibility of germfree or antibiotic-treated adult mice to Cryptosporidium parvum. Infect Immun 56, 2006-2010.

Hayward, A.R., Chmura, K., Cosyns, M., 2000. Interferon-gamma is required for innate immunity to Cryptosporidium parvum in mice. J Infect Dis 182, 1001-1004.

Hayward, A.R., Levy, J., Facchetti, F., Notarangelo, L., Ochs, H.D., Etzioni, A., Bonnefoy, J.Y., Cosyns, M., Weinberg, A., 1997. Cholangiopathy and tumors of the pancreas, liver, and biliary tree in boys with X-linked immunodeficiency with hyper-IgM. J Immunol 158, 977-983.

He, S.H., Song, C.H., Liu, Z., Zhang, H., Ma, W., Zhou, L.F., Mahmood, T., Yang, P.C., 2012. Eosinophil-derived interferon-lambda contributes to initiation of allergen-related inflammation in the intestine. Cytokine 58, 186-192.

Heine, J., Moon, H.W., Woodmansee, D.B., 1984. Persistent Cryptosporidium infection in congenitally athymic (nude) mice. Infect Immun 43, 856-859.

Henderson, K.S., 2008. Murine norovirus, a recently discovered and highly prevalent viral agent of mice. Lab animal 37, 314-320.

Hernandez, P.P., Mahlakoiv, T., Yang, I., Schwierzeck, V., Nguyen, N., Guendel, F., Gronke, K., Ryffel, B., Hoelscher, C., Dumoutier, L., Renauld, J.C., Suerbaum, S., Staeheli, P., Diefenbach, A., 2015. Interferon-lambda and interleukin 22 act synergistically for the induction of interferon-stimulated genes and control of rotavirus infection. Nat Immunol 16, 698-707.

Hong, M., Schwerk, J., Lim, C., Kell, A., Jarret, A., Pangallo, J., Loo, Y.M., Liu, S., Hagedorn, C.H., Gale, M., Jr., Savan, R., 2016. Interferon lambda 4 expression is suppressed by the host during viral infection. J Exp Med 213, 2539-2552.

Hou, L., Li, X., Dunbar, L., Moeller, R., Palermo, B., Atwill, E.R., 2004. Neonatal-mouse infectivity of intact Cryptosporidium parvum oocysts isolated after optimized in vitro excystation. Appl Environ Microbiol 70, 642-646.

Hu, G., Gong, A.Y., Roth, A.L., Huang, B.Q., Ward, H.D., Zhu, G., Larusso, N.F., Hanson, N.D., Chen, X.M., 2013. Release of luminal exosomes contributes to TLR4-mediated epithelial antimicrobial defense. Plos Pathog 9, e1003261.

Hu, G.K., Zhou, R., Liu, J., Gong, A.Y., Chen, X.M., 2010. MicroRNA-98 and let-7 Regulate Expression of Suppressor of Cytokine Signaling 4 in Biliary Epithelial Cells in Response to Cryptosporidium parvum Infection. J Infect Dis 202, 125-135.

Huang, B.Q., Chen, X.M., LaRusso, N.F., 2004. Cryptosporidium parvum attachment to and internalization by human biliary epithelia in vitro: a morphologic study. J Parasitol 90, 212-221.

Hunt, E., Fu, Q., Armstrong, M.U., Rennix, D.K., Webster, D.W., Galanko, J.A., Chen, W.N., Weaver, E.M., Argenzio, R.A., Rhoads, J.M., 2002. Oral bovine serum concentrate improves cryptosporidial enteritis in calves. Pediatr Res 51, 370-376.

Inomata, A., Murakoshi, F., Ishiwa, A., Takano, R., Takemae, H., Sugi, T., Cagayat Recuenco, F., Horimoto, T., Kato, K., 2015. Heparin interacts with elongation factor 1α of Cryptosporidium parvum and inhibits invasion. Scientific Reports 5, 11599.

Khaldi, S., Gargala, G., Le Goff, L., Parey, S., Francois, A., Fioramonti, J., Ballet, J.J., Dupont, J.P., Ducrotte, P., Favennec, L., 2009. Cryptosporidium parvum Isolate-Dependent Postinfectious Jejunal Hypersensitivity and Mast Cell Accumulation in an Immunocompetent Rat Model. Infect Immun 77, 5163-5169.

Kirkpatrick, B.D., Noel, F., Rouzier, P.D., Powell, J.L., Pape, J.W., Bois, G., Alston, W.K., Larsson, C.J., Tenney, K., Ventrone, C., Powden, C., Sreenivasan, M., Sears, C.L., 2006. Childhood cryptosporidiosis is associated with a persistent systemic inflammatory response. Clinical infectious diseases: an official publication of the Infectious Diseases Society of America 43, 604-608.

Kohler, H., Sakaguchi, T., Hurley, B.P., Kase, B.A., Reinecker, H.C., McCormick, B.A., 2007. Salmonella enterica serovar Typhimurium regulates intercellular junction proteins and facilitates transepithelial neutrophil and bacterial passage. American journal of physiology. Gastrointestinal and liver physiology 293, G178-187.

Kotenko, S.V., Gallagher, G., Baurin, V.V., Lewis-Antes, A., Shen, M., Shah, N.K., Langer, J.A., Sheikh, F., Dickensheets, H., Donnelly, R.P., 2003a. IFN-lambdas mediate antiviral protection through a distinct class II cytokine receptor complex. Nat Immunol 4, 69-77.

Kotenko, S.V., Gallagher, G., Baurin, V.V., Lewis-Antes, A., Shen, M.L., Shah, N.K., Langer, J.A., Sheikh, F., Dickensheets, H., Donnelly, R.P., 2003b. IFN-lambda s mediate antiviral protection through a distinct class II cytokine receptor complex. Nat Immunol 4, 69-77.

Kotloff, K.L., Nataro, J.P., Blackwelder, W.C., Nasrin, D., Farag, T.H., Panchalingam, S., Wu, Y., Sow, S.O., Sur, D., Breiman, R.F., Faruque, A.S., Zaidi, A.K., Saha, D., Alonso, P.L., Tamboura, B., Sanogo, D., Onwuchekwa, U., Manna, B., Ramamurthy, T., Kanungo, S., Ochieng, J.B., Omore, R., Oundo, J.O., Hossain, A., Das, S.K., Ahmed, S., Qureshi, S., Quadri, F., Adegbola, R.A., Antonio, M., Hossain, M.J., Akinsola, A., Mandomando, I., Nhampossa, T., Acacio, S., Biswas, K., O'Reilly, C.E., Mintz, E.D., Berkeley, L.Y., Muhsen, K., Sommerfelt, H., Robins-Browne, R.M., Levine, M.M., 2013. Burden and aetiology of diarrhoeal disease in infants and young children in developing countries (the Global Enteric Multicenter Study, GEMS): a prospective, case-control study. Lancet 382, 209-222.

Kuang, Z., Seo, E.J., Leis, J., 2011. Mechanism of inhibition of retrovirus release from cells by interferon-induced gene ISG15. J Virol 85, 7153-7161.

Kumar, A., Chatterjee, I., Anbazhagan, A.N., Jayawardena, D., Priyamvada, S., Alrefai, W.A., Sun, J., Borthakur, A., Dudeja, P.K., 2018. Cryptosporidium parvum disrupts intestinal epithelial barrier function via altering expression of key tight junction and adherens junction proteins. Cell Microbiol.

Lacroix, S., Mancassola, R., Naciri, M., Laurent, F., 2001. Cryptosporidium parvum-specific mucosal immune response in C57BL/6 neonatal and gamma interferon-deficient mice: role of tumor necrosis factor alpha in protection. Infect Immun 69, 1635-1642.

Langer, R.C., Riggs, M.W., 1999. Cryptosporidium parvum apical complex glycoprotein CSL contains a sporozoite ligand for intestinal epithelial cells. Infect Immun 67, 5282-5291.

Langer, R.C., Schaefer, D.A., Riggs, M.W., 2001. Characterization of an intestinal epithelial cell receptor recognized by the Cryptosporidium parvum sporozoite ligand CSL. Infect Immun 69, 1661-1670.

Lantier, L., Drouet, F., Guesdon, W., Mancassola, R., Metton, C., Lo-Man, R., Werts, C., Laurent, F., Lacroix-Lamande, S., 2014. Poly(I:C)-Induced Protection of Neonatal Mice Against Intestinal Cryptosporidium parvum Infection Requires an Additional TLR5 Signal Provided by the Gut Flora. J Infect Dis 209, 457-467.

Laurent, F., Kagnoff, M.F., Savidge, T.C., Naciri, M., Eckmann, L., 1998. Human intestinal epithelial cells respond to Cryptosporidium parvum infection with increased prostaglandin H synthase 2 expression and prostaglandin E2 and F2alpha production. Infect Immun 66, 1787-1790.

Lazear, H.M., Daniels, B.P., Pinto, A.K., Huang, A.C., Vick, S.C., Doyle, S.E., Gale, M., Jr., Klein, R.S., Diamond, M.S., 2015. Interferon-lambda restricts West Nile virus neuroinvasion by tightening the blood-brain barrier. Science translational medicine 7, 284ra259.

Lean, I.S., Lacroix-Lamande, S., Laurent, F., McDonald, V., 2006. Role of tumor necrosis factor alpha in development of immunity against Cryptosporidium parvum infection. Infect Immun 74, 4379-4382.

Leav, B.A., Yoshida, M., Rogers, K., Cohen, S., Godiwala, N., Blumberg, R.S., Ward, H., 2005. An early intestinal mucosal source of gamma interferon is associated with resistance to and control of Cryptosporidium parvum infection in mice. Infect Immun 73, 8425-8428.

Lebreton, A., Lakisic, G., Job, V., Fritsch, L., Tham, T.N., Camejo, A., Mattei, P.J., Regnault, B., Nahori, M.A., Cabanes, D., Gautreau, A., Ait-Si-Ali, S., Dessen, A., Cossart, P., Bierne, H., 2011. A bacterial protein targets the BAHD1 chromatin complex to stimulate type III interferon response. Science 331, 1319-1321.

Lee, S., Harwood, M., Girouard, D., Meyers, M.J., Campbell, M.A., Beamer, G., Tzipori, S., 2017. The therapeutic efficacy of azithromycin and nitazoxanide in the acute pig model of Cryptosporidium hominis. Plos One 12, e0185906.

Leitch, G.J., He, Q., 1994. Arginine-derived nitric oxide reduces fecal oocyst shedding in nude mice infected with Cryptosporidium parvum. Infect Immun 62, 5173-5176.

Leitch, G.J., He, Q., 1999. Reactive nitrogen and oxygen species ameliorate experimental cryptosporidiosis in the neonatal BALB/c mouse model. Infect Immun 67, 5885-5891.

Liu, L., Johnson, H.L., Cousens, S., Perin, J., Scott, S., Lawn, J.E., Rudan, I., Campbell, H., Cibulskis, R., Li, M., Mathers, C., Black, R.E., Child Health Epidemiology Reference Group of, W.H.O., Unicef, 2012. Global, regional, and national causes of child mortality: an updated systematic analysis for 2010 with time trends since 2000. Lancet 379, 2151-2161.

Ludington, J.G., Ward, H.D., 2016. The Cryptosporidium parvum C-Type Lectin CpClec Mediates Infection of Intestinal Epithelial Cells via Interactions with Sulfated Proteoglycans. Infect Immun 84, 1593-1602.

Lukin, K., Cosyns, M., Mitchell, T., Saffry, M., Hayward, A., 2000. Eradication of Cryptosporidium parvum infection by mice with ovalbumin-specific T cells. Infect Immun 68, 2663-2670.

Mahlakoiv, T., Hernandez, P., Gronke, K., Diefenbach, A., Staeheli, P., 2015. Leukocyte-Derived IFN-alpha/beta and Epithelial IFN-lambda Constitute a Compartmentalized Mucosal Defense System that Restricts Enteric Virus Infections. Plos Pathog 11.

Maillot, C., Gargala, G., Delaunay, A., Ducrotte, P., Brasseur, P., Ballet, J.J., Favennec, L., 2000. Cryptosporidium parvum infection stimulates the secretion of TGF-beta, IL-8 and RANTES by Caco-2 cell line. Parasitol Res 86, 947-949.

Malakhova, O.A., Zhang, D.E., 2008. ISG15 inhibits Nedd4 ubiquitin E3 activity and enhances the innate antiviral response. J Biol Chem 283, 8783-8787.

Manjunatha, U.H., Vinayak, S., Zambriski, J.A., Chao, A.T., Sy, T., Noble, C.G., Bonamy, G.M.C., Kondreddi, R.R., Zou, B., Gedeck, P., Brooks, C.F., Herbert, G.T., Sateriale, A., Tandel, J., Noh, S., Lakshminarayana, S.B., Lim, S.H., Goodman, L.B., Bodenreider, C., Feng, G., Zhang, L., Blasco, F., Wagner, J., Leong, F.J., Striepen, B., Diagana, T.T., 2017. A Cryptosporidium PI(4)K inhibitor is a drug candidate for cryptosporidiosis. Nature 546, 376-380.

Matsubayashi, M., Teramoto-Kimata, I., Uni, S., Lillehoj, H.S., Matsuda, H., Furuya, M., Tani, H., Sasai, K., 2013. Elongation Factor-1 alpha Is a Novel Protein Associated with Host Cell Invasion and a Potential Protective Antigen of Cryptosporidium parvum. J Biol Chem 288, 34111-34120.

Maudet, C., Mano, M., Eulalio, A., 2014. MicroRNAs in the interaction between host and bacterial pathogens. Febs Lett 588, 4140-4147.

McClure, R., Massari, P., 2014. TLR-Dependent Human Mucosal Epithelial Cell Responses to Microbial Pathogens. Front Immunol 5, 386.

McDonald, V., Korbel, D.S., Barakat, F.M., Choudhry, N., Petry, F., 2013. Innate immune responses against Cryptosporidium parvum infection. Parasite Immunol 35, 55-64.

Mead, J.R., Arrowood, M.J., Sidwell, R.W., Healey, M.C., 1991. Chronic Cryptosporidium parvum infections in congenitally immunodeficient SCID and nude mice. J Infect Dis 163, 1297-1304.

Meloni, B.P., Thompson, R.C., 1996. Simplified methods for obtaining purified oocysts from mice and for growing Cryptosporidium parvum in vitro. J Parasitol 82, 757-762.

Meunier, E., Dick, M.S., Dreier, R.F., Schurmann, N., Kenzelmann Broz, D., Warming, S., Roose-Girma, M., Bumann, D., Kayagaki, N., Takeda, K., Yamamoto, M., Broz, P., 2014. Caspase-11 activation requires lysis of pathogen-containing vacuoles by IFN-induced GTPases. Nature 509, 366-370.

Miller, R.A., Bronsdon, M.A., Morton, W.R., 1990. Experimental cryptosporidiosis in a primate model. J Infect Dis 161, 312-315.

Ming, Z., Zhou, R., Chen, X.M., 2017. Regulation of host epithelial responses to Cryptosporidium infection by microRNAs. Parasite Immunol 39.

Mirhashemi, M.E., Noubary, F., Chapman-Bonofiglio, S., Tzipori, S., Huggins, G.S., Widmer, G., 2018. Transcriptome analysis of pig intestinal cell monolayers infected with Cryptosporidium parvum asexual stages. Parasit Vectors 11, 176.

Morada, M., Lee, S., Gunther-Cummins, L., Weiss, L.M., Widmer, G., Tzipori, S., Yarlett, N., 2016. Continuous culture of Cryptosporidium parvum using hollow fiber technology. Int J Parasitol 46, 21-29.

Mordstein, M., Neugebauer, E., Ditt, V., Jessen, B., Rieger, T., Falcone, V., Sorgeloos, F., Ehl, S., Mayer, D., Kochs, G., Schwemmle, M., Gunther, S., Drosten, C., Michiels, T., Staeheli, P., 2010a. Lambda interferon renders epithelial cells of the respiratory and gastrointestinal tracts resistant to viral infections. J Virol 84, 5670-5677.

Mordstein, M., Pott, J., Mahlakoiv, T., Neugebauer, E., Dirt, V., Drosten, C., Hornef, M.W., Michiels, T., Staeheli, P., 2010b. A non-redundant role of IFN-lambda in antiviral defense of the intestinal tract. Cytokine 52, 48-48.

Mosier, D.A., Cimon, K.Y., Kuhls, T.L., Oberst, R.D., Simons, K.R., 1997. Experimental cryptosporidiosis in adult and neonatal rabbits. Vet Parasitol 69, 163-169.

Naciri, M., Mancassola, R., Yvore, P., Peeters, J.E., 1993. The effect of halofuginone lactate on experimental Cryptosporidium parvum infections in calves. Vet Parasitol 45, 199-207.

Nice, T.J., Baldridge, M.T., McCune, B.T., Norman, J.M., Lazear, H.M., Artyomov, M., Diamond, M.S., Virgin, H.W., 2015. Interferon-lambda cures persistent murine norovirus infection in the absence of adaptive immunity. Science 347, 269-273.

Nydam, D.V., Mohammed, H.O., 2005. Quantitative risk assessment of Cryptosporidium species infection in dairy calves. J Dairy Sci 88, 3932-3943.

O'Connor R, M., Shaffie, R., Kang, G., Ward, H.D., 2011. Cryptosporidiosis in patients with HIV/AIDS. Aids 25, 549-560.

O'Hara, S.P., Bogert, P.S.T., Trussoni, C.E., Chen, X.M., LaRusso, N.F., 2011. Tlr4 Promotes Cryptosporidium Parvum Clearance in a Mouse Model of Biliary Cryptosporidiosis. J Parasitol 97, 813-821.

O'Hara, S.P., Small, A.J., Chen, X.M., LaRusso, N.F., 2008. Host cell actin remodeling in response to Cryptosporidium. Subcell Biochem 47, 92-100.

Odendall, C., Dixit, E., Stavru, F., Bierne, H., Franz, K.M., Durbin, A.F., Boulant, S., Gehrke, L., Cossart, P., Kagan, J.C., 2014. Diverse intracellular pathogens activate type III interferon expression from peroxisomes. Nat Immunol 15, 717-726.

Odendall, C., Voak, A.A., Kagan, J.C., 2017. Type III IFNs Are Commonly Induced by Bacteria-Sensing TLRs and Reinforce Epithelial Barriers during Infection. J Immunol 199, 3270-3279.

Okumura, A., Lu, G.S., Pitha-Rowe, I., Pitha, P.M., 2006. Innate antiviral response targets HIV-1 release by the induction of ubiquitin-like protein ISG15. P Natl Acad Sci USA 103, 1440-1445.

Okumura, A., Pitha, P.M., Harty, R.N., 2008. ISG15 inhibit Ebola VP40VLP budding in an L-domain-dependent manner by blocking Nedd4 ligase activity. P Natl Acad Sci USA 105, 3974-3979.

Oura, C.A., McKellar, S., Swan, D.G., Okan, E., Shiels, B.R., 2006. Infection of bovine cells by the protozoan parasite Theileria annulata modulates expression of the ISGylation system. Cell Microbiol 8, 276-288.

Pereira, S.J., Ramirez, N.E., Xiao, L., Ward, L.A., 2002. Pathogenesis of human and bovine Cryptosporidium parvum in gnotobiotic pigs. J Infect Dis 186, 715-718.

Perkins, M.E., Riojas, Y.A., Wu, T.W., Le Blancq, S.M., 1999. CpABC, a Cryptosporidium parvum ATP-binding cassette protein at the host-parasite boundary in intracellular stages. Proc Natl Acad Sci U S A 96, 5734-5739.

Perryman, L.E., Kegerris, K.A., Mason, P.H., 1993. Effect of orally administered monoclonal antibody on persistent Cryptosporidium parvum infection in scid mice. Infect Immun 61, 4906-4908.

Pervolaraki, K., Stanifer, M.L., Munchau, S., Renn, L.A., Albrecht, D., Kurzhals, S., Senis, E., Grimm, D., Schroder-Braunstein, J., Rabin, R.L., Boulant, S., 2017. Type I and Type III Interferons Display Different Dependency on Mitogen-Activated Protein Kinases to Mount an Antiviral State in the Human Gut. Front Immunol 8, 459.

Piedade, D., Azevedo-Pereira, J.M., 2016. The Role of microRNAs in the Pathogenesis of Herpesvirus Infection. Viruses 8.

Pincetic, A., Kuang, Z.Z., Seo, E.J., Leis, J., 2010. The Interferon-Induced Gene ISG15 Blocks Retrovirus Release from Cells Late in the Budding Process. J Virol 84, 4725-4736.

Planchon, S.M., Martins, C.A., Guerrant, R.L., Roche, J.K., 1994. Regulation of intestinal epithelial barrier function by TGF-beta 1. Evidence for its role in abrogating the effect of a T cell cytokine. J Immunol 153, 5730-5739.

Platanias, L.C., 2005. Mechanisms of type-I- and type-II-interferon-mediated signalling. Nat Rev Immunol 5, 375-386.

Pollok, R.C., Farthing, M.J., Bajaj-Elliott, M., Sanderson, I.R., McDonald, V., 2001. Interferon gamma induces enterocyte resistance against infection by the intracellular pathogen Cryptosporidium parvum. Gastroenterology 120, 99-107.

Pott, J., Mahlakoiv, T., Mordstein, M., Duerr, C.U., Michiels, T., Stockinger, S., Staeheli, P., Hornef, M.W., 2011. IFN-lambda determines the intestinal epithelial antiviral host defense. P Natl Acad Sci USA 108, 7944-7949.

Prokunina-Olsson, L., Muchmore, B., Tang, W., Pfeiffer, R.M., Park, H., Dickensheets, H., Hergott, D., Porter-Gill, P., Mumy, A., Kohaar, I., Chen, S., Brand, N., Tarway, M., Liu, L., Sheikh, F., Astemborski, J., Bonkovsky, H.L., Edlin, B.R., Howell, C.D., Morgan, T.R., Thomas, D.L., Rehermann, B., Donnelly, R.P., O'Brien, T.R., 2013. A variant upstream of IFNL3 (IL28B) creating a new interferon gene IFNL4 is associated with impaired clearance of hepatitis C virus. Nat Genet 45, 164-171.

Putignani, L., Menichella, D., 2010. Global distribution, public health and clinical impact of the protozoan pathogen cryptosporidium. Interdisciplinary perspectives on infectious diseases 2010.

Radoshevich, L., Impens, F., Ribet, D., Quereda, J.J., Tham, T.N., Nahori, M.A., Bierne, H., Dussurget, O., Pizarro-Cerda, J., Knobeloch, K.P., Cossart, P., 2015. ISG15 counteracts Listeria monocytogenes infection. Elife 4.

Raetz, M., Hwang, S.H., Wilhelm, C.L., Kirkland, D., Benson, A., Sturge, C.R., Mirpuri, J., Vaishnava, S., Hou, B., Defranco, A.L., Gilpin, C.J., Hooper, L.V., Yarovinsky, F., 2013. Parasite-induced TH1 cells and intestinal dysbiosis cooperate in IFN-gamma-dependent elimination of Paneth cells. Nat Immunol 14, 136-142.

Raki, M., Beitnes, A.C., Lundin, K.E., Jahnsen, J., Jahnsen, F.L., Sollid, L.M., 2013. Plasmacytoid dendritic cells are scarcely represented in the human gut mucosa and are not recruited to the celiac lesion. Mucosal Immunol 6, 985-992.

Rasmussen, K.R., Healey, M.C., 1992. Experimental Cryptosporidium parvum infections in immunosuppressed adult mice. Infect Immun 60, 1648-1652.

Rehg, J.E., 1995. The activity of halofuginone in immunosuppressed rats infected with Cryptosporidium parvum. The Journal of antimicrobial chemotherapy 35, 391-397.

Rehg, J.E., Hancock, M.L., Woodmansee, D.B., 1987. Characterization of cyclophosphamide-rat model of cryptosporidiosis. Infect Immun 55, 2669-2674.

Reijasse, D., Patey-Mariaud de Serre, N., Canioni, D., Huerre, M., Haddad, E., Leborgne, M., Blanche, S., Brousse, N., 2001. Cytotoxic T cells in AIDS colonic cryptosporidiosis. Journal of clinical pathology 54, 298-303.

Riggs, M.W., Stone, A.L., Yount, P.A., Langer, R.C., Arrowood, M.J., Bentley, D.L., 1997. Protective monoclonal antibody defines a circumsporozoite-like glycoprotein exoantigen of Cryptosporidium parvum sporozoites and merozoites. J Immunol 158, 1787-1795.

Robinson, P., Okhuysen, P.C., Chappell, C.L., Lewis, D.E., Shahab, I., Janecki, A., White, A.C., Jr., 2001. Expression of tumor necrosis factor alpha and interleukin 1 beta in jejuna of volunteers after experimental challenge with Cryptosporidium parvum correlates with exposure but not with symptoms. Infect Immun 69, 1172-1174.

Roche, J.K., Martins, C.A., Cosme, R., Fayer, R., Guerrant, R.L., 2000. Transforming growth factor beta1 ameliorates intestinal epithelial barrier disruption by Cryptosporidium parvum in vitro in the absence of mucosal T lymphocytes. Infect Immun 68, 5635-5644.

Rogers, K.A., Rogers, A.B., Leav, B.A., Sanchez, A., Vannier, E., Uematsu, S., Akira, S., Golenbock, D., Ward, H.D., 2006. MyD88-dependent pathways mediate resistance to Cryptosporidium parvum infection in mice. Infect Immun 74, 549-556.

Rossi, P., Pozio, E., Besse, M.G., Gomez Morales, M.A., La Rosa, G., 1990. Experimental cryptosporidiosis in hamsters. J Clin Microbiol 28, 356-357.

Sang, Y., Rowland, R.R., Blecha, F., 2010a. Molecular characterization and antiviral analyses of porcine type III interferons. Journal of interferon & cytokine research: the official journal of the International Society for Interferon and Cytokine Research 30, 801-807.

Sang, Y., Rowland, R.R., Hesse, R.A., Blecha, F., 2010b. Differential expression and activity of the porcine type I interferon family. Physiol Genomics 42, 248-258.

Saxena, K., Simon, L.M., Zeng, X.L., Blutt, S.E., Crawford, S.E., Sastri, N.P., Karandikar, U.C., Ajami, N.J., Zachos, N.C., Kovbasnjuk, O., Donowitz, M., Conner, M.E., Shaw, C.A., Estes, M.K., 2017. A paradox of transcriptional and functional innate interferon responses of human intestinal enteroids to enteric virus infection. Proc Natl Acad Sci U S A 114, E570-E579.

Scallan, E., Hoekstra, R.M., Angulo, F.J., Tauxe, R.V., Widdowson, M.A., Roy, S.L., Jones, J.L., Griffin, P.M., 2011. Foodborne illness acquired in the United States--major pathogens. Emerg Infect Dis 17, 7-15.

Schnoor, M., Betanzos, A., Weber, D.A., Parkos, C.A., 2009. Guanylate-binding protein-1 is expressed at tight junctions of intestinal epithelial cells in response to interferon-gamma and regulates barrier function through effects on apoptosis. Mucosal Immunol 2, 33-42.

Schoggins, J.W., 2014. Interferon-stimulated genes: roles in viral pathogenesis. Current opinion in virology 6, 40-46.

Seth, R.B., Sun, L., Ea, C.K., Chen, Z.J., 2005. Identification and characterization of MAVS, a mitochondrial antiviral signaling protein that activates NF-kappaB and IRF 3. Cell 122, 669-682.

Seydel, K.B., Zhang, T., Champion, G.A., Fichtenbaum, C., Swanson, P.E., Tzipori, S., Griffiths, J.K., Stanley, S.L., Jr., 1998. Cryptosporidium parvum infection of human intestinal xenografts in SCID mice induces production of human tumor necrosis factor alpha and interleukin-8. Infect Immun 66, 2379-2382.

Shen, L., Weber, C.R., Raleigh, D.R., Yu, D., Turner, J.R., 2011. Tight junction pore and leak pathways: a dynamic duo. Annual review of physiology 73, 283-309.

Sheppard, P., Kindsvogel, W., Xu, W., Henderson, K., Schlutsmeyer, S., Whitmore, T.E., Kuestner, R., Garrigues, U., Birks, C., Roraback, J., Ostrander, C., Dong, D., Shin, J., Presnell, S., Fox, B., Haldeman, B., Cooper, E., Taft, D., Gilbert, T., Grant, F.J., Tackett, M., Krivan, W., McKnight, G., Clegg, C., Foster, D., Klucher, K.M., 2003. IL-28, IL-29 and their class II cytokine receptor IL-28R. Nat Immunol 4, 63-68.

Siegel, R., Eskdale, J., Gallagher, G., 2011. Regulation of IFN-lambda 1 Promoter Activity (IFN-lambda 1/IL-29) in Human Airway Epithelial Cells. J Immunol 187, 5636-5644.

Sischo, W.M., Atwill, E.R., Lanyon, L.E., George, J., 2000. Cryptosporidia on dairy farms and the role these farms may have in contaminating surface water supplies in the northeastern United States. Prev Vet Med 43, 253-267.

Snodgrass, D.R., Angus, K.W., Gray, E.W., 1984. Experimental cryptosporidiosis in germfree lambs. J Comp Pathol 94, 141-152.

Sow, S.O., Muhsen, K., Nasrin, D., Blackwelder, W.C., Wu, Y.K., Farag, T.H., Panchalingam, S., Sur, D., Zaidi, A.K.M., Faruque, A.S.G., Saha, D., Adegbola, R., Alonso, P.L., Breiman, R.F., Bassat, Q., Tamboura, B., Sanogo, D., Onwuchekwa, U., Manna, B., Ramamurthy, T., Kanungo, S., Ahmed, S., Qureshi, S., Quadri, F., Hossain, A., Das, S.K., Antonio, M., Hossain, M.J., Mandomando, I., Nhampossa, T., Acacio, S., Omore, R., Oundo, J.O., Ochieng, J.B., Mintz, E.D., O'Reilly, C.E., Berkeley, L.Y., Livio, S., Tennant, S.M., Sommerfelt, H., Nataro, J.P., Ziv-Baran, T., Robins-Browne, R.M., Mishcherkin, V., Zhang, J.X., Liu, J., Houpt, E.R., Kotloff, K.L., Levine, M.M., 2016. The Burden of Cryptosporidium Diarrheal Disease among Children < 24 Months of Age in Moderate/High Mortality Regions of Sub-Saharan Africa and South Asia, Utilizing Data from the Global Enteric Multicenter Study (GEMS). Plos Neglect Trop D 10.

Stephens, J., Cosyns, M., Jones, M., Hayward, A., 1999. Liver and bile duct pathology following Cryptosporidium parvum infection of immunodeficient mice. Hepatology 30, 27-35.

Stewart, M.J., Smoak, K., Blum, M.A., Sherry, B., 2005. Basal and reovirus-induced beta interferon (IFN-beta) and IFN-beta-stimulated gene expression are cell type specific in the cardiac protective response. J Virol 79, 2979-2987.

Storey, J.D., 2002. A direct approach to false discovery rates. J. R. Statist. Soc. B 64, 479-498.

Striepen, B., 2013. Parasitic infections: Time to tackle cryptosporidiosis. Nature 503, 189-191.

Syedbasha, M., Egli, A., 2017. Interferon Lambda: Modulating Immunity in Infectious Diseases. Front Immunol 8, 119.

Tang, V.W., Goodenough, D.A., 2003. Paracellular ion channel at the tight junction. Biophysical journal 84, 1660-1673.

Tarver, A.P., Clark, D.P., Diamond, G., Russell, J.P., Erdjument-Bromage, H., Tempst, P., Cohen, K.S., Jones, D.E., Sweeney, R.W., Wines, M., Hwang, S., Bevins, C.L., 1998. Enteric beta-defensin: molecular cloning and characterization of a gene with inducible intestinal epithelial cell expression associated with Cryptosporidium parvum infection. Infect Immun 66, 1045-1056.

Thomson, S., Hamilton, C.A., Hope, J.C., Katzer, F., Mabbott, N.A., Morrison, L.J., Innes, E.A., 2017. Bovine cryptosporidiosis: impact, host-parasite interaction and control strategies. Vet Res 48, 42.

Topouchian, A., Kapel, N., Huneau, J.F., Barbot, L., Magne, D., Tome, D., Gobert, J.G., 2001. Impairment of amino-acid absorption in suckling rats infected with Cryptosporidium parvum. Parasitol Res 87, 891-896.

Travar, M., Vucic, M., Petkovic, M., 2014. Interferon lambda-2 levels in sputum of patients with pulmonary Mycobacterium tuberculosis infection. Scand J Immunol 80, 43-49.

Tsai, P.Y., Zhang, B., He, W.Q., Zha, J.M., Odenwald, M.A., Singh, G., Tamura, A., Shen, L., Sailer, A., Yeruva, S., Kuo, W.T., Fu, Y.X., Tsukita, S., Turner, J.R., 2017. IL-22 Upregulates Epithelial Claudin-2 to Drive Diarrhea and Enteric Pathogen Clearance. Cell Host Microbe 21, 671-681 e674.

Turner, J.R., 2009. Intestinal mucosal barrier function in health and disease. Nat Rev Immunol 9, 799-809.

Tzipori, S., Angus, K.W., Campbell, I., Gray, E.W., 1982. Experimental infection of lambs with Cryptosporidium isolated from a human patient with diarrhoea. Gut 23, 71-74.

Ueki, I.F., Min-Oo, G., Kalinowski, A., Ballon-Landa, E., Lanier, L.L., Nadel, J.A., Koff, J.L., 2013. Respiratory virus-induced EGFR activation suppresses IRF1-dependent interferon lambda and antiviral defense in airway epithelium. J Exp Med 210, 1929-1936.

Upton, S.J., Tilley, M., Brillhart, D.B., 1994. Comparative development of Cryptosporidium parvum (Apicomplexa) in 11 continuous host cell lines. Fems Microbiol Lett 118, 233-236.

Vakil, N.B., Schwartz, S.M., Buggy, B.P., Brummitt, C.F., Kherellah, M., Letzer, D.M., Gilson, I.H., Jones, P.G., 1996. Biliary cryptosporidiosis in HIV-infected people after the waterborne outbreak of cryptosporidiosis in Milwaukee. The New England journal of medicine 334, 19-23.

Vargas-Inchaustegui, D.A., Xin, L., Soong, L., 2008. Leishmania braziliensis infection induces dendritic cell activation, ISG15 transcription, and the generation of protective immune responses. J Immunol 180, 7537-7545.

Varughese, E.A., Bennett-Stamper, C.L., Wymer, L.J., Yadav, J.S., 2014. A new in vitro model using small intestinal epithelial cells to enhance infection of Cryptosporidium parvum. J Microbiol Meth 106, 47-54.

Vignali, D.A., Kuchroo, V.K., 2012. IL-12 family cytokines: immunological playmakers. Nat Immunol 13, 722-728.

Waters, W.R., Harp, J.A., 1996. Cryptosporidium parvum infection in T-cell receptor (TCR)-alpha- and TCR-delta-deficient mice. Infect Immun 64, 1854-1857.

Wen, H., Watry, D.D., Marcondes, M.C., Fox, H.S., 2004. Selective decrease in paracellular conductance of tight junctions: role of the first extracellular domain of claudin-5. Mol Cell Biol 24, 8408-8417.

Witola, W.H., Zhang, X., Kim, C.Y., 2017. Targeted gene knockdown validates the essential role of lactate dehydrogenase in Cryptosporidium parvum. Int J Parasitol 47, 867-874.

Witte, K., Gruetz, G., Volk, H.D., Looman, A.C., Asadullah, K., Sterry, W., Sabat, R., Wolk, K., 2009. Despite IFN-lambda receptor expression, blood immune cells, but not keratinocytes or melanocytes, have an impaired response to type III interferons: implications for therapeutic applications of these cytokines. Genes and Immunity 10, 702-714.

Witte, K., Witte, E., Sabat, R., Wolk, K., 2010. IL-28A, IL-28B, and IL-29: promising cytokines with type I interferon-like properties. Cytokine Growth Factor Rev 21, 237-251.

Xu, P., Widmer, G., Wang, Y., Ozaki, L.S., Alves, J.M., Serrano, M.G., Puiu, D., Manque, P., Akiyoshi, D., Mackey, A.J., Pearson, W.R., Dear, P.H., Bankier, A.T., Peterson, D.L., Abrahamsen, M.S., Kapur, V., Tzipori, S., Buck, G.A., 2004. The genome of Cryptosporidium hominis. Nature 431, 1107-1112.

Yamamoto, M., Takeda, K., 2010. Current views of toll-like receptor signaling pathways. Gastroenterol Res Pract 2010, 240365.

Yang, Y.L., Buck, G.A., Widmer, G., 2010. Cell Sorting-Assisted Microarray Profiling of Host Cell Response to Cryptosporidium parvum Infection. Infect Immun 78, 1040-1048.

Yang, Z., Fu, Y., Gong, P., Zheng, J., Liu, L., Yu, Y., Li, J., Li, H., Yang, J., Zhang, X., 2015. Bovine TLR2 and TLR4 mediate Cryptosporidium parvum recognition in bovine intestinal epithelial cells. Microb Pathog 85, 29-34.

Zaalouk, T.K., Bajaj-Elliott, M., George, J.T., McDonald, V., 2004. Differential regulation of beta-defensin gene expression during Cryptosporidium parvum infection. Infect Immun 72, 2772-2779.

Zadrozny, L.M., Stauffer, S.M., Armstrong, M.U., Jones, S.L., Gookin, J.L., 2006. Neutrophils mediate barrier function in Cryptosporidium parvum infection. Gastroenterology 130, A233-A233.

Zhang, D., Zhang, D.E., 2011. Interferon-stimulated gene 15 and the protein ISGylation system. Journal of interferon & cytokine research : the official journal of the International Society for Interferon and Cytokine Research 31, 119-130.

Zhang, H.L., Guo, F.G., Zhu, G., 2015. Cryptosporidium Lactate Dehydrogenase Is Associated with the Parasitophorous Vacuole Membrane and Is a Potential Target for Developing Therapeutics. Plos Pathog 11.

Zhang, H.L., Zhu, G., 2015. Quantitative RT-PCR assay for high-throughput screening (HTS) of drugs against the growth of Cryptosporidium parvum in vitro. Front Microbiol 6.

Zhang, X.T., Gong, A.Y., Wang, Y., Chen, X., Lim, S.S., Dolata, C.E., Chen, X.M., 2016. Cryptosporidium parvum infection attenuates the ex vivo propagation of murine intestinal enteroids. Physiol Rep 4.

Zhang, Y., Lee, B., Thompson, M., Glass, R., Lee, R.C., Figueroa, D., Gilman, R., Taylor, D., Stephenson, C., Grp, D.W., 2000. Lactulose-mannitol intestinal permeability test in children with diarrhea caused by rotavirus and Cryptosporidium. J Pediatr Gastr Nutr 31, 16-21.

Zhou, R., Gong, A.Y., Eischeid, A.N., Chen, X.M., 2012. miR-27b Targets KSRP to Coordinate TLR4-Mediated Epithelial Defense against Cryptosporidium parvum Infection. Plos Pathog 8.

Zhou, R., Hu, G.K., Liu, J., Gong, A.Y., Drescher, K.M., Chen, X.M., 2009. NF-kappaB p65-Dependent Transactivation of miRNA Genes following Cryptosporidium parvum Infection Stimulates Epithelial Cell Immune Responses. Plos Pathog 5.

Zhou, Z., Hamming, O.J., Ank, N., Paludan, S.R., Nielsen, A.L., Hartmann, R., 2007. Type III interferon (IFN) induces a type I IFN-like response in a restricted subset of cells through signaling pathways involving both the Jak-STAT pathway and the mitogen-activated protein kinases. J Virol 81, 7749-7758.